ABSTRACT

Title of dissertation: FLAVOR PHYSICS
IN THE MODELS WITH WARPED
EXTRA DIMENSION

Aleksandr Azatov, Doctor of Philosophy, 2010

Dissertation directed by: Professor Rabindra N. Mohapatra
Department of Physics

I will first briefly review the Standard Model and gauge hierarchy problem. Then I will present the Randall-Sundrum model with warped extra dimension, which provides an elegant geometrical solution to the hierarchy problem. The main focus of this thesis will be an analysis of the flavor violation in the models with warped extra dimension. First I will discuss the bounds on the scale of the extra dimension arising from the low energy physics. I will show that there is a tension in the parameter space coming from different low energy observables, and I will also discuss possible ways to relax these bounds. Another interesting feature of the warped models is that they generically predict flavor violation in the Higgs sector. I will discuss low energy flavor constraints on the Higgs mediated flavor violation as well as its signatures at the collider experiments. In the last part of this thesis I will discuss the physics of radion, a scalar degree of freedom of the five dimensional gravity multiplet, and I will show why it has interactions which are generically flavor misaligned leading to the observable flavor violation. This, combined with the fact that radion is likely to be

the lightest new physics degree of freedom will lead to the interesting phenomenology both from perspective of collider phenomenology and low energy observables.

FLAVOR PHYSICS IN THE MODELS WITH WARPED EXTRA DIMENSION

by

Aleksandr Azatov

Dissertation submitted to the Faculty of the Graduate School of the
University of Maryland, College Park in partial fulfillment
of the requirements for the degree of
Doctor of Philosophy
2010

Advisory Committee:
Professor Rabindra N. Mohapatra, Chair/Advisor
Professor Kaustubh Agashe
Professor Zacharia Chacko
Professor Nicholas Hadley
Professor Jonathan Rosenberg

Acknowledgments

It is a pleasure to thank the many people who made this thesis possible.

First and for all I would like to thank my advisor, Prof. Rabi Mohapatra, for his guidance during my research and studies at University of Maryland, for his patience, motivation, and immense knowledge. His guidance helped me during the all time of my research, I could not have imagined having a better advisor and mentor for my Ph.D study.

I owe my deepest gratitude to my co-advisor Prof. Kaustubh Agashe, for his guidance on the projects that laid down foundation for this thesis. His perpetual energy and enthusiasm in research had motivated and guided me through the last two years of my research studies. He was always accessible and willing to help me and answer my questions and as a result, research life became smooth and rewarding for me.

I would like to thank Prof. Zacharia Chacko, Prof. Nick Hadley and Prof. Jonathan Rosenberg for agreeing to be committee members and for sparing their invaluable time reviewing the manuscript.

I would like to thank faculty members of the High Energy Theory Group for providing a stimulating environment in which I learned and grown, Prof. Jim Gates, Prof. Kev Abazajian, Prof. Raman Sundrum, special thanks to Prof. Wally Greenberg for his great class on particle physics. I would also like to thank Prof Zacharia Chacko for his great class on particle physics and a lot of stimulating discussions during my graduate studies, from which I benefited a lot.

I am grateful to post-doctoral fellows of High Energy Theory group, Steve Blanchet, Andrey Katz and Take Okui for enlightening discussions and especially I would like to thank Manuel Toharia who was my collaborator on the projects that become essential part of this thesis. It was a great pleasure to collaborate with Manuel during the last two years and hopefully we will continue this collaboration in the future.

I would like to thank my friend and collaborator Lijun Zhu, with whom we worked together on all the projects that now have become my thesis. It was a great fun to work with Lijun and discussing physics with him helped me to understand it better. I hope we will continue working together in the future.

I would like to thank my fellow graduate students Minho Son, Chris Krenke, Kostas Koutrolikos, Dan Chapman, Nick Setzer, Sogee Spinner, Haibo Yu, Ken Hsieh, Bhupal Dev, Prateek Agrawal, Rashmish Mishra, Pat Harding, Mike Buchoff, I benefited a lot from discussing physics with them.

Last and most important, I would like to thank my brother Mike Azatov and my mother Marina Zhamkochyan who supported me throughout my life.

Table of Contents

List of Figures

List of Abbreviations

vev	Vacuum Expectation Value
SM	Standard Model
BSM	Beyond Standard Model
RS	Randall Sundrum
CFT	Conformal Field Theory
AdS	Anti -deSitter
CKM	Cabibbo Kobayashi Maskawa
GIM	Glashow Illiopoulos Maiani
FCNC	Flavor Changing Neutral Currents
FV	Flavor Violation
UV	Ultraviolet
IR	Infrared
4D	fourdimensional
5D	fivedimensional
LHC	Large Hadron Collider
EWSB	Electroweak Symmetry Breaking
EDM	Electric Dipole Moment
RG	Renormalization Group

1.1 Introduction

In 2010 when the Large Hadron Collider (LHC) has already started running, and the high energy physics community is waiting for new experimental results, interest in particle physics has experienced a great rebirth. But what do we know about the properties and interactions of the elementary particles? We know that in the universe there are four fundamental interactions: gravitational, electromagnetic, weak and strong. Standard Model (SM) of particle physics is a theory that describes all of these interactions (except gravitational) at scales from $10-100$GeV. SM agrees to a very high precision with all the experimental observations, and the only missing ingredient of the SM, the Higgs boson, is waiting to be discovered soon at LHC.

Although SM is a very successful theory it still fails to address several important questions. One of the most serious drawbacks of the SM is that it provides no explanation for a huge difference between scales of the gravitational and weak interactions. This is a problem because the Higgs mass receives quantum corrections which are quadratically sensitive to the physics at the highest energy scale, thus making the natural size of the Higgs mass to be of the order of Planck scale ($\sim 10^{19}$GeV). On the other hand, we know that the Higgs mass is of the order of few hundred GeV, and this enormous 10^{16} magnitude of separation between scales, which naturally should be of the same size, is called the hierarchy problem. Another problem with the SM is that from cosmological observations we know that 23% of the energy density of the universe comes from invisible matter, which we call Dark Matter. The SM does not contain particles that can be considered as Dark Matter

candidates. Another problem of the SM is that neutrinos are massless within the minimal SM, but from experimental observations of neutrino oscillations we know that they have mass. These questions motivate us to search for the physics Beyond Standard Model(BSM), which will be free of all the SM drawbacks. Hierarchy problem requires that the new physics states should be somewhere close to the scale of the weak interactions, thus making them accessible at the LHC.

One of the most attractive BSM physics scenarios is provided by the models with warped extra dimension suggested by L.Randall and R.Sundrum [1]. This thesis will be devoted to the analysis of the flavor violation of Randall-Sundrum (RS) models both in the low energy physics observables and at the collider scales. Here is a plan of my thesis. First I will briefly review the SM and the questions it fails to address. Then I will review models with a warped extra dimension. In such models, it is assumed that our universe has an additional spatial dimension which is compact and extremely curved, this warped geometry results in redshifting an effecting cutoff of the theory from the Planck scale down to the electroweak scale, thus addressing the hierarchy problem. Another interesting feature of these theories is that due to the AdS/CFT correspondence [2, 3, 4] such models can become dual to some strongly coupled theory. So in a way RS can be considered as a dual description of the models with strong dynamics, where Higgs is a composite field. Another attractive property of such models is that they have a built in mechanism (so called RS Glashow-Illiopoulos-Maiani(GIM) mechanism [5, 6]) to explain hierarchies of the fermion masses and suppress flavor violating processes mediated by the new physics states. Furthermore, it is interesting that within such models we can easily explain

the spectrum of the neutrino masses[7], achieve precision coupling unification [8] as well as have a Dark Matter candidate [9].

After briefly reviewing warped models, I will present an analysis of the low energy bounds. This analysis will be carried out using so called "two site" approach [10]. Two site is a model which is much simpler than RS, but at the same time it possesses most of the interesting phenomenological aspects of the warped models. We will analyze the bounds coming from $K_0 - \bar{K}_0$ oscillations[11, 12, 13, 14, 15, 16] and $B \to X_s\gamma$ [14, 15] exotic decays, as well as ways to suppress them without introducing flavor symmetries. At the end constraints arising from two processes will lead us to the combined bound of $O(5)$TeV on the scale of the lightest Kaluza-Klein (KK) spin one excitation. In the chapter 3 I will discuss Higgs mediated flavor violation [17, 18]. I will show that these effects will remain important independently of whether Higgs is a five dimensional (5D) or four dimensional (4D) field, and can be understood as a mixing between a zero mode and KK fermions coming from the nonzero Higgs vev. After deriving the formulae for the misalignment between SM fermion masses and their Yukawa couplings, I will discuss some phenomenological implications coming from low energy experiments such as $K_0 - \bar{K}_0$ oscillations and possible effects at the collider such as exotic Higgs and top decays $h \to tc, h \to \mu\tau, t \to ch$. In chapter 4 I will discuss physics of the radion, a graviscalar degree of freedom. I will start with a description of the Goldberger-Wise mechanism[19] which stabilizes the size of the extra dimension, and gives mass to the radion. Then I will discuss the interactions of the radion with SM fields and show that interactions of the radion with fermions are flavor misaligned leading to the radion mediated flavor

violation[20]. Flavor violation in the radion sector becomes important because in Goldberger-Wise stabilization, radion generically is the lightest new physics state. I will again analyze the low energy bounds from $K_0 - \bar{K}_0$ oscillations and flavor violating decays at the collider $r \to tc$. After this I will conclude by summarizing bounds on the scale of the warped extra dimension as well as prospects for the collider physics.

1.2 Standard Model

Before reviewing SM let us a consider a very simple toy model which can illustrate some of the very important features of the SM, a single complex scalar field. The Lagrangian of this toy example will be

$$\begin{aligned} \mathcal{L} &= -\frac{1}{4}F_{\mu\nu}F^{\mu\nu} + |D_\mu\phi|^2 - V(|\phi|) \\ F_{\mu\nu} &= \partial_\mu A_\nu - \partial_\nu A_\mu \\ D_\mu\phi &= (\partial_\mu - ieA_\mu)\,\phi. \end{aligned} \tag{1}$$

One can see that this theory is invariant under the following local transformations

$$\begin{aligned} \phi(x) &\to e^{i\theta(x)}\phi(x) \\ A_\mu(x) &\to A_\mu(x) + \frac{1}{e}\partial_\mu\theta(x). \end{aligned} \tag{2}$$

Now let us suppose that the potential $V(\phi)$ has the following form

$$V(|\phi|) = -\frac{m^2}{2}\phi\phi^\dagger + \frac{\lambda}{4}\left(\phi\phi^\dagger\right)^2, \quad m^2 > 0 \tag{3}$$

then the minimum of the potential will be located at

$$< \phi >= \frac{v}{\sqrt{2}} = \sqrt{\frac{2m^2}{\lambda}}. \tag{4}$$

So the field ϕ will develop a vacuum expectation value (vev), $v \neq 0$ and can be expanded around its vacuum in the following way

$$\phi = \frac{1}{\sqrt{2}} (v + \rho) \, e^{\frac{i\eta}{v}}. \tag{5}$$

Plugging it back to the Lagrangian and performing a gauge transformation to eliminate phase $e^{\frac{i\eta}{v}}$ we will get:

$$\mathcal{L} = -\frac{1}{4} F_{\mu\nu} F^{\mu\nu} + \frac{1}{2} \left| \partial_\mu \rho - ieA_\mu (v + \rho) \right|^2 - V(\rho). \tag{6}$$

We see now that this theory will contain one massive vector field A_μ with mass ev and one massive real scalar field ρ, and that the gauge invariance of the initial Lagrangian of Eq. (1) is broken. This breaking happened because the ground state of the system was not invariant under $U(1)$ symmetry of the Lagrangian. This mechanism of symmetry breaking is called spontaneous symmetry breaking.

Now we can proceed to the discussion of the Standard Model. SM is a quantum field theory based on the $SU(3) \otimes SU(2)_L \otimes U(1)_Y$ gauge group. Lagrangian of the gauge sector is given by,

$$\mathcal{L}_{gauge} = -\frac{1}{4} G^{\mu\nu} G_{\mu\nu} - \frac{1}{4} W^{\mu\nu} W_{\mu\nu} - \frac{1}{4} F^{\mu\nu} F_{\mu\nu}, \tag{7}$$

where $G^{\mu\nu}, W^{\mu\nu}, F^{\mu\nu}$ are the strengths of the $SU(3), SU(2)_L, U(1)_Y$ gauge fields respectively. The subgroup $SU(2)_L \otimes U(1)_Y$ is broken spontaneously down to the $U(1)_{em}$ which describes usual electromagnetic interactions. This symmetry breaking happens in the same way as we have discussed in our toy model example by the non vanishing vev of the scalar field, only in this case our scalar field (Higgs) should have the following quantum numbers under $SU(3) \otimes SU(2)_L \otimes U(1)_Y$ gauge group:

$(1,2,1)$. The Lagrangian describing Higgs interactions will be

$$\begin{aligned} \mathcal{L}_{Higgs} &= |D_\mu H|^2 + \frac{m^2}{2} H H^\dagger - \frac{\lambda}{4}\left(H^\dagger H\right)^2, \\ D_\mu H &= \left(\partial_\mu - igW_\mu^2 \frac{\sigma^a}{2} - \frac{i}{2} g' B_\mu\right) H. \end{aligned} \tag{8}$$

where σ^a are Pauli matrices, generators of the $SU(2)$ group. One can see that the potential will have a minimum for the $< H > \neq 0$ and Higgs field will develop a vev of the form

$$< H >= \begin{pmatrix} 0 \\ \\ \frac{v}{\sqrt{2}} \end{pmatrix}, \quad \frac{v}{\sqrt{2}} = \sqrt{\frac{2m^2}{\lambda}}. \tag{9}$$

This results in the following combinations of the gauge bosons becoming massive

$$\begin{aligned} W_\mu^\pm &= \frac{1}{\sqrt{2}}\left(W_\mu^1 \mp i W_\mu^2\right), \quad m_W = \frac{gv}{2}, \\ Z_\mu &= \frac{1}{\sqrt{g^2 + g'^2}}\left(g W_\mu^3 - g' B_\mu\right), \quad m_Z = \sqrt{g^2 + g'^2}\frac{v}{2}. \end{aligned} \tag{10}$$

The field combination that stays massless

$$A_\mu = \frac{1}{\sqrt{g^2 + g'^2}}\left(g' W_\mu^3 + g B_\mu\right) \tag{11}$$

we can identify with a photon. It will couple to the fields with the following coupling constant

$$e = \frac{g g'}{\sqrt{g^2 + g'^2}} \tag{12}$$

and the $U(1)_{em}$ charge will be related to the $SU(2)_L \times U(1)_Y$ generators in the following way $Q = T^3 + \frac{Y}{2}$. We can see that the neutral mass eigenstates Z_μ, A_μ are related to the eigenstates of the gauge group B_μ, W_μ^3 by the following rotation

$$\begin{pmatrix} Z_\mu \\ \\ A_\mu \end{pmatrix} = \begin{pmatrix} \cos\theta_w & -\sin\theta_w \\ \\ \sin\theta_w & \cos\theta_w \end{pmatrix} \begin{pmatrix} W_\mu^3 \\ \\ B_\mu \end{pmatrix}, \qquad \sin\theta_w = \frac{g'}{\sqrt{g^2 + g'^2}}. \tag{13}$$

Then the generic coupling of the gauge fields to the matter can be described in terms of the following covariant derivative

$$\begin{aligned} D_\mu &= \partial_\mu - \frac{ig}{\sqrt{2}}\left(W_\mu^+ T^+ + W_\mu^- T^-\right) - \frac{ig}{\cos\theta_w} Z_\mu \left(T^3 - Q\sin^2\theta_w\right) - ieQA_\mu \\ T^\pm &= \frac{1}{2}\left(\sigma^1 \pm i\sigma^2\right), \quad T^3 = \frac{\sigma^3}{2}. \end{aligned} \tag{14}$$

This concludes the discussion of the gauge sector of the SM and now we can proceed to the fermion sector.

1.2.1 Fermions

In the SM fermions fermions are sitting in the following representations of the gauge group $SU(3) \otimes SU(2)_L \otimes U(1)_Y$

- electroweak doublets $\left(3, 2, \frac{1}{3}\right)$: $\begin{pmatrix} u_L \\ d_L \end{pmatrix}, \begin{pmatrix} c_L \\ s_L \end{pmatrix}, \begin{pmatrix} t_L \\ b_L \end{pmatrix}$
- up type singlets $\left(3, 1, \frac{4}{3}\right)$: $u_R,\ c_R,\ t_R$
- down type singlets $\left(3, 1, -\frac{2}{3}\right)$: $d_R,\ s_R,\ b_R$

where we explicitly indicated the chiralities of the fermions. In the SM fermions belong to the chiral representations of the gauge group, so prior to the spontaneous symmetry breaking all of them are massless. Fermions will obtain masses only from the interactions with Higgs. The following interaction is consistent with the quantum numbers of the fields

$$\mathcal{L}_{Yukawa} = y_d^{ij} \bar{q}_L^i H d_R^j + y_u^{ij} \bar{q}_L^i \tilde{H} u_R^j, \quad \tilde{H} \equiv i\sigma^2 H^\dagger, \tag{15}$$

where q_L stands for the electroweak doublet and u_R, d_R for the singlets and indices $(i, j = 1, 2, 3)$ refer to the fermion generations (u, c, t) for the up quarks and (d, s, b) for the down quarks. Then after Higgs develops a vev, this will lead to the following mass term for the fermion fields,

$$\mathcal{L}_{Mass} = \frac{y_d^{ij} v}{\sqrt{2}} \bar{d}_L^i d_R^j + \frac{y_u^{ij} v}{\sqrt{2}} \bar{u}_L^i u_R^j. \tag{16}$$

Rotating fermions back to the physical (mass eigenstate basis) generates mixing between different generations (flavors) of the fermions in the interactions with charged gauge bosons ($W^{\pm}$),

$$\mathcal{L}_{W^+} = \frac{g}{\sqrt{2}} \bar{u}_L^i \gamma^\mu V_{CKM}^{ij} d_L^j W_\mu^+ + h.c. \tag{17}$$

where the mixing is parametrized by the unitary Cabibbo-Kobayashi-Maskawa(CKM) matrix V_{CKM}. Similarly we can introduce the leptons

- electroweak doublets $\left(1, 2, -\frac{1}{2}\right)$: $\quad l_L \quad \begin{pmatrix} \nu_L^e \\ e_L \end{pmatrix}, \begin{pmatrix} \nu_L^\mu \\ \mu_L \end{pmatrix}, \begin{pmatrix} \nu_L^\tau \\ \tau_L \end{pmatrix}$
- electroweak singlets $(1, 1, -1)$: $\quad e_R,\ \mu_R,\ \tau_R.$

Leptons also get their masses from the couplings with Higgs

$$\mathcal{L}_{leptons} = \frac{y_e v}{\sqrt{2}} \bar{e}_L e_R. \tag{18}$$

In the SM there are no right handed neutrinos, so neutrinos are massless.

1.2.2 Hierarchy problem

From experimental data we know that electroweak symmetry breaking scale is $v = 246$ GeV, so the Higgs mass should be of the order of $O(100)$ GeV, but if we

will look at the quantum corrections to the Higgs mass (see Fig. 1) we will see that

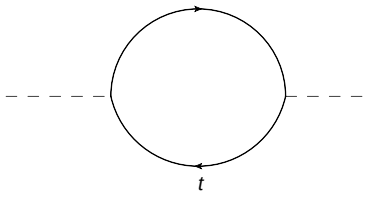

Figure 1: Radiative correction to the Higgs mass due to the fermion loop

this diagram diverges quadratically,

$$\delta m_H^2 \sim -y^2 \int \frac{d^4p}{(2\pi)^4} Tr\left(\frac{\not{p}+m}{p^2-m^2}\frac{\not{p}+m}{p^2-m^2}\right) \sim -\frac{\Lambda^2 y^2}{16\pi^2} \tag{19}$$

The cutoff Λ of the SM is around the Planck scale and the largest of the Yukawa couplings, Yukawa coupling of the top quark is close one, thus the natural scale of the Higgs mass should be of the order of $M_{Planck} \sim 10^{18}$ GeV and not a hundred GeV. There are few solutions to this problem like supersymmetry, strongly coupled theories, extra dimensions. In this thesis we will talk about solution to this problem coming from the models with warped extra dimension.

1.2.3 Fermion masses

Fermions in the SM get their masses from interactions with Higgs (see Eq.(15)) and large hierarchies in the fermion masses are explained by the large hierarchies of the corresponding Yukawa couplings, however the models with warped extra dimensions can provide an interesting explanation of these hierarchies [6, 22]. The nice feature of this type of models is that the same mechanism that generates hierarchies in the fermion sector suppresses flavor violation from the new physics states. An-

other interesting puzzle of the SM is neutrino mass. As we have mentioned before, neutrinos in the SM are massless, but this contradicts neutrino oscillation experiments. Of course we can easily evade this problem by extending the SM fermion sector and introducing a right handed singlet neutrino, but then the question of the smallness of the neutrino masses arises, because Yukawa couplings in the neutrino sector should be 10^{-6} times smaller than the smallest coupling of the other fermions. Models with warped extra dimension provide a simple solution to this problem [7].

1.3 Review of RS

In this section I will briefly review the original model suggested by L.Randall and R.Sundrum (RS) [1]. Their idea was to assume that our world has an additional compact spatial dimension and the metric has the following nonfactorizable form,

$$ds^2 = e^{-2ky}dx^2 - dy^2, \quad 0 < y < \pi r. \tag{20}$$

Let us look at how such geometry might arise from the Einstein equations and how it can address the hierarchy problem. We start with a five dimensional action for gravity, and we will assume that there is a cosmological constant term. We will also assume cosmological constant terms located at the boundaries of the system, then

the action of the system will be,

$$\begin{aligned} S &= S_{gravity} + S_{UV} + S_{IR}, \\ S_{gravity} &= \int d^4x \int_0^{\pi r} dy \sqrt{-G} \left(\Lambda + 2M^3 R\right), \\ S_{IR} &= \int d^4x \sqrt{-g_{IR}} \left(\mathcal{L}_{IR} - V_{IR}\right), \\ S_{UV} &= \int d^4x \sqrt{-g_{UV}} \left(\mathcal{L}_{UV} - V_{UV}\right), \end{aligned} \tag{21}$$

where $S_{UV,IR}$ correspond to the terms of the action localized on the boundaries of the system, so called ultraviolet(UV) and infrared(IR) branes[1]. These branes are located at $(y = 0, (y = \pi r))$ coordinates in 5D space respectively, and $g^{\mu\nu}_{UV(IR)} = G^{\mu\nu}|_{y=0(\pi r)}$ is metric induced on the branes. It is important to remember that we introduced extra spatial dimension in order to address hierarchy problem and we do not want to introduce additional hierarchies in the action, thus all the dimensional parameters should be of the same size $\Lambda^{\frac{1}{5}} \sim V^{\frac{1}{4}}_{UV,IR} \sim M$. We will search for the solutions of the Einstein equations for this system using the following ansatz:

$$ds^2 = e^{-2\sigma(y)}\eta_{\mu\nu}dx^\mu dx^\nu - dy^2, \quad 0 < y < \pi r. \tag{22}$$

It will lead to the following equations

$$\begin{aligned} 6\sigma'(y)^2 &= -\frac{\Lambda}{4M^3} \\ 3\sigma''(y) &= \frac{V_{UV}}{4M^3}\delta(y) + \frac{V_{IR}}{4M^3}\delta(y - \pi r), \end{aligned} \tag{23}$$

and the solution will be

$$\sigma(y) = |y|\sqrt{\frac{-\Lambda}{24M^3}}. \tag{24}$$

[1]In this thesis I will also use notations Planck and TeV branes for the UV and IR branes respectively

In order to have this solution, bulk cosmological constant Λ and brane cosmological constants V_{UV}, V_{IR} should be related in the following way

$$V_{UV} = -V_{IR} = 24M^3k, \quad \Lambda = -24M^3k^2, \tag{25}$$

where curvature k is of the order of 5D Planck mass M. Then the solution for the metric will be given by

$$ds^2 = e^{-2ky}\eta_{\mu\nu}dx^\mu dx^\nu + dy^2. \tag{26}$$

Let us see now how the parameters of our five dimensional theory are related to the parameters of four dimensional theory of gravity, namely to the Planck mass M_{Pl}. To see this we can consider small perturbations of the metric

$$ds^2 = e^{-2ky}\left[\eta_{\mu\nu} + \bar{h}_{\mu\nu}\right]dx^\mu dx^\nu + dy^2 \tag{27}$$

this will lead to the following four dimensional action

$$S_{4D} \sim \int_0^{\pi r} dy \left(2M^3 e^{-2k|y|}\sqrt{-\bar{g}}\bar{R}\right) \tag{28}$$

where $\bar{R}, \bar{g}$ are Ricci scalar and metric calculated for the four dimensional metric $\bar{g}_{\mu\nu} = \eta_{\mu\nu} + h_{\mu\nu}$. This leads to the following relation between four dimensional Planck mass and the parameters of the five dimensional action

$$M_{Pl}^2 = M^3\int_0^{\pi r} dy e^{-2k|y|} = \frac{M^3}{k}\left[1 - e^{-2k\pi r}\right] \tag{29}$$

So in the limit of large $k\pi r$

$$M_{Pl}^2 \sim \frac{M^3}{k}, \tag{30}$$

where 5D Planck mass M is of the same size order as 4D M_{Pl}. Now, after we have shown that we can achieve metric (20) as a solution to the Einstein equations, and that this theory leads to the usual 4D gravity, we can look at how gauge hierarchy problem might be addressed within this framework. Let us assume that the Higgs field is localized on the IR brane, then the corresponding action will be

$$S_{IR} = \int d^4x\sqrt{-g_{IR}}\left[g_{IR}^{\mu\nu}\left(D_\mu H\right)^\dagger D_\nu H - \lambda(|H|^2 - v_0^2)^2\right]. \tag{31}$$

On the other hand g_{IR} in our case is equal to $g_{IR} = e^{-2k\pi R}\bar{g}_{\mu\nu}$ so substituting it back we will get

$$S_{IR} = \int d^4x\sqrt{-\bar{g}}e^{-4k\pi r}\left[\bar{g}^{\mu\nu}e^{2k\pi r}\left(D_\mu H\right)^\dagger D_\nu H - \lambda(|H|^2 - v_0^2)^2\right]. \tag{32}$$

We have to make substitution $H \to e^{k\pi r}H$ to normalize kinetic term properly and this will lead us to

$$S_{eff} = \int d^4x\sqrt{-\bar{g}}\left[\bar{g}^{\mu\nu}\left(D_\mu H\right)^\dagger D_\nu H - \lambda(|H|^2 - v_0^2e^{-2k\pi r})^2\right]. \tag{33}$$

We can see now, that effective electroweak symmetry breaking scale is given by

$$v \equiv e^{-k\pi r}v_0. \tag{34}$$

This result is completely general and it will hold for arbitrary mass scale of the IR localized action

$$m \to e^{-k\pi r}m. \tag{35}$$

So if the exponent $e^{k\pi r} \sim 10^{15} - 10^{16}$, we can easily get desired hierarchy between Planck and weak scales. The new physics states in this model will be Kaluza-Klein excitations of the graviton, i.e. spin 2 massive fields, with a mass around

TeV scale. In the original RS model (RS1) SM Lagrangian was located on the IR brane. Unfortunately this leads to a very serious problem: generically flavor violating contribution of new physics should be suppressed only by the cutoff scale, which is roughly $\sim M_{Pl}e^{-k\pi r} \sim O(10\text{TeV})$. But from low energy experiments we know that constraints from flavor violation are very severe, looking for example at four fermion operator

$$\frac{\bar{d}_L s_R \bar{d}_R s_L}{\Lambda^2}, \tag{36}$$

we see that bounds from ϵ_K parameter of the $K_0 - \bar{K}_0$ oscillations requires $\Lambda > 2.4 \times 10^5$ TeV(see [21] for model independent analysis). We see that the RS1 requires some additional mechanism to suppress flavor violation. On the other hand from AdS/CFT correspondence we know that the RS1 corresponds to the theory with strong dynamics, where all the SM fields are composite, but we know that to make the Higgs mass stable under radiative corrections we only need the Higgs field to be composite. So in RS picture we do not need fermions to be localized on the IR brane, and even more we can use RS dual of the partial compositeness mechanism of [23] to address fermion hierarchy problem as well as to suppress flavor violation.

1.3.0.1 Fermions in the bulk

Before putting every SM field in the 5D bulk[22], let us consider just a single fermion in the bulk. For simplicity we will use the conformal coordinates

$$\begin{aligned} & z \equiv e^{-ky}, \\ & ds^2 = \frac{R}{z^2}\left(\eta_{\mu\nu}dx^\mu dx^\nu - dz^2\right), \\ & R < z < R', \quad R = \frac{1}{k}, \quad R' = \frac{e^{k\pi r}}{k}. \end{aligned} \tag{37}$$

The action for the fermion will be given by

$$S = \int d^4x \int_R^{R'} dz\sqrt{-g}\left[\frac{i}{2}\bar{\psi}e_A^M\Gamma^A D_M\psi - \frac{i}{2}\left(D_M\psi\right)^\dagger\Gamma_0 e_A^M\Gamma^A\psi + \frac{c}{R}\bar{\psi}\psi\right], \tag{38}$$

where e_A^M and D_M are funfbein and covariant derivative(see for the details Appendix A). After simplifications the action will look like

$$\int d^4x \int_R^{R'} dz\left(\frac{R}{z}\right)^4\left[\frac{i}{2}\bar{\psi}\Gamma^M\partial_M\psi - \frac{i}{2}\left(\partial_M\psi\right)^\dagger\Gamma^0\Gamma^M\psi - \frac{c\bar{\psi}\psi}{z}\right]. \tag{39}$$

Now we can apply action variation principle to derive equation of motions for the fermion fields. But we have to take care of the finiteness of the extra dimension, in this case the integration of a full divergence over z coordinate will lead to the additional surface term

$$\frac{1}{2}\int d^4x\left(\frac{R}{z}\right)^4\left[\overline{\psi}_L\delta\psi_R - \overline{\psi}_R\delta\psi_L - \delta\overline{\psi}_L\psi_R + \delta\overline{\psi}_R\psi_L\right]|_R^{R'} \tag{40}$$

where we decompose 5D fermion

$$\psi = \begin{pmatrix} \psi_R \\ \\ \psi_L \end{pmatrix} \tag{41}$$

in terms of the usual 4D chiral fermions. Now we can see that in order to have a consistent theory we need to impose Dirichlet boundary condition [25] on one of the two chiralities of the fermion on each of the branes,

$$\begin{aligned} \psi_L|_{z=R} = 0 \quad \text{or} \quad \psi_R|_{z=R} = 0 \\ \psi_L|_{z=R'} = 0 \quad \text{or} \quad \psi_R|_{z=R'} = 0. \end{aligned} \tag{42}$$

So at the end in the equation of motion will look like

$$\left(i\partial\!\!\!/ + \gamma_5 \partial_z - \frac{2}{z}\gamma_5 - \frac{c}{z} \right) \psi = 0 \tag{43}$$

or in terms of the 4D chiral fields

$$\begin{aligned} i\partial\!\!\!/ \psi_L + \partial_z \psi_R - \left(\frac{2+c}{z} \right) \psi_R = 0 \\ i\partial\!\!\!/ \psi_R - \partial_z \psi_L + \left(\frac{2-c}{z} \right) \psi_L = 0. \end{aligned} \tag{44}$$

First one can see that equations of motion for the left and right handed fields are coupled and the Dirichlet boundary condition for the one field will lead to the Neumann boundary condition for the other field. In the future we will denote Dirichlet (odd) and Neumann (even)boundary conditions by $(-), (+)$ signs and for example, $\psi_L(+,-)$ will mean that ψ_L satisfies even boundary condition at UV and odd boundary condition at IR brane.

We can now decompose our field in terms of the KK excitations

$$\begin{aligned} \psi_L = \sum_n f_L^n(z) \psi_L^n(x) \\ \psi_R = \sum_n f_R^n(z) \psi_R^n(x) \\ p\!\!\!/ \psi_L^n(x) = m_n \psi_R^n(x). \end{aligned} \tag{45}$$

This leads to the following equations for the profiles ($f_{L,R}$)

$$\begin{aligned} -m_n f_L^n - \partial_z f_R^n + \frac{c+2}{z} f_R^n = 0 \\ -m_n f_R^n + \partial_z f_L^n + \frac{c-2}{z} f_L^n = 0 \end{aligned} \tag{46}$$

Solving these equations will lead us to the spectrum of the KK masses. It is interesting to point out that in the case of the $(+,+)$ fields we will have a massless mode, so for example for the $\psi_L(+,+)$ boundary conditions we will have massless left handed fermion with 5D profile

$$\begin{aligned} f_L(z) &= z^{2-c} \frac{(R')^{-1/2+c}}{R^2} f(c) \\ f(c) &\equiv \sqrt{\frac{1-2c}{1-\left(\frac{R}{R'}\right)^{1-2c}}}. \end{aligned} \tag{47}$$

The solution for the $\psi_R(+,+)$ case we can get just by simply resubstituting $c \leftrightarrow -c$. Generically solutions are given in terms of the bessel functions (see AppendixA). For the case of the $(\psi_L(+,+))$ boundary conditions KK mass spectrum can be calculated from

$$\begin{aligned} \frac{J_{-1/2+c}(m_n R')}{Y_{-1/2+c}(m_n R')} = \frac{J_{-1/2+c}(m_n R)}{Y_{-1/2+c}(m_n R)} \\ m_n \sim \frac{\pi}{R'}\left(n + \frac{c+1}{2}\right), \quad 1/R' < m_n < 1/R \end{aligned} \tag{48}$$

1.3.0.2 Fermion couplings to Higgs

Right now we know how to get a single massless fermion, but in SM model fermions are chiral and they get their masses from the Higgs vev. To reproduce this in RS, we will need two 5D fermions Q, U, one of which should be a doublet and another a singlet under SM $SU(2)_L$. Q_L, U_R fields should satisfy even boundary

conditions $(+,+)$, in order to have zero modes, and their interaction with Higgs will be given by the following overlap integral

$$\int d^4x \left(\frac{R}{R'}\right)^4 Y_{5D} HQU,$$
$$\text{where } \dim[Y_{5D}] = -1. \tag{49}$$

Then the effective 4D interaction of the fermions with Higgs will given by

$$\int d^4x \left(\frac{R}{R'}\right)^4 Y_{5D} HQU = \frac{Y_{5D}}{R} f(c_Q) f(-c_U) H, \tag{50}$$

where $f(c)$ is defined in Eq.(47). The mass of the fermion in this case will be equal to,

$$Y_* f(c_Q) f(-c_U) v, \quad Y_* \equiv \frac{Y_{5D}}{R} \tag{51}$$

At the same time we know that fermion profiles $f(c)$ depend exponentially on the bulk masses c, so by small variation of the 5D bulk masses c we can easily explain observed hierarchies in the fermion mass sector. This leads us to the so called "flavor anarchy" scenario[6], where all the 5D Yukawa couplings are of the same order and the hierarchies of fermions masses come only from their 5D profiles.

1.4 Realistic Model

The minimal extension of the SM in the RS scenario naively should be the model, where all the SM fields are promoted to be the bulk fields. However this simple model does not work, because bounds from electroweak precision T parameter [26] become extremely severe and require $1/R' \gtrsim 11$ TeV [27], because the custodial

$SU(2)_R$ is broken. But as was shown in [28], simple extention of the gauge sector of the model from $SU(3) \times SU(2)_L \otimes U(1)_Y$ to $SU(3) \otimes SU(2)_L \otimes SU(2)_R \otimes U(1)_{B-L}$ relaxes T parameter bound a lot, and the mass scale of the $1/R' \gtrsim 1.3$ TeV becomes compatible with current electroweak precision data. The action for the gauge sector of the model will become

$$S_{gauge} = \int d^4xdz \left(\frac{R}{z}\right) \left[-\frac{1}{4} Tr W^L_{MN} W^{L,MN} - \frac{1}{4} Tr W^R_{MN} W^{R,MN} \right.$$
$$\left. -\frac{1}{4} Tr G_{MN} G^{MN} - \frac{1}{4} F_{MN} F^{MN} \right], \qquad (52)$$

where W^L_{MN}, W^R_{MN}, are field strengths for the $SU(2)_L$ and $SU(2)_R$ gauge fields respectively, G_{MN} is a field strength for gluon and F_{MN} is for $B-L$ gauge boson. The following boundary conditions are assigned for the fields:

$$W^{R,1,2}_\mu \quad (-,+),$$
$$\text{everything else} \quad (+,+). \qquad (53)$$

So the boundary conditions on the UV brane break $SU(2)_R$ down to $U(1)_R$, and then resulting $U(1)_{B-L} \times U(1)_R$ is broken down to $U(1)_Y$ by vev at the UV brane. As a result two linear combinations of W^3_R and B' (B' is a gauge boson of the $U(1)_{B-L}$) will become mass eigenstates

$$Z'_\mu = \frac{g^R_5 W^{R,3}_\mu - g^{B-L}_5 B'_\mu}{\sqrt{(g^R_5)^2 + (g^{B-L}_5)^2}},$$
$$B_\mu = \frac{g^{B-L}_5 W^{R,3}_\mu + g^R_5 B'_\mu}{\sqrt{(g^R_5)^2 + (g^{B-L}_5)^2}}. \qquad (54)$$

B_μ field satisfies $(+,+)$ boundary conditions and covariant derivative for the B_M fields will look like,

$$D_M = \partial_M - ig_5' B_M \left(\tau_R^3 + \frac{B-L}{2} \right), \tag{55}$$

now we can identify B_μ with $U(1)_Y$ gauge boson of the SM and $Y = \tau_R^3 + \frac{B-L}{2}$ with the hypercharge.

Now we can look at the fermions, SM left handed doublet (u_L, d_L) in the simplest set up will be part of the 5D $SU(2)_L$ doublet

$$Q : (3, 2, 1, 1/3) \quad \begin{pmatrix} u_L(+,+) \\ \\ d_L(+,+) \end{pmatrix} \tag{56}$$

where we have written down only the lefthanded part of the 5D fermion, which satisfies $(+,+)$ boundary conditions and contains chiral zero modes. There are different ways to embed SM singlet fermions in the multiplets of the $SU(2)_R$ and one of the simplest ones is to introduce extra u', d', so that we will have two doublets of $SU(2)_R$

- $q_1 : (3, 1, 2, 1/3) \quad \begin{pmatrix} u_R'(-,+) \\ \\ d_R(+,+) \end{pmatrix}$ contains SM d_R
- $q_2 : (3, 1, 2, 1/3) \quad \begin{pmatrix} u_R(+,+) \\ \\ d_R'(-,+) \end{pmatrix}$ contains SM u_R,

and similarly for the other two generations of the SM fermions. Higgs field in such models becomes bidoublet of $SU(2)_L \otimes SU(2)_R$.

1.4.1 "Flavor anarchy" scenario

This scenario assumes that all the parameters of the 5D Lagrangian are not hierarchical, and the hierarchies of the fermion sector come only from 5D profiles (47). The mass matrices for the SM "up" and "down" quarks in this case will become

$$m^u_{ij} = Y^{ij}_* v f(c^i_q) f(-c^j_u)$$
$$m^d_{ij} = Y^{ij}_* v f(c^i_q) f(-c^j_d). \tag{57}$$

One can see that the four dimensional mass matrices for the SM fermions are hierarchical because $f(c^1_{q,u,d}) << f(c^2_{q,u,d}) << f(c^3_{q,u,d})$, where subscripts q, u, d refer to the profiles of the electroweak doublets and up and down type singlets. In the case of hierarchical mass matrices the following approximate relations will hold

$$m^u_i \sim Y_* v f(c^i_q) f(-c^i_u) \quad m^d_i \sim Y_* v f(c^i_q) f(-c^i_d)$$
$$\left(O_{d(u)_L}\right)^{ij} \sim V^{ij}_{CKM} \sim \left|\frac{f(c^i_q)}{f(c^j_q)}\right| \text{ for j> i,}$$
$$\left(O_{d(u)_R}\right)^{ij} \sim \left|\frac{f(c^i_{d(u)})}{f(c^j_{d(u)})}\right| \text{ for j> i,} \tag{58}$$

where Y_* is typical value of the Y^{ij}_*(again we are assuming that all the elements of the Y^{ij}_* are of the same order)and $O_{d(u)_{L,R}}$ are left and right rotation matrices defined in the following way

$$m^{d(u)}_{diag} = \left(O_{d(u)_L}\right)^\dagger m^{d(u)} \left(O_{d(u)_R}\right). \tag{59}$$

Then we can estimate the typical values of the profiles on the IR brane.

$$
\begin{aligned}
f(-c_3^u) \sim 1, \quad f(c_3^q) \sim \frac{m_t}{Y_*^u v}, \quad f(-c_3^d) \sim \frac{m_b Y_*}{m_t Y_* d}, \\
f(-c_2^u) \sim \frac{m_s}{m_t \lambda^2}, \quad f(c_2^q) \sim \lambda^2 \frac{m_t}{Y_*^u v}, \quad f(-c_2^d) \sim \frac{m_b Y_*^u}{m_t Y_*^d \lambda^2}, \\
f(-c_1^u) \sim \frac{m_u}{m_t \lambda^3}, \quad f(c_1^q) \sim \lambda^3 \frac{m_t}{Y_*^u v}, \quad f(-c_1^d) \sim \frac{m_u Y_*^u}{m_t Y_*^d \lambda^3},
\end{aligned}
\tag{60}
$$

where λ is Cabibbo angle of the CKM matrix. So generically this scenario becomes very predictive, because all the values of the fermion profiles are fixed on the IR brane from SM observables.

So let us state some qualitative properties of the models with "flavor anarchy". Profiles of the zero modes of the fermions are hierarchical on the IR brane. Profiles of the KK excitations are localized near IR brane (see Appendix A), and they do not depend strongly on the values of the 5D Lagrangian parameters. The same is true for the masses of the KK fermions, they only mildly depend on the values of the bulk mass parameter c. Then one can immediately see that the couplings of the zero mode fermions to the heavy states are controlled by the smallness of their profiles at IR brane $f(c)$. At the same time we know that profiles of the light quarks should be small at IR brane to explain their masses, so the new physics contribution to the flavor violating interactions involving light quarks will become suppressed by the parameter which is related to their mass.

In the end I would like to summarize this chapter by saying that models with warped extra dimension with SM in the bulk provide a very attractive scenario of BSM physics, which can address both hierarchy problem and explain observed

hierarchies of the fermion masses.

Chapter 2

Low energy bounds on the warped models

2.1 Review of two -site model

In this chapter we will analyze low energy bounds arising from flavor violating observables on the scale of the warped extra dimension. Instead of using some specific warped model we will use so called "two site" model, which comes from the deconstruction of the 5D extra dimension. Two site model is much simpler to analyze and at the same time it is good enough to capture most of the robust predictions of the warped phenomenology. We will start by reviewing the basic features of the two-site model (for more details see [10]). The particle content of the model is divided into two sectors: composite and elementary. The elementary sector of the model is equal exactly to that of SM except for the Higgs field. The SM gauge fields $(SU(3) \otimes SU(2)_L \otimes U(1)_Y)$ will be denoted in the following way,

$$A_\mu \equiv \{G_\mu, W_\mu, B_\mu\} \tag{2.1}$$

and fermion $SU(2)_L$ doublets by,

$$\psi_L \equiv \{q_{Li} = (u_{Li}, d_{Li}), l_{Li} = (\nu_{Li}, e_{Li})\} \tag{2.2}$$

and finally $SU(2)_L$ singlets as,

$$\tilde{\psi}_R \equiv \{u_{Ri}, d_{Ri}, \nu_{Ri}, e_{Ri}\}. \tag{2.3}$$

The only renormalizable interactions are the gauge interactions.

$$\mathcal{L}^{\text{elementary}} = -\frac{1}{4}F_{\mu\nu}^2 + \bar{\psi}_L i\not{D}\psi_L + \bar{\tilde{\psi}}_R i\not{D}\tilde{\psi}_R. \tag{2.4}$$

where the covariant derivative only involves elementary sector gauge bosons: $D_\mu \equiv \partial_\mu - ig_{el}A_\mu$, with g_{el} the elementary sector gauge couplings.

The composite boson sector (containing SM Higgs and massive spin 1 particles) has $SU(3) \otimes SU(2)_L \otimes SU(2)_R \otimes U(1)_X$ global symmetries, where we need the additional custodial $SU(2)_R$ to suppress new physics contribution to the T parameter [28]. There are fifteen heavy vector mesons (ρ_μ) that belong to adjoint representation of the $SU(3) \otimes SU(2)_L \otimes SU(2)_R \otimes U(1)_X$, and they can be decomposed into two sets: ρ_*, which are in the adjoint representation of the SM gauge group and their orthogonal combinations $\tilde{\rho}$

$$\rho_\mu^* = \{G_\mu^*, W_\mu^*, \mathcal{B}_\mu^*\}, \qquad \tilde{\rho}_\mu = \left\{\tilde{W}_\mu^\pm \equiv \frac{\tilde{W}_1 \mp i\,\tilde{W}_2}{\sqrt{2}}, \tilde{\mathcal{B}}_\mu\right\}. \tag{2.5}$$

We associate $\mathcal{B}^*, \tilde{\mathcal{B}}$ with the generators $T_{\mathcal{B}^*} = Y_{\text{hypercharge}} = \frac{T^{3R}+\sqrt{2/3}T_X}{\sqrt{5/3}}$ and $T_{\tilde{\mathcal{B}}} = \frac{T^{3R}-\sqrt{2/3}T_X}{\sqrt{5/3}}$, where $T_{\mathcal{B}^*}$ is hypercharge generator in the SO(10) normalization. Higgs field belongs to the composite sector and is a real bidoublet under $SU(2)_L \otimes SU(2)_R$: $(H, \tilde{H})$.

Every SM fermion representation will be accompanied by a heavy composite Dirac fermion, so the composite sector will consist of $SU(2)_L$ doublets :

$$\chi \equiv (Q_i = \{U_i, D_i\}, L_i = \{N_i, E_i\}) \tag{2.6}$$

and $SU(2)_L$ singlets:

$$\tilde{\chi} = \left(\tilde{U}_i, \tilde{D}_i, \tilde{E}_i, \tilde{N}_i\right) \tag{2.7}$$

They are all singlets under $SU(2)_R$. The Dirac masses of the composite sector doublets and singlets are $m_*, \tilde{m}_*$, respectively, which we assume to be the same (and generation-independent) for simplicity. $U(1)_X$ charges for fermions are chosen to reproduce the usual SM hypercharges.

The Lagrangian of the composite sector is

$$\mathcal{L}_{\text{composite}} = -\frac{1}{4}\rho_{\mu\nu}^2 + \frac{M_*^2}{2}\rho_\mu^2 + |D_\mu H|^2 - V(H) +$$
$$+\bar{\chi}(i\not{D} - m_*)\chi + \bar{\tilde{\chi}}(i\not{D} - \tilde{m}_*)\tilde{\chi} - \bar{\chi}(Y_*^u \tilde{H}\tilde{\chi}^u + Y_*^d H\tilde{\chi}^d) + h.c. \tag{2.8}$$

where M_* is the mass of the composite sector vector boson (again, assumed to be the same for all gauge bosons for simplicity), and the covariant derivative here involves only composite sector gauge bosons: $D_\mu \equiv \partial_\mu - ig_*\rho_\mu^* - i\tilde{g}_*\tilde{\rho}_\mu$, with g_* and $\tilde{g}_*$ the corresponding composite sector gauge couplings. One can see that Yukawa couplings explicitly break $SU(2)_R$ in composite sector (see Eq. (2.8)). But this breaking gives a small contribution to the T parameter and is thus technically natural as mentioned in [10].[1]

2.1.1 Mixing and Diagonalization

The two sectors (composite and elementary) are connected to each other by the mixing terms

$$\mathcal{L}_{\text{mixing}} = -M_*^2 \frac{g_{el}}{g_*} A_\mu \rho_\mu^* + \frac{M_*^2}{2}\left(\frac{g_{el}}{g_*}A_\mu\right)^2 + (\bar{\psi}_L \Delta \chi_R + \bar{\tilde{\psi}}_R \tilde{\Delta}\tilde{\chi}_L + \text{h.c.}). \tag{2.9}$$

[1] Alternatively, we can add extra composite site fermions so that Yukawa interactions respect $SU(2)_R$. This corresponds to choosing $5D$ fermions in complete multiplets of $SU(2)_R$ in the $5D$ AdS models [28]. We will not pursue this option here.

This structure of mixing terms are motivated by the corresponding 5D warped extra dimension models. We assume small mixings between elementary and composite sectors, i.e., $\frac{g_{el}}{g_*} \ll 1$ and $\frac{\Delta}{m_*} \ll 1$. Due to the presence of the gauge boson mixing terms the following combination of the vector bosons will remain massless

$$\frac{g_*}{\sqrt{g_{el}^2 + g_*^2}} A_\mu + \frac{g_{el}}{\sqrt{g_{el}^2 + g_*^2}} \rho_\mu^*. \tag{2.10}$$

The original elementary and composite states will be re-written using the mass eigenstates as follows

$$\begin{pmatrix} A_\mu \\ \rho_\mu^* \end{pmatrix} \to \begin{pmatrix} \cos\theta & -\sin\theta \\ \sin\theta & \cos\theta \end{pmatrix} \begin{pmatrix} A_\mu \\ \rho_\mu^* \end{pmatrix}, \qquad \tan\theta = \frac{g_{el}}{g_*}, \tag{2.11}$$

$$\begin{pmatrix} \psi_L \\ \chi_L \end{pmatrix} \to \begin{pmatrix} \cos\varphi_{\psi_L} & -\sin\varphi_{\psi_L} \\ \sin\varphi_{\psi_L} & \cos\varphi_{\psi_L} \end{pmatrix} \begin{pmatrix} \psi_L \\ \chi_L \end{pmatrix}, \qquad \tan\varphi_{\psi_L} = \frac{\Delta}{m_*}, \tag{2.12}$$

$$\begin{pmatrix} \tilde{\psi}_R \\ \tilde{\chi}_R \end{pmatrix} \to \begin{pmatrix} \cos\varphi_{\tilde{\psi}_R} & -\sin\varphi_{\tilde{\psi}_R} \\ \sin\varphi_{\tilde{\psi}_R} & \cos\varphi_{\tilde{\psi}_R} \end{pmatrix} \begin{pmatrix} \tilde{\psi}_R \\ \tilde{\chi}_R \end{pmatrix}, \qquad \tan\varphi_{\tilde{\psi}_R} = \frac{\tilde{\Delta}}{\tilde{m}_*}. \tag{2.13}$$

In the new, i.e., mass eigenstate basis, $(A_\mu, \psi_L, \tilde{\psi}_R)$ are the SM fields, which are massless *before* EWSB, and $(\rho_*^\mu, \chi_L, \tilde{\chi}_R)$ are the heavy mass eigenstates (i.e. the heavy partners of SM), again prior to EWSB. To shorten our notations we will denote

$$\theta \equiv \theta_1, \theta_2, \theta_3, \quad \varphi_{\psi_L} \equiv \varphi_{q_{Li}}, \varphi_{l_{Li}}, \quad \varphi_{\tilde{\psi}_R} \equiv \varphi_{u_{Ri}}, \varphi_{d_{Ri}}, \varphi_{\nu_{Ri}}, \varphi_{e_{Ri}}$$

$$\sin\varphi_{u_R^i} \equiv s_u, \quad \sin\varphi_{d_R^i} \equiv s_d, \quad \sin\varphi_{q_{Li}} \equiv s_q. \tag{2.14}$$

2.1.2 Couplings in mass eigenstates before EWSB

Substituting Eq. (2.11) (2.12) (2.13) in Eq. (2.8), we get the Lagrangian for the Yukawa interaction between quarks and Higgs field in mass eigenstates before EWSB (the same expression will be true for leptons too, one just has to substitute $L, E, N \Longleftrightarrow Q, D, U$)

$$\begin{aligned}
\mathcal{L}_Y = \quad & \mathcal{L}_Y^{\text{SM-SM}} + \mathcal{L}_Y^{\text{SM-Heavy}} + \mathcal{L}_Y^{\text{Heavy-Heavy}} \\
= \quad & -Y_{*u}\tilde{H} s_q s_u \bar{q}_L u_R - Y_{*d} H s_q s_d \bar{q}_L d_R \\
& -Y_{*u}\tilde{H}\left[c_q s_u \bar{Q}_L u_R + s_q c_u \bar{q}_L \tilde{U}_R\right] - Y_{*d} H\left[c_q s_d \bar{Q}_L d_R + s_q c_d \bar{q}_L \tilde{D}_R\right] \\
& -Y_{*u}\tilde{H}\left[c_q c_u \bar{Q}_L \tilde{U}_R + \bar{Q}_R \tilde{U}_L\right] - Y_{*d} H\left[c_q c_d \bar{Q}_L \tilde{D}_R + \bar{Q}_R \tilde{D}_L\right] + \text{h.c.}
\end{aligned} \tag{2.15}$$

where $c_{q,u,d}$ stands for $\cos(\varphi_{q,u,d})$. We have split the Yukawa interactions into three parts, (SM-SM): interaction between two SM fermions, (SM-Heavy): interaction between SM fermion and heavy fermions, and (Heavy-Heavy): interaction between two heavy fermions.

Similarly interactions between fermions (including SM and heavy) and heavy partners of SM gauge bosons are

$$\begin{aligned}
& \mathcal{L} = \mathcal{L}^{\text{SM-SM}} + \mathcal{L}^{\text{SM-Heavy}} + \mathcal{L}^{\text{Heavy-Heavy}} \\
& = \rho_\mu^* g\left[\bar{q}_L \gamma_\mu q_L (-c_q^2 t + s_q^2 \frac{1}{t})\right] \\
& + \rho_\mu^* g\left[(\bar{q}_L \gamma_\mu Q_L + \bar{Q}_L \gamma_\mu q_L)(s_q c_q (1 + \frac{1}{t}))\right] \\
& + \rho_\mu^* g\left[\bar{Q}_L \gamma_\mu Q_L (c_q^2 \frac{1}{t} - s_q^2 t)\right] \\
& + \{L \leftrightarrow R\},
\end{aligned} \tag{2.16}$$

where $t \equiv \tan\theta$, and g is usual SM gauge coupling constant, and it is equal to $g = g_{el}\cos\theta = g_*\sin\theta$. In the same way as we have done for the Yukawa interactions we split total Lagrangian into three parts ((SM-SM), (SM-Heavy), (Heavy-Heavy)) . In the limit when all the SM fermions are made up of mostly elementary sector particles, i.e. $s_q \ll 1$, then the flavor non-universal interaction between SM quarks and heavy gauge bosons will be $\frac{gs_q^2}{\tan\theta} = g_* s_q^2 \cos\theta \approx g_* s_q^2$, and similarly for the right handed quarks.

The interactions between Higgs field, massless vector bosons and their heavy partners are

$$\begin{aligned}
\mathcal{L} \quad &= \mathcal{L}^{\text{SM-SM}} + \mathcal{L}^{\text{SM-Heavy}} + \mathcal{L}^{\text{Heavy-Heavy}} = |D_\mu H|^2 \\
&+ \left[H^\dagger i g \cot\theta \rho_\mu^* D_\mu H - i\frac{g_1}{2\sin\theta_1}\left(\frac{1}{\sqrt{2}}\tilde{H}^\dagger \tilde{W}_\mu^- D_\mu H + \frac{1}{\sqrt{2}} H^\dagger \tilde{W}_\mu^+ D_\mu \tilde{H} - \sqrt{\frac{3}{5}} H^\dagger \tilde{\mathcal{B}} D_\mu H \right) \right] \\
&+ \left[-g_1 g \frac{\cot\theta}{2\sin\theta_1}\left(\frac{1}{\sqrt{2}}\tilde{H}^\dagger \tilde{W}_\mu^- \rho_\mu^* H + \frac{1}{\sqrt{2}} H^\dagger \tilde{W}_\mu^+ \rho_\mu^* \tilde{H} - \sqrt{\frac{3}{5}} H^\dagger \tilde{\mathcal{B}} \rho_\mu^* H \right) \right. \\
&\left. + H^\dagger \left((g\cot\theta\rho_\mu^*)^2 + \frac{g_1^2}{\sin^2\theta_1}\left(\frac{1}{2}\tilde{W}_\mu^+ \tilde{W}_\mu^- + \frac{3}{20}\mathcal{B}_\mu^2\right) \right) H \right]
\end{aligned} \tag{2.17}$$

2.1.3 Including EWSB

Plugging in the Higgs vev in Eq. (2.15)(2.17) will lead to new mixings between SM massless fields and their heavy partners which can be classified in the same way as was done in Eq. (2.15),(2.16),(2.17): (SM-SM)- mixing between different generations of the SM massless fermions and the mixing between (W^3, B) SM gauge fields ; (SM-Heavy)- mixing between SM massless fermions and heavy fermions and the mixing between (B, W^3) SM gauge bosons and $(W_*^3, \mathcal{B}_*, \tilde{\mathcal{B}}_*, W_*)$ heavy vector bosons; (Heavy-Heavy)- mixing between the heavy fermions corresponding to the

different generations of SM and the mixing between $(W_*^3, \mathcal{B}_*, \tilde{\mathcal{B}}_*, W_*)$ heavy vector bosons. These mixings lead to many new contributions to flavor violating processes, which we will study in detail in later sections.

2.2 Matching 4D and 5D theories

As we have said in the beginning of this chapter two -site represents an effective description of the warped models so here we present a relations between parameters of the 4D and 5D theories

$$\begin{aligned} \text{light states} \quad &\leftrightarrow \text{zero modes} \\ \text{heavy states} \quad &\leftrightarrow \text{1st KK modes} \\ s_{q,u,d} \quad &\leftrightarrow f(c_{q,u,d}) \\ Y_* \quad &\leftrightarrow \text{coupling of the KK fermions to Higgs} \end{aligned} \tag{2.18}$$

so we can see that in the 4D theory which is an effective theory of RS with fermions in the bulk $s_{q,d,u}$ elementary/composite mixing angles should be hierarchical, and the Yukawa couplings should be of the same order.

2.3 $\Delta F = 2$ processes: ϵ_K

2.3.1 Formulae for Two-Site Model

We want to find the bound on composite sector scale from CP violation in the $\Delta S = 2$ process, i.e., ϵ_K parameter of the $K_0 - \bar{K}_0$ oscialltions . The most general effective Hamiltonian for $\Delta S = 2$ processes can be parameterized in the following

way [29]

$$H_{\Delta S=2} = C_1\mathcal{O}_1 + C_2\mathcal{O}_2 + C_3\mathcal{O}_3 + C_4\mathcal{O}_4 + C_5\mathcal{O}_5 \text{ with}$$

$$\mathcal{O}_1 = \bar{d}_L^\alpha \gamma_\mu s_L^\alpha \bar{d}_L^\beta \gamma_\mu s_L^\beta, \quad \mathcal{O}_2 = \bar{d}_R^\alpha s_L^\alpha \bar{d}_R^\beta s_L^\beta$$

$$\mathcal{O}_3 = \bar{d}_R^\alpha s_L^\beta \bar{d}_R^\beta s_L^\alpha, \quad \mathcal{O}_4 = \bar{d}_R^\alpha s_L^\alpha \bar{d}_L^\beta s_R^\beta, \quad \mathcal{O}_5 = \bar{d}_R^\alpha s_L^\beta \bar{d}_L^\beta s_R^\alpha, \tag{2.19}$$

where α, β are color indices. There are also $\mathcal{O}'_{1,\,2}$ operators with L replaced by R. The dominant contributions to these Wilson coefficients in the two-site model come from tree-level exchange of heavy gauge bosons for example gluon (see Fig. 2.1) with flavor violating couplings. These flavor violating couplings arise mainly from

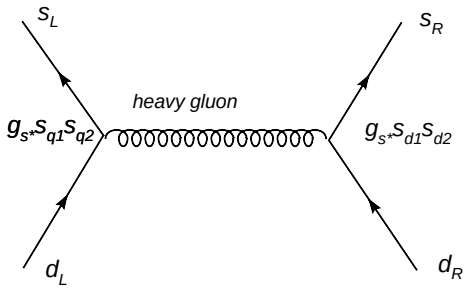

Figure 2.1: Contribution to the ϵ_k from KK gluon exchange

the mixings between SM fermions induced after EWSB (see section 2.1.3) which we now focus on – the other two types of mixings (SM-Heavy, Heavy-Heavy) have sub-leading effects for ϵ_K and so will be neglected for the analysis in this section.

The point is that the couplings between heavy gluon and SM quarks are diagonal but non-universal in the gauge eigenstate basis for quarks, i.e., before EWSB, in $\mathcal{L}^{\text{SM-SM}}$ term of Eq. (2.16). After EWSB, one has to use unitary transformations: $(O_{D_L},\, O_{D_R})$ and $(O_{U_L},\, O_{U_R})$ to go to mass eigenstate basis for down and

up-type quarks respectively (just like in the SM). These rotations thus lead to off-diagonal couplings between SM quarks (in mass eigenstate basis) and heavy gluon. From the analysis of the $5D$ models [11, 12, 13], it is well-known that the dominant contribution comes from the heavy/KK gluon exchange between left-handed and right-handed down-type quark currents, i.e., $(V-A)\times(V+A)$-type operators. Therefore, we focus here on heavy gluon exchange of the above type. The main contribution comes from the different amount of composite components of SM quarks. We assume here that $s_{q,d1} \ll s_{q,d2} \ll s_{q,d3} \ll 1$ and $O_{D_{L,R}}$ are nearly diagonal, since we need hierarchical elementary/composite mixings to reproduce hierarchical quark masses. It is straightforward to show that such exchange gives (upon Fierzing)

$$\begin{aligned} C_4(M_*) &= -3C_5(M_*) \\ &\approx \frac{(g_{s*})^2}{M_*^2}\left[(s_{q2})^2 (O_{D_L})_{12} + (s_{q3})^2 (O_{D_L})_{13} (O_{D_L})_{23}\right] \times \\ &\quad \left[(s_{d2})^2 (O_{D_R})_{12} + (s_{d3})^2 (O_{D_R})_{13} (O_{D_R})_{23}\right]^* \end{aligned} \tag{2.20}$$

where g_{s*} is composite QCD coupling. Each $\Big[...\Big]$ in this formula includes two terms, i.e., one from the "direct" $1-2$ mixing (present even with two generations) and another from the $(1-3)\times(2-3)$ mixing (i.e., via 3rd generation) for the left and right-handed flavor-violating couplings.

Assumption of anarchic Yukawa couplings Y_* in the original Lagrangian of Eq. (2.15) implies that mixing angles in SM Yukawa couplings are given by ratios of elementary-composite mixings[6] (see Eq.(58)), for example,

$$\left(O_{D_{L,R}}\right)_{ij} \sim \frac{(s_{q,d})_i}{(s_{q,d})_j} \text{ for } i<j \tag{2.21}$$

So, the two terms (inside each of the brackets $\Big[...\Big]$) in Eq. (2.20) (for each of left and right-handed sectors) are of same size, but uncorrelated.

On the other hand from the $\mathcal{L}_Y^{\text{SM-SM}}$ term of Eq. (2.15) we have

$$m_d \sim Y_*^d s_{q1} s_{d1} v/\sqrt{2} \tag{2.22}$$
$$m_s \sim Y_*^d s_{q2} s_{d2} v/\sqrt{2},$$

so we can estimate the size of the mixing angles s_{qi}, s_{di}.

Now we can estimate new physics contribution to $C_{4,\,5}$ using the following assumptions: (i) considering one term in each of the brackets $\Big[...\Big]$ of Eq. (2.20) at a time, (ii) mixing angles set to "natural" size (i.e., with "=" in Eq.(2.21) above), and (iii) quark masses given by natural size of the parameters (i.e., with "=" in Eq.(2.22) above). Plugging Eq. (2.21) and (2.22) into Eq. (2.20) leads to the estimate, up to an $O(1)$ complex factor:

$$C_4^{2-\text{site}}{}_{\text{ estimate}} \;=\; \frac{g_{s*}^2}{(Y_*^d)^2}\frac{2m_s m_d}{v^2}\frac{1}{M_*^2} \tag{2.23}$$

with $v = 246$ GeV, where subscript "estimate" stands for the above three assumptions. To repeat, the assumption of anarchy tells us that the four terms in Eq. (2.20) are of the same size as Eq. (2.23) and have *un*correlated phases. Therefore, our estimate using one term gives us the correct result up to $O(1)$ factor.

2.3.2 Experimental limit

The model independent bound from ϵ_K is strongest on the Wilson coefficient C_4 due to (i) enhancement (as compared to for the other Wilson coefficients) from

RG scaling from the new physics scale to the hadronic scale and (ii) from chiral enhancement of matrix element (see reference [21]).[2] This bound on C_4 is :

$$\mathrm{Im}\, C_4 \lesssim \frac{1}{(\Lambda_F)^2}, \qquad \Lambda_F = 1.6 \times 10^5\, \mathrm{TeV}. \tag{2.24}$$

where the coefficient is renormalized at the ~ 3 TeV scale [11]. Note that the bound on Im C_4 is only mildly (logarithmically) sensitive to the renormalization scale and hence it remains almost the same as the above number (which is again for a scale of ~ 3 TeV) for heavy mass scales of up to ~ 10 TeV that we will consider in this paper. Using Eqs. (2.23) and (2.24), and assuming order one phase, we get

$$M_* \gtrsim \frac{11 g_{s*}}{Y^d_*}\ \mathrm{TeV} \tag{2.25}$$

We can see the bound on the composite mass scale *decreases* as Y^d_* increases.

2.4 Radiative processes: $b \to s\gamma$

The rare decay $B \to X_s\gamma$ gives very powerful constraints on new physics. We follow the standard notation and define the effective Hamiltonian for $b \to s\gamma$ [29]:

$$\mathcal{H}_{eff}(b \to s\gamma) = -\frac{G_F}{\sqrt{2}} V^*_{ts} V_{tb} [C_7(\mu_b) Q_7 + C'_7(\mu_b) Q'_7 + \ldots] \tag{2.26}$$

where $Q_7 = e\ m_b/\,(8\pi^2)\,\bar{b}\sigma^{\mu\nu} F_{\mu\nu}(1-\gamma_5)s$ and $Q'_7 = m_b\ e\,(8\pi^2)\,\bar{b}\sigma^{\mu\nu} F_{\mu\nu}(1+\gamma_5)s$. Here we have neglected other operators that only enter through renormalization of

[2] The effect of C_5 (M_*) in the two-site model is sub-leading because firstly the model-independent bound is weaker relative to C_4 (see reference [21]) and secondly in this model C_5 (M_*) is suppressed by a color factor relative to C_4 (see Eq. 2.20).

C_7 and C_7'. In SM, the Wilson coefficient $C_7(\mu_w)$ evaluated at weak scale is[29]

$$\begin{aligned} C_7^{SM}(\mu_w) &= -\frac{1}{2}\left[-\frac{(8x_t^3+5x_t^2-7x_t)}{12(1-x_t)^3}+\frac{x_t^2(2-3x_t)}{2(1-x_t)^4}\ln(x_t)\right]; \\ C_7'^{SM}(\mu_w) &= \frac{m_s}{m_b}C_7^{SM}(\mu_w) \end{aligned} \tag{2.27}$$

with $x_t = m_t^2/M_w^2$. The Wilson coefficient $C_7'(\mu_w)$ can be neglected in SM due to a suppression by m_s/m_b. The leading order QCD correction gives us [29]

$$\begin{aligned} C_7(\mu_b) &= 0.695C_7(\mu_w)+0.085C_8(\mu_w)-0.158C_2(\mu_w) \\ &= 0.695(-0.193)+0.085(-0.096)-0.158 = -0.300 \end{aligned} \tag{2.28}$$

where C_2 and C_8 are Wilson coefficients for operators $Q_2 \equiv (\bar{c}b)_{V-A}(\bar{s}c)_{V-A}$ and $Q_{8G} \equiv$

$m_b\ g/\left(8\pi^2\right)\bar{b}_\alpha\sigma^{\mu\nu}(1-\gamma_5)T^a_{\alpha\beta}s_\beta G^a_{\mu\nu}$. The latest higher order calculations for BR($b \longrightarrow s\gamma$) are given in [30] but the above order results suffice for our purposes.

2.4.1 Estimate in two-site model

In two-site model, the largest new physics contribution to $\Gamma(b \to s\gamma)$ comes from diagrams with heavy states in the loop because of their larger coupling constants. First, we consider diagrams with heavy gluons and fermions (see Fig. 2.2). We can get an idea of the flavor structure of this diagram by treating the EWSB-induced fermion mass terms of Eq. (2.15) as being small compared to the masses of the heavy partners of SM fermions (henceforth called by the mass insertion approximation). From $\mathcal{L}^{\text{SM-Heavy}}$ term of Eq. (2.16), we see that mass insertion approximation gives us a new contribution to Wilson coefficients of operators $\bar{d}_j\sigma^{\mu\nu}F_{\mu\nu}(1-\gamma_5)d_i$

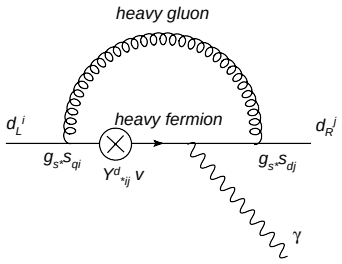

Figure 2.2: Contribution to the $b \to s\gamma$ from the loop with KK fermion anf KK gluon

(with quarks in gauge basis before EWSB)

$$C^G_{7\,ij} \propto s_{q_i} g^2_{s*} Y^d_{*ij} s_{d_j} \tag{2.29}$$

Notice that $C^G_{7\,ij}$ has the same flavor structure as quark mass matrix $m_{d\,ij} \approx Y^d_{*ij} s_{q_i} s_{d_j}$. Therefore, after unitary rotation into the mass eigenstates after EWSB, $C^G_{7\,ij}$ will be approximately diagonal in flavor space, and contribution from heavy gluon and heavy fermion exchange to $\Gamma(b \to s\gamma)$ is suppressed. (see reference [6] for a similar discussion in warped extra dimension, where KK gluons and KK fermions correspond to heavy gluons and fermions here.)

Next, we consider diagrams with heavy fermions and Higgs in the loop (including physical Higgs and longitudinal W/Z bosons). Similar to the previous analysis, we can get the flavor structure of these diagrams from mass insertion approximation. For the purpose of estimating flavor structure, we consider only neutral Higgs diagram (see Fig. 2.3). From the Yukawa couplings between SM fermion, heavy fermion and Higgs ($\mathcal{L}^{\text{SM-Heavy}}$ term of Eq. 2.15), we find that

$$C^H_{7\,ij} \propto s_{q_i} Y^d_{*ik} Y^d_{*kl} Y^d_{*lj} s_{d_j} \tag{2.30}$$

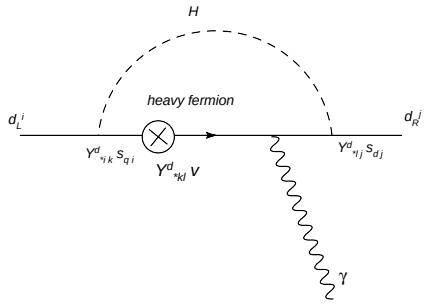

Figure 2.3: Contribution to the $b \to s\gamma$ from the loop with KK fermion and Higgs

It is obvious that $C^H_{7\,ij}$ is not aligned with $m_{d\,ij}$, assuming no particular structure in the Y_* (i.e., anarchy). Thus these diagrams will give the leading new contribution to C_7 and C'_7, and we will focus on these diagrams (see reference [6] for a similar discussion in warped extra dimension).

Because of the near degeneracy of heavy fermion masses, we can*not* use mass insertion approximation to *calculate* the loop diagrams. Instead, we need to diagonalize the 9×9 mass matrix (once we include EWSB-induced mass terms, i.e., coming from Yukawa couplings in Eq. (2.15)) for all down type quarks in order to determine the mass eigenstates and their couplings. Since it is difficult to obtain an exact analytical formulae for this effect, the analysis is performed numerically in Section 2.6. However, it is insightful to obtain an approximate analytical formulae for $b \to s\gamma$ as follows. First, we calculate the dipole operator for the case of *one* generation quark together with its heavy partners (say, as in the calculation of $(g-2)_\mu$)) with*out* using the mass insertion approximation and then we simply multiply it by factors from generational mixing effects in order to obtain the amplitude for $b \to s\gamma$.

In more detail, we diagonalize the 3×3 mass matrix (including the EWSB-

induced mass terms) for one generation quarks analytically to first order in $x \equiv Y_*^{u,d} v / \left(m_* \sqrt{2}\right)$ in Appendix B.3: the results for dipole moment operator of one generation with charged and neutral Higgs in the loop are shown in Eqs. (B.39) and (B.43). In order to *estimate* the effect of mixing between different generations, we again use mass insertion approximation (see Fig. 2.3). For example, the operator $\bar{b}_L \sigma^{\mu\nu} F_{\mu\nu} s_R$ can be generated via the mass insertions/Yukawa couplings (as in Eq. 2.30, but dropping the flavor indices on Y_{d*} for simplicity)

$$Y_{d*} s_{q3} Y_{d*} v Y_{d*} s_{d2} \tag{2.31}$$

Based on our assumption of anarchy and the formulae for Yukawa couplings and mixing angles (Eq. (2.15) (2.21)), we know that

$$Y_{d*} v s_{q3} s_{d2} = Y_{d*} v s_{q3} s_{d3} \frac{s_{d2}}{s_{d3}} \sim m_b (O_{D_R})_{23} \tag{2.32}$$

and

$$\frac{m_s}{m_b} \sim (O_{D_L})_{23} (O_{D_R})_{23} \tag{2.33}$$

In addition, since left-handed down and up-type quarks have the same elementary-composite mixing, we get (again assuming anarchy of Y_{d*})

$$\begin{aligned} (D_L)_{23} &\sim (U_L)_{23} \\ &\sim V_{ts} \text{ or } V_{cb} \end{aligned} \tag{2.34}$$

where in the second line we have used that $V_{CKM} = O_{U_L}^\dagger O_{D_L}$. Combining Eq (2.31) through (2.34), we can find that generational mixing gives a factor $\sim \frac{m_s}{m_b V_{ts}}$. Similarly, for the operator $\bar{b}_R \sigma^{\mu\nu} F_{\mu\nu} s_L$ we have (as in Eq. 2.30)

$$Y_{d*} s_{d3} Y_{d*} v Y_{d*} s_{q2} \sim (Y_{d*})^2 m_b (O_{D_L})_{23} \sim (Y_{d*})^2 m_b V_{ts} \tag{2.35}$$

i.e., generational mixing gives a factor $\sim V_{ts}$. Note that for neutral Higgs diagram the amplitude is proportional to Y_{d*}^3. The flavor structure for *charged* Higgs (would-be Goldstone) diagram is similar, expect that there are two types of contributions (schematically $\propto Y_{d*}^3$ and $Y_{u*}^2 Y_{d*}$). For simplicity, we set $Y_{u*} = Y_{d*} \equiv Y_*$ in our estimation.

Then, multiplying the one generation results for dipole operator in Eqs. (B.39) and (B.43) by the above generational mixing factors, we get the following effective Hamiltonians:

$$\mathcal{H}^{eff}_{\text{charged Higgs}} \approx \frac{5}{12}(Y_*)^2 m_b \frac{ie}{16\pi^2}\frac{(2\epsilon\cdot p)}{(m_*)^2}[V_{ts}\bar{b}(1-\gamma_5)s + \frac{m_s}{m_b V_{ts}}\bar{b}(1+\gamma_5)s] \quad (2.36)$$

$$\mathcal{H}^{eff}_{\text{neutral Higgs}} \approx -\frac{1}{4}(Y_*)^2 m_b \frac{ie}{16\pi^2}\frac{(2\epsilon\cdot p)}{(m_*)^2}[V_{ts}\bar{b}(1-\gamma_5)s + \frac{m_s}{m_b V_{ts}}\bar{b}(1+\gamma_5)s] \quad (2.37)$$

We present the results for both charged Higgs and neutral Higgs contribution since they generally have different phase and cannot be simply added together. Since their sizes are of the same order, we will *focus just on charged Higgs contribution in the analytical estimates*. Then, the new physics contribution to the Wilson coefficients are[3]

$$\begin{aligned} C_{7\,\text{estimate}}^{2-\text{site}}(m_*) &= -\frac{5}{48}\frac{(Y_*)^2}{(m_*)^2}\frac{\sqrt{2}}{G_F} \\ C'^{\,2-\text{site}}_{7\,\text{estimate}}(m_*) &= -\frac{5}{48}\frac{(Y_*)^2}{(m_*)^2}\frac{\sqrt{2}}{G_F}\frac{m_s}{m_b\lambda^4} \end{aligned} \quad (2.38)$$

where we used $V_{ts} \sim \lambda^2$ ($\lambda \approx 0.22$). As explained earlier, (based on assumption of

[3]Note that such a size for these Wilson coefficients can be *estimated*, i.e., derived up to $O(1)$ factors, using *purely* mass insertion approximation. As explained above, here instead we have *calculated* the $O(1)$ factor from loop diagram (with*out* using mass insertion approximation), although we still used mass insertion approximation to estimate the generational mixing factors.

anarchy) in the exact result for $b \to s\gamma$ there will be several terms of the above order but with uncorrelated phases. Thus Eq. (2.38) is only an *estimate* for $b \to s\gamma$, i.e., the natural size of *one* term that contribute to the new physics effective Hamiltonian. We expect the final result of the coherent sum of such terms to be of the same order as this one-term estimates. From these estimates we can conclude that $C_7'^{2-\text{site}}(m_*)$ is bigger than $C_7^{2-\text{site}}(m_*)$ by a factor of $m_s/\left(m_b V_{ts}^2\right) \sim 8$, which is different than the case in SM (where $C_7' \approx C_7\, m_s/m_b$).

As mentioned earlier, in Section 2.6, we will apply the exact diagonalization of the 9×9 mass matrix for three generations to the results from general loop calculation of $b \to s\gamma$ in Appendix B.2 to obtain $C_7^{2-\text{site}}$ and $C_7'^{2-\text{site}}$ numerically.

2.4.2 Experimental limit

The leading order QCD corrections will suppress the new physics contribution to the Wilson coefficients

$$C_7^{2-\text{site}}(\mu_w) = \left[\frac{\alpha_s(m_*)}{\alpha_s(m_t)}\right]^{16/21} \left[\frac{\alpha_s(m_t)}{\alpha_s(\mu_w)}\right]^{16/23} C_7^{2-\text{site}}(m_*) \approx 0.73\; C_7^{2-\text{site}}(m_*) \quad (2.39)$$

We add it to $C_7^{\text{SM}}(\mu_w)$ in Eq. (2.27) and then use this sum, i.e., $C_7^{\text{total}}(\mu_w) = C_7^{\text{SM}}(\mu_w) + C_7^{2-\text{site}}(\mu_w)$ in Eq. (2.28) to obtain $C_7(\mu_b)$. Whereas, the SM contribution to C_7' is negligible compared to that in the two-site model so that we have

$$\begin{aligned} C_7'^{\text{total}}(\mu_b) &\approx C_7'^{2-\text{site}}(\mu_b) \\ &= \left[\frac{\alpha_s(m_*)}{\alpha_s(m_t)}\right]^{16/21} \left[\frac{\alpha_s(m_t)}{\alpha_s(\mu_b)}\right]^{16/23} C_7'^{2-\text{site}}(m_*) \\ &\approx 0.48\; C_7'^{2-\text{site}}(m_*) \end{aligned} \quad (2.40)$$

The contributions from $C_7(\mu_b)$ and $C_7'(\mu_b)$ sum incoherently (without interference) in the total (i.e., SM and new physics) decay width $\Gamma^{\rm total}(b \to s\gamma)$:

$$\Gamma^{\rm total}(b \to s\gamma) \propto |C_7(\mu_b)|^2 + |C_7'(\mu_b)|^2 \tag{2.41}$$

For convenience, we define $\delta_7 \equiv C_7^{2-\rm site}(m_*)/C_7^{SM}(\mu_w)$ and $\delta_7' \equiv C_7'^{2-\rm site}(m_*)/C_7^{SM}(\mu_w)$. Adding these new contributions, we have

$$\frac{\Gamma^{\rm total}(b \to s\gamma)}{\Gamma^{SM}(b \to s\gamma)} \approx 1 + 0.68 Re(\delta_7) + 0.11|\delta_7'|^2 \tag{2.42}$$

The experimental average value for the branching ratio is $BR(b \to s\gamma) = (352 \pm 23 \pm 9) \times 10^{-6}$[31]. The theoretical calculation gives $BR(b \to s\gamma) = (315 \pm 23) \times 10^{-6}$[32]. Adding the 2σ uncertainties by quadrature we find that a 20% deviation from SM prediction is allowed. If we consider the two contributions separately, we will get the bound $|\delta_7'| \lesssim 1.4$ and $\mathrm{Re}(\delta_7) \lesssim 0.3$. Using Eqs. (2.38) and (2.27), the first condition gives

$$m_* \gtrsim (0.63) Y_* \ \mathrm{TeV} \tag{2.43}$$

and the second condition gives us a weaker bound. From this rough estimate, we can see the bound on composite mass scale *increases* with composite Yukawa coupling.

2.4.3 Tension and lowest heavy SM partner mass scale scenario

We see that the bounds on M_* and m_* from ϵ_K and $\mathrm{BR}(b \to s\gamma)$ have opposite dependence on Y_*. Thus we cannot use this parameter to decouple flavor-violation. *For simplicity, we set $M_* = m_*$ henceforth.* Then the lowest allowed value for M_*

that satisfies both bounds Eqs.(2.25) and (2.43) is

$$\begin{aligned} M_* &\gtrsim 2.6\sqrt{g_{s*}}\ \text{TeV} \quad \text{for} \quad Y_* \sim 4.2\sqrt{g_{s*}} \\ &\sim 4.5\ \text{TeV for}\ g_{s*} \sim 3 \\ &\sim 6.4\ \text{TeV for}\ g_{s*} \sim 6 \end{aligned} \tag{2.44}$$

where in last two lines, we have set $g_{s*} \sim 3, 6$ which is motivated by the $5D$ AdS model, although the latter value might not be allowed by $5D$ perturbativity. We can check that with the values of Y_* in Eq. (2.44), the loop expansion parameter $Y_*^2/(16\pi^2)$ is less than one, and the two-site model is thus perturbative (but barely so in the case of $Y_* \sim 10$ for $g_{s*} \sim 6$): see Appendix B.1.3 about perturbativity bound on KK Yukawa couplings in the $5D$ AdS model.

We reiterate that the bounds in Eq. (2.44) are only *estimates* in the sense that they are based on *one* among multiple, *uncorrelated* terms in the amplitudes for both ϵ_K and $b \to s\gamma$. Also, note that the contributions to $b \to s\gamma$ in the two-site model, being at the loop-level (as opposed to the tree-level contributions to ϵ_K), can be quite sensitive to the composite sector content – for example, as mentioned in section 2.1, we could add $SU(2)_R$ partners for the composite site u_R and d_R (as in $5D$ models) which can easily modify the new physics amplitude for $b \to s\gamma$ by $\sim O(1)$ factors due to their appearance in the loops. In this sense, the constraints from $b \to s\gamma$ presented for this model should especially be considered as a ballpark guide to the viable parameter space of this framework: the main motivation for using $b \to s\gamma$ in our analysis is to put an upper bound on the composite site Yukawa coupling.

As discussed in references [6, 33] for the $5D$ model, the Higgs-heavy fermion loop contributions to electric dipole moments (EDMs) of SM fermions also increase with the size of the composite Yukawa coupling (just like $b \to s\gamma$). Thus, EDMs can also be used to put an upper bound on the size of this coupling (for a given heavy mass scale). However, EDMs depend on a different (flavor-*preserving*) combination of phases than the flavor-violating observables ϵ_K and $b \to s\gamma$ and so we will leave a study of these constraints for the future. Note that $5D$ flavor symmetries can suppress EDM's as well as the flavor violating effects.

2.5 Correction to $Zb\bar{b}$ coupling

There is another important constraint coming from non-universal correction to $Zb_L\bar{b}_L$ coupling which arises from mixing between SM and heavy states after EWSB (see [10])

$$\frac{\delta g_{Z\bar{b}b}}{g_{Z\bar{b}b}} \approx \sum_{i=1}^{3} \left(\frac{Y_{*di3}}{Y_{*u33}}\right)^2 \left(\frac{m_t}{M_* s_{u3}}\right)^2 + \frac{1}{2}\left(\frac{m_t}{M_* s_{u3}}\right)^2 \left(\frac{g_{*2}}{Y_{*U33}}\right)^2 \tag{2.45}$$

Experimentally, it is measured to have less than 0.25% deviation from its SM value. If we assume that all composite Yukawa couplings are of the same order, then we can get a bound on M_* from the first term alone:

$$M_* \gtrsim 4.7 \quad \text{TeV} \tag{2.46}$$

This bound is similar to what we found from ϵ_K and $b \to s\gamma$. However, if we allow a little hierarchy between the Yukawa couplings, e.g., $Y_{*d} > Y_{*u}$, then the bound on

M_* will be enhanced. We mention that $Z\bar{b}_L b_L$ coupling can be protected by another custodial symmetry [34]. But we will not use this idea here.

2.6 Numerical Analysis

In previous sections we presented semi-analytical *estimates* for the new physics contributions to the ϵ_K and $b \to s\gamma$ processes, but to get the precise values one has to perform a numerical scan over the parameter space. The scan procedure is discussed in detail in Appendix B.4. Here we summarize some important features and results of our scan. We require that our composite Yukawa coupling matrices are anarchical, i.e. all entries of the same order, with the results presented here corresponding to the variation of the Yukawa couplings by a factor of three, and we varied the elementary/composite mixings also by a factor of three. First, we generate the points in parameter space with $Y_{u*}, Y_{d*}, s_Q, s_u, s_d$ such that the SM quark masses and CKM mixing angles are reproduced. Then we calculated $|\frac{\Gamma^{\rm total}(b\to s\gamma)}{\Gamma^{\rm SM}(b\to s\gamma)} - 1|/(20\%)$, $|\delta g_{Z\bar{b}b}/g_{Z\bar{b}b}|$ and $\mathrm{Im}\, C_{4K}\Lambda_F^2$ (with $\Lambda_F = 1.6\times 10^5$ TeV) for different values of M_* and $Y_*^{u,d}$.

In Fig. *B*.2, we show the plots of $|\frac{\Gamma^{\rm total}(b\to s\gamma)}{\Gamma^{\rm SM}(b\to s\gamma)} - 1|/(20\%)$ and $\mathrm{Im}\, C_{4K}\Lambda_F^2$ for $M_* = 5$ TeV and different values of $Y_*^{u,d}$ (defined here as the geometric *average* value for $Y_{*ij}^{u,d}$). We focus on the case with $g_{s*} = 3$. Points to the left and below the solid lines satisfy both bounds from BR $(b \to s\gamma)$ and ϵ_K. We begin with the cases with no hierarchy between the up and down-type quark composite site Yukawa coupling, i.e., $Y_*^d = Y_*^u$. In the top left plot, we choose this value to be $\in (3, 4)$.

We see that a small fraction of points satisfy the bounds from ϵ_K and BR $(b \to s\gamma)$. Next we increase the common value for Y_*^d and Y_*^u to $(6, 7)$ (top right plot). We expect that the larger Yukawa coupling will enhance the contribution to $\Gamma(b \to s\gamma)$ and suppress the contribution to $\mathrm{Im}\, C_{4K}$, which is clearly shown in the plots and illustrates the tension discussed in section 2.4.3. In the end, there are fewer points satisfying both bounds with these larger Yukawa couplings.

Finally, we consider a mild hierarchy between the Yukawa couplings: $Y_*^u \in (1, 2)$ and $Y_*^d \in (5, 6)$ (bottom plot). We find that more points satisfy both bounds than in the previous two cases. This is expected since small Y_*^u suppresses one of the contributions to $\Gamma(b \to s\gamma)$[4] while larger Y_*^d suppresses contribution to $\mathrm{Im}\, C_{4K}$. However, the bound from non-universal $Z\bar{b}_L b_L$ coupling correction is more constrained in this case due to the $(\frac{Y_*^{di3}}{Y_*^{u33}})^2$ enhancement in $\delta g_{Z\bar{b}_L b_L}$ (see Eq. (2.45)) so that we have to study the consequence of this bound. In Fig. $B.3$, we present the result from the scan for $\mathrm{Im}\, C_{4K}$ and $\delta g_{Z\bar{b_L} b_L}$. We can see that when $Y_*^d = 5 \sim 6$ and $Y_*^u = 1 \sim 2$ (right plot) the $\delta g_{Z\bar{b_L} b_L}$ bound eliminates a majority of the points. However, for $Y_*^u = Y_*^d \in (3, 4)$ (left plot), the bound on $\delta g_{Z\bar{b_L} b_L}$ is easily satisfied, as expected from our analysis in Section 2.5.

We show the same scatter plots for $M_* = 10\,\mathrm{TeV}$ (Fig. B.4, B.5) and $M_* = 3\,\mathrm{TeV}$ (Fig. B.6, B.7). As it is clearly shown in the plots, all bounds can be easily satisfied for $M_* = 10\,\mathrm{TeV}$, while almost no point satisfy all bounds for $M_* = 3\,\mathrm{TeV}$. Note that, with our choices of Y_*, higher-order loop diagrams with these couplings will give us corrections to all our observables of $\sim Y_*^2/\left(16\pi^2\right) \sim O\left(1/\text{a few}\right) - 1/10$,

[4]There is also a contribution $\propto Y_d$ only as discussed in section 2.4.1.

which is the main source of error in our analysis.

Now we consider the case with a larger composite site gluon coupling, i.e., $g_{s*} = 6$. The contribution in the two-site model to $\Gamma(b \to s\gamma)$ is the same as in the case $g_{s*} = 3$ while $\mathrm{Im}\, C_{4K}$ increases by a factor of 4. Thus, rather than showing separate plots for $g_{s*} = 6$, we can present the *bounds* for this case on the same plots as for $g_{s*} = 3$ by just moving the line from the $\mathrm{Im}\, C_{4K}$ bound downward by factor of 4. So all the points satisfying both constraints for $g_{s*} = 6$ are below the *dashed* line and to the left of the solid line in the same plots. As expected, for $g_{s*} = 6$, few (a sizable fraction of) points satisfy the bounds for $M_* = 5(10)$ TeV.

Combining the results of the numerical analysis shown in the plots with our earlier estimate in Eqs. (2.44) and (2.46) of ~ 4.5 TeV as the lowest heavy SM partner mass scale allowed, we then conclude M_* as low as $\sim O(5)$ TeV with $g_* \sim 3$ can satisfy all the constraints we considered.

2.7 Summary

In this chapter we analyzed bounds from $b \to s\gamma$ decays and ϵ_K parameter of $K_0 - \bar{K}_0$ oscillations. We have shown that constraints from these two processes have opposite dependence on the parameter Y_*. We have shown that the combined bound on the mass of the lightest spin one new physics resonance is $O(5)$ TeV, and argued (see for details Appendix B.1.1) that the bounds from ϵ_K are relaxed, when Higgs becomes bulk field, and this effect is reflected in two site model.

Chapter 3

Higgs mediated flavor violation

3.1 Flavor misalignment estimate

In this chapter I will discuss modifications of the interactions between SM fermions and the Higgs field, which appear after integrating out all the KK states, and generically lead to the flavor violation. From an effective field theory approach it is easy to write the lowest order operators responsible for generating a misalignment in flavor space between the Higgs Yukawa couplings and the SM fermion masses. For simplicity we focus on the down quark sector and write the following dimension 6 operators of the 4D effective Lagrangian [17, 35, 36, 37, 38]

$$\lambda_{ij}\frac{H^2}{\Lambda^2}\, H\overline{Q}_{L_i}D_{R_j}, \quad k^D_{ij}\frac{H^2}{\Lambda^2}\,\overline{D}_{R_i}\partial\!\!\!/ D_{R_j} \quad \text{and} \quad k^Q_{ij}\frac{H^2}{\Lambda^2}\,\overline{Q}_{L_i}\partial\!\!\!/ Q_{L_j}, \tag{3.1}$$

where Q_{L_i} and D_{R_j} are the fermionic $SU(2)$ doublets and singlets of the SM, with λ_{ij}, k^D_{ij} and k^Q_{ij} being complex coefficients and i, j are flavor indices; Λ is the cut-off or the threshold scale of the effective Lagrangian. Upon electroweak symmetry breaking (EWSB), these operators will give a correction to the fermion kinetic terms and to the fermion mass terms. Calling y_{ij} the original Yukawa couplings, the corrected fermion mass and kinetic terms become:

$$v_4\left(y_{ij}+\lambda_{ij}\tfrac{v_4^2}{\Lambda^2}\right)\overline{Q}_{L_i}D_{R_j}, \quad \left(\delta_{ij}/2+k^D_{ij}\tfrac{v_4^2}{\Lambda^2}\right)\overline{D}_{R_i}\partial\!\!\!/ D_{R_j}$$
$$\text{and}\left(\delta_{ij}/2+k^Q_{ij}\tfrac{v_4^2}{\Lambda^2}\right)\overline{Q}_{L_i}\partial\!\!\!/ Q_{L_j}, \tag{3.2}$$

where $v_4 = 174$ GeV is the Higgs electroweak *vev*, i.e. $H = h/\sqrt{2} + v_4$, with h being the physical Higgs scalar. On the other hand, the induced operators involving two fermions and one physical Higgs h become:

$$\left(y_{ij} + 3\lambda_{ij}\frac{v_4^2}{\Lambda^2}\right)\frac{h}{\sqrt{2}}\overline{Q}_{L_i}D_{R_j}, \qquad \left(2k_{ij}^{D}\frac{v}{\Lambda^2}\right)\frac{h}{\sqrt{2}}\overline{D}_{R_i}\partial\!\!\!/ D_{R_j}$$
$$\text{and} \qquad \left(2k_{ij}^{Q}\frac{v_4}{\Lambda^2}\right)\frac{h}{\sqrt{2}}\overline{Q}_{L_i}\partial\!\!\!/ Q_{L_j}. \tag{3.3}$$

From Eq.(3.2) it is clear that one has to redefine the fermion fields to canonically normalize the new kinetic terms and then perform a bi-unitary transformation to diagonalize the resulting mass matrix. These fermion redefinitions and rotations will not in general diagonalize the couplings from Eq. (3.3) and therefore, we will obtain tree-level flavor changing Higgs couplings, with a generic size controlled by $\frac{v^2}{\Lambda^2}$.

Before doing the calculation in the warped model let us see what will be the two-site estimate of this process. For simplicity let us start with the calculation for the one family of the fermions. Corrections to the mass and to the Yukawa coupling will arise from the following diagrams (Fig. 3.1-3.2) The diagram with three Higgs insertions (Fig. 3.1) will give the following contribution to the mass

$$m \sim Y_* v s_q s_d + \frac{Y_*^3 v^3 s_q s_d}{M_*^2}, \tag{3.4}$$

and the diagram with two higgs insertions (3.2) will lead to the correction of the kinetic term SM quark fields

$$\bar{Q}\partial\!\!\!/ Q\left(1 + \frac{Y_*^2 v^2 s_q^2}{M_*^2}\right) + \bar{D}\partial\!\!\!/ D\left(1 + \frac{Y_*^2 v^2 s_d^2}{M_*^2}\right) \tag{3.5}$$

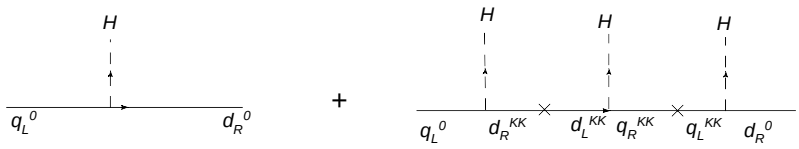

Figure 3.1: Shift in masses and Yukawa couplings of SM fermions using the mass insertion approximation.

After normalizing kinetic terms canonically and combining all the contributions together we will get

$$m \sim Y_* v s_q s_d + \frac{Y_*^3 v^3 s_q s_d}{M_*^2} + \frac{Y_*^3 v^3 s_q {s_d}^3}{2M_*^2} + \frac{Y_*^3 v^3 {s_q}^3 s_d}{2M_*^2}. \tag{3.6}$$

To find an effective Yukawa coupling we can just take a derivative of the mass with respect to the Higgs vev. Although it is meaningless to speak about flavor violation for the one generation we still can introduce parameter $\Delta = m_{SM} - y_{SM} v$ which will quantify the misalignment between Yukawa couplings and the masses of the SM fermions

$$\Delta = \Delta_1 + \Delta_2 + \Delta_3 = \frac{s_q s_d Y_*^3 v^3}{M_*^2} \left[-2 + {s_q}^2 + {s_d}^2 \right], \tag{3.7}$$

where the first term comes from the diagram with three insertions and the other two from the corrections to the kinetic term of the quark field. In the case of three generations this misalignment will lead to the flavor violation, and in the rest of this chapter we will analyze the effects arising from this misalignment.

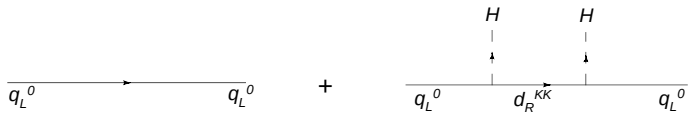

Figure 3.2: Correction to kinetic terms using insertion approximation.

3.1.1 Brane Higgs subtlety

In the previous section we presented a two-site estimate of the flavor misalignment, so we should expect effect of the same size in the warped models, however there is a subtlety in the case of an exactly brane localized Higgs. As pointed out in [12, 16], since the wavefunctions of q_R^{KK} and d_L^{KK} vanish at TeV brane (due to Dirichlet boundary conditions), their couplings to a brane localized Higgs should also vanish. This means that the second diagram in Fig. 3.1 should give no contribution to the fermion mass-Yukawa shift (or at best a highly suppressed one). We would then expect to be left with only the correction coming from the kinetic term (Fig. 3.2), which as stated above is negligible for light quarks. We observe, however, that upon EWSB, the wavefunctions q_R^{KK} and d_L^{KK} become discontinuous at the brane location [25], with the jump of the wavefunctions being proportional to the brane Higgs vev v_4. This discontinuity requires some sort of regularization of the brane location, meaning that the couplings of q_R^{KK} and d_L^{KK} with the brane Higgs would be infinitesimally small, but non-zero. But we note that in the second diagram of Fig. 3.1, one has to sum over infinite KK modes and even though each KK mode will give an infinitesimally small contribution, the sum of infinite terms can lead to a finite (non-zero) result (and as it turns out, this is what happens, as

shown explicitly in Appendix C.3 for this mass insertion approximation).

This brane Higgs issue is avoided in [13] because the authors did not include in their brane action any operator of the type HQ_RD_L. By avoiding these, the contribution to the shift Δ^d coming from the diagrams of Fig. 3.1 is simply not present (except for highly suppressed corrections of order $\frac{v_4^2 m_f^2}{M_{KK}^4}$ which are safe to ignore).

We will address thoroughly this issue in the next two Sections and again in Appendix C.3, since we do find that the flavor misalignment produced by the diagrams of Fig. 3.1 is large and of the same order for both bulk Higgs and brane Higgs scenarios.

3.2 5D calculation: Bulk Higgs Scenario

In this section we perform a 5D calculation in order to evaluate more precisely the shift between Yukawa couplings and masses of SM fermions. We start by working with a single fermion generation for clarity but will later extend our results to the three generations case.

To proceed, we will need to solve for the wavefunctions of SM fermions along the fifth dimension in the bulk Higgs [39, 40] scenario. This corresponds to including the contribution of all KK modes of the mass insertion approximation, and not just the lightest ones. As we will see, the most important shift does not go away as we push the Higgs profile towards the IR brane. In the bulk Higgs scenario, the Higgs

comes from a 5D scalar with the following action [39]

$$\mathcal{L}_{\text{Higgs}} = \int dz d^4x \left(\frac{R}{z}\right)^3 \left[Tr|\mathcal{D}_M H|^2 - \frac{\mu^2}{z^2} Tr|H|^2\right] - V_{UV}(H)\delta(z-R) - V_{IR}(H)\delta(z-R') \tag{3.8}$$

where μ is the 5D mass for Higgs in unit of k. The boundary potentials $V_{UV}(H)$ and $V_{IR}(H)$ give the boundary conditions for the Higgs wavefunction. We can choose these boundary conditions such that the profile of the Higgs vev takes the simple form

$$v(z) = V(\beta)\ z^{2+\beta} \tag{3.9}$$

where $\beta = \sqrt{4+\mu^2}$ and

$$V(\beta) = \sqrt{\frac{2(1+\beta)}{R^3(1-(R'/R)^{2+2\beta})}} \frac{v_4}{(R')^{1+\beta}} \tag{3.10}$$

where v_4 is the SM Higgs vev. This nontrivial vev $v(z)$ is localized towards the IR brane solving the Planck-weak hierarchy problem. Nevertheless we will treat the brane Higgs case separately later to review possible subtleties inherent to its localization by a Dirac delta function. The action for the fermions will look like

$$\begin{aligned} S_{\text{fermion}} \quad &= \int d^4x dz \sqrt{g} \left[\frac{i}{2}\left(\bar{Q}\Gamma^A \mathcal{D}_A Q - \mathcal{D}_A \bar{Q}\Gamma^A Q\right) + \frac{c_q}{R}\bar{Q}Q + \right. \\ &\left. (Q \to D) + \left(Y_d\ \bar{Q} H D + h.c.\right)\right] \end{aligned} \tag{3.11}$$

where Q is electrweak doublet and D singlet. After writing the 5D fermions in two component notation, $Q = \begin{pmatrix} \mathcal{Q}_L \\ \\ \mathcal{Q}_R \end{pmatrix}$ and $D = \begin{pmatrix} \mathcal{D}_L \\ \\ \mathcal{D}_R \end{pmatrix}$, we perform a "mixed" KK

decomposition as

$$\mathcal{Q}_L(x,z) = q_L(z)\,Q_L(x) + ... \tag{3.12}$$

$$\mathcal{Q}_R(x,z) = q_R(z)\,D_R(x) + ... \tag{3.13}$$

$$\mathcal{D}_L(x,z) = d_L(z)\,Q_L(x) + ... \tag{3.14}$$

$$\mathcal{D}_R(x,z) = d_R(z)\,D_R(x) + ... \tag{3.15}$$

where $Q_L(x),\ D_R(x)$ correspond to the light 4D SM fermions and the ... include the rest of heavy KK fermion fields. $q_{L,R}(z),\ d_{L,R}(z)$ are the corresponding profiles of the 4D SM fermions $Q_L(x)$ and $D_R(x)$ which verify the Dirac equation

$$-i\bar{\sigma}^\mu\partial_\mu Q_L(x) + m_d\,D_R(x) = 0, \tag{3.16}$$

$$-i\sigma^\mu\partial_\mu D_R(x) + m_d^*\,Q_L(x) = 0, \tag{3.17}$$

with m_d being the 4D SM down-type quark mass (the analysis can be carried out for up-type quarks in similar fashion).

The four profiles $q_{L,R}(z)$ and $d_{L,R}(z)$ must verify the coupled equations coming from the equations of motion.

$$-m_d\ q_L - q_R' + \frac{c_q+2}{z}q_R + \left(\frac{R}{z}\right)v(z)Y_d\ d_R = 0 \tag{3.18}$$

$$-m_d^*\ q_R + q_L' + \frac{c_q-2}{z}q_L + \left(\frac{R}{z}\right)v(z)Y_d\ d_L = 0 \tag{3.19}$$

$$-m_d\ d_L - d_R' + \frac{c_d+2}{z}d_R + \left(\frac{R}{z}\right)v(z)Y_d^*\ q_R = 0 \tag{3.20}$$

$$-m_d^*\ d_R + d_L' + \frac{c_d-2}{z}d_L + \left(\frac{R}{z}\right)v(z)Y_d^*\ q_L = 0 \tag{3.21}$$

where the $'$ denotes derivative with respect to the extra coordinate z and $[Y_d] = -1/2$ is 5D Yukawa coupling. Even if one knows the analytical form of the nontrivial

Higgs vev $v(z)$, solving analytically this system of equations might still be quite hard. Nevertheless it is simple to find the misalignment between Higgs Yukawa couplings and fermion masses based on the previous equations. To proceed, let us first multiply Eq. (3.18) by $q_L^*(z)$ and the conjugate of Eq. (3.19) by $q_R(z)$, and then subtract them. One obtains

$$m_d(|q_L|^2 - |q_R|^2) + z^4 \left(\frac{q_L^* q_R}{z^4}\right)' - \left(\frac{R}{z}\right) v(z)(Y_d d_R q_L^* - Y_d^* q_R d_L^*) = 0 \qquad (3.22)$$

We can now multiply by $\frac{R^4}{z^4}$ and integrate the whole expression between $z = R$ and $z = R'$ and obtain

$$R^4 \int_R^{R'} dz \left(\frac{m_d}{z^4}(|q_L|^2 - |q_R|^2) - \frac{Rv(z)}{z^5}(Y_d d_R q_L^* - Y_d^* q_R d_L^*)\right) + \left(q_L^* q_R \frac{R^4}{z^4}\right)\Big|_R^{R'} \;=\; 0 \qquad (3.23)$$

The boundary conditions for the profile $q_R(z)$ are chosen to be Dirichlet at both boundaries, i.e. $q_R(R) = q_R(R') = 0$, which means that the last term of Eq. (3.23) identically vanishes. Moreover, canonical normalization of the SM d-quark imposes the extra constraint

$$R^4 \int_R^{R'} \frac{dz}{z^4}(|q_L|^2 + |d_L|^2) \;=\; 1. \qquad (3.24)$$

We can therefore rewrite Eq. (3.23) as

$$m_d = R^4 \int_R^{R'} dz \left(\frac{m_d}{z^4}(|d_L|^2 + |q_R|^2) + \frac{Rv(z)}{z^5}(Y_d d_R q_L^* - Y_d^* q_R d_L^*)\right) \qquad (3.25)$$

Note that this identity is exact, but also that each profile $q_{R,L}(z)$ and $d_{R,L}(z)$ depend on the mass m_d. In the zero mode approximation, the profiles with Dirichlet boundary conditions, $q_R^0(z)$ and $d_L^0(z)$ vanish, and the identity can be expressed as

$$m_d \simeq m_d^0 = R^5 \int_R^{R'} dz \frac{v(z)}{z^5} Y_d d_R^0 q_L^{0*} \qquad (3.26)$$

which agrees with the intuition that fermion mass is mostly generated by the 5D Yukawa couplings between the 5D Higgs and the zero mode fermion profiles. From the action in Eq. (3.11) we also extract the 4D Yukawa coupling of the Higgs field (the lightest KK mode of the 5D Higgs) and the SM down type quark.

$$y_4^d = R^5 \int_R^{R'} dz \frac{h(z)}{z^5} (Y_d d_R q_L^* + Y_d^* q_R d_L^*) \tag{3.27}$$

where $h(z)$ is the profile of the physical Higgs field. It is easy to show that the Higgs vev solution $v(z)$ is related to the profile of the physical light Higgs $h(z)$ (lightest KK mode) by

$$h(z) = \frac{v(z)}{v_4} \left(1 + \mathcal{O}\left(\frac{m_h^2 z^2}{1+\beta}\right)\right) \tag{3.28}$$

so for a light enough Higgs field both profiles $h(z)$ and $v(z)$ are proportional to each other. For a moderately heavy physical Higgs, there will be a misalignment between the profiles of the Higgs vev and the physical Higgs, leading to a misalignment between fermion masses and Yukawa couplings. However, this effect can actually be decoupled if the Higgs is pushed towards the IR brane (by increasing the parameter β). In this case, the Higgs vev profile will be more and more aligned with that of the physical Higgs, so that they become identical in the brane Higgs limit. This source of Higgs flavor violating couplings will be controlled by the parameter $\frac{1}{\beta+1}$ and for the sake of clarity we will ignore its effects in the rest of the paper because, as we discuss in Appendix C.2, they are numerically small and can be decoupled by pushing the Higgs towards the IR brane.

We can then compute the shift $\Delta^d = m_d - v_4\ y_4^d$ between the fermion mass m_d

and the Yukawa coupling y_4^d as

$$\Delta^d = R^4 \int_R^{R'} dz \left(\frac{m_d}{z^4}(|d_L|^2 + |q_R|^2) - 2Y_d^* \frac{Rv(z)}{z^5} q_R d_L^* \right). \tag{3.29}$$

This identity shows that the shift has to be relatively small since it vanishes in the zero mode approximation.

To proceed further, we will use a perturbative approach such that we assume that $(v_4 R') \ll 1$ where v_4 is the SM Higgs vev. Thus, once we know the analytical form of the vev profile $v(z)$ (see Eq. (3.9)) we can solve perturbatively the system of coupled equations (3.18-3.21).

We find

$$q_L(z) = Q_L \; z^{2-c_q} \left[1 + \; \mathcal{O}(v_4^2 R'^2) \right] \tag{3.30}$$

$$d_R(z) = D_R \; z^{2+c_d} \left[1 + \; \mathcal{O}(v_4^2 R'^2) \right] \tag{3.31}$$

and

$$q_R(z) = \left[m_d \; Q_L \left(\frac{R^{1-2c_q}}{1-2c_q} z^{2+c_q} - \frac{1}{1-2c_q} \; z^{3-c_q} \right) + \; Y_d \frac{RV(\beta)}{(2+\beta-c_q+c_d)} D_R \; z^{4+\beta+c_d} \; \right] \left[1 + \; \mathcal{O}(v_4^2 R'^2) \right] \tag{3.32}$$

$$d_L(z) = \left[m_d^* \; D_R \left(-\frac{R^{1+2c_d}}{1+2c_d} z^{2-c_d} + \frac{1}{1+2c_d} \; z^{3+c_d} \right) - \; Y_d^* \frac{RV(\beta)}{(2+\beta-c_q+c_d)} Q_L \; z^{4+\beta-c_q} \right] \left[1 + \; \mathcal{O}(v_4^2 R'^2) \right] \tag{3.33}$$

with the constants Q_L and D_R fixed by canonical normalization of the kinetic terms giving

$$Q_L = \sqrt{\frac{1-2c_q}{\epsilon^{2c_q-1}-1}} R^{c_q-5/2} \tag{3.34}$$

$$D_R = \sqrt{\frac{1+2c_d}{\epsilon^{-2c_d-1}-1}} R^{-c_d-5/2} \tag{3.35}$$

Equipped with the solutions from Eqs. (3.30) to (3.33) one can evaluate perturbatively the shift Δ^d defined in Eq. (3.29). For simplicity, we present here the results for UV localized fermions ($c_q > 0.5, c_d < -0.5$). The general results for both UV and IR localized fermions are presented in Appendix C.1. We find that the main contribution to the shift coming from the last term in Eq. (3.29) can be written as

$$\Delta_1^d = \frac{2|m_d|^3 R'^2}{f(c_q)^2 f(-c_d)^2} \cdot \left[\frac{(2+\beta+c_d-c_q)}{(6+3\beta+c_d-c_q)} - 2\frac{(2+\beta+c_d-c_q)}{(2\beta+4)} + \frac{(2+\beta+c_d-c_q)}{(2+\beta+c_q-c_d)}\right] \quad (3.36)$$

This result corresponds to the first term of (Eq. (3.7)) which we obtained using two site approximation.

The first term in Eq. (3.29) gives a subleading contribution to the shift

$$\Delta_2^d = |m_d|^3 R'^2 \left[\frac{1}{f(c_q)^2}\left(\frac{2c_q-1}{2c_q+1} + \frac{1}{5+2\beta+2c_d} - \frac{1}{3+c_q+c_d+\beta}\right)\right] + (c_{q,d} \to -c_{d,q}) \quad (3.37)$$

which corresponds to the last two terms of the expression from two site approximation (Eq.3.7).

Even if the fermion mass m_d is small, the large warp factor $\frac{1}{f(c_q)^2 f(-c_d)^2} \approx \epsilon^{2-2c_q+2c_d}$ will overcome most of the suppression, rendering the shift to be of the order $\Delta^d \sim m_d v_4^2 R'^2$. The shift is generally on the percent level with respect to fermion masses, but a misalignment of this order in the Higgs Yukawa couplings should introduce strong constraints due to FCNC's.

3.2.1 Pushing the Higgs from the bulk to the brane

Note that in the $\beta \to \infty$ limit, the profile of the Higgs vev tends to become brane localized, as well as the light physical Higgs and the rest of Higgs KK modes. In this limit, the shift Δ_1^d produced between the fermion mass and the Yukawa coupling, coming from the diagrams of Fig. 3.1, reduces to

$$\Delta_1^d = \frac{2}{3}|m_d|^2 m_d R'^2 \frac{1}{f(c_q)^2 f(-c_d)^2}, \tag{3.38}$$

and in particular we see that the effect does not decouple (i.e. it is non-zero). The fact that the expected misalignment is more or less independent on the localization of the Higgs is one of our main results since the bounds and predictions that we will extract can then be considered a general feature of RS models with fields in the bulk (and a Higgs scalar localized near or at IR brane)[1]. The shift Δ_2^d coming from the corrections to the fermion kinetic terms (Fig. 3.2) becomes in the $\beta \to \infty$ limit

$$\Delta_2^d = m_d |m_d|^2 R'^2 \left[\frac{1}{f(c_q)^2} \left(\frac{2c_q - 1}{2c_q + 1} \right) + \frac{1}{f(-c_d)^2} \left(\frac{2c_d + 1}{2c_d - 1} \right) \right], \tag{3.39}$$

in agreement with the results found in [13] (for a brane Higgs scenario).

Maybe it can be useful to discuss the validity of the $\beta \to \infty$ limit starting from a bulk Higgs scenario. Let's first look at the mass spectrum in this case. The Higgs profile is given by Eq. (C.3) and to find its mass eigenvalues one has to satisfy the appropriate boundary conditions at the IR brane [39]

$$\partial_z h + \left(\frac{R'}{R} \right) m_{\rm TeV} h \Big|_{R'} = 0. \tag{3.40}$$

[1] An interesting exception to these results in the Higgs sector, proposed in [17], would be to eliminate the Higgs as a fundamental scalar and consider the fifth component of a gauge field as playing the Higgs role in EWSB.

This will lead to one light mode (i.e. SM Higgs) and a tower of heavy modes with masses proportional to $\sim \beta/R'$, and so in the $\beta \to \infty$ limit all the KK Higgs excitations are decoupled from the low energy spectrum. This means that in this limit we can treat Higgs field as an effective four dimensional field, and thus it corresponds to the brane Higgs scenario. As mentioned earlier (and in Appendix C.2), the misalignment caused by a difference in profiles between the Higgs physical field and its vev (and which we have neglected) will also disappear, as one can interpret that specific misalignment as a result of the mixing between SM Higgs and the heavy Higgs KK modes, which is controlled by $\frac{1}{\beta} \sim \frac{1}{M_{\rm KK}^{\rm Higgs} R'}$.

Let us now look on the couplings of fermions to the Higgs in this limit. For the zero modes we will get:

$$y_d^{SM} = \frac{\sqrt{2(1+\beta)}}{(2 - c_q + c_d + \beta)} \frac{Y_d}{\sqrt{R}} f(c_q) f(-c_d) \tag{3.41}$$

where $[y_d^{SM}] = 0, [Y_d] = -1/2$; similarly one can look at the couplings of two KK fermions to the Higgs and in this case one finds its dependence to be $\sim \frac{1}{\sqrt{\beta}} \frac{Y_d}{\sqrt{R}}$. Naively both couplings do vanish in the $\beta \to \infty$ limit. But if the 5D couplings Y_d scale as $\sqrt{\beta}$ then these couplings will have a finite limit given by the usual brane Higgs results. One can argue whether we can scale the 5D Yukawas as $\sqrt{\beta}$ because such large Yukawas should violate perturbativity of the theory, but as was shown above the couplings of the Higgs to the KK fermions are still $O(1)$. One can see that only the KK excitations of the Higgs will have couplings with KK fermions $\sim Y_d R^{-1/2} \propto O(\sqrt{\beta})$, but their masses are $O(\frac{\beta}{R'})$ and they are completely decoupled from the spectrum. So we conclude this discussion by stressing that it is consistent

to consider the limit $\beta \to \infty$ with $Y_d \propto \sqrt{\beta}$ and it coincides with the usual brane Higgs scenario.

3.3 5D calculation: Brane Higgs Scenario

We argued in Section 3.1 that one might expect that the major contribution to the misalignment Δ_1^d vanishes in the brane Higgs case since the odd KK modes q_R^{KK}, d_L^{KK} have vanishing wavefunctions on the IR brane. We also briefly mentioned that in the mass insertion approximation, one actually might need to sum the infinite tower of fermion KK modes to obtain a non-vanishing contribution (see Appendix C.3 for details). However, without invoking that explanation, we just saw that in the $\beta \to \infty$ limit, Δ_1^d approaches a nonzero value of same numerical order as the $\beta = finite$ case. Since the $\beta \to \infty$ limit of bulk Higgs corresponds to a brane localized Higgs, there seems to be a counter-intuitive subtlety. In this section we try to address and resolve this point in a more precise way, by performing the 5D calculation of the shift Δ_1^d for the specific scenario of a brane Higgs.

For brane Higgs, we can write the Yukawa couplings in the Lagrangian as

$$S_{\text{brane}} = \int d^4x dz\, \delta(z - R') \left(\frac{R}{z}\right)^4 H \left(Y_1^{5D} R \bar{\mathcal{Q}}_L \mathcal{D}_R + Y_2^{5D} R \bar{\mathcal{Q}}_R \mathcal{D}_L + \text{h.c.}\right) \quad (3.42)$$

Here we choose the convention with $\dim[Y_{1,2}^{5D}] = 0$. Note that compared to the bulk Higgs case, the Yukawa couplings Y_1^{5D} an Y_2^{5D} are independent and both $\sim O(1)$. However, they should be of the same order due to the philosophy of flavor anarchy and naturalness. We can do KK decomposition as before, then the equations

satisfied by the wavefunctions are

$$-m_d q_L - \partial_z q_R + \frac{c_q + 2}{z} q_R + v_4 \delta(z - R') Y_1^{5D} R' d_R = 0 \tag{3.43}$$

$$-m_d^* q_R + \partial_z q_L + \frac{c_q - 2}{z} q_L + v_4 \delta(z - R') Y_2^{5D} R' d_L = 0 \tag{3.44}$$

$$-m_d d_L - \partial_z d_R + \frac{c_u + 2}{z} d_R + v_4 \delta(z - R') Y_2^{5D*} R' q_R = 0 \tag{3.45}$$

$$-m_d^* d_R + \partial_z d_L + \frac{c_u - 2}{z} d_L + v_4 \delta(z - R') Y_1^{5D*} R' q_L = 0 \tag{3.46}$$

Notice that the odd wavefunctions q_R and d_L vanish at the IR brane. But the delta functions in equations above give a jump for q_R and d_L at the IR brane, which makes their values at IR brane ambiguous [25]. To remove this ambiguity, we "regularize" the delta in the following way

$$\delta(z - R') = \lim_{\varepsilon \to 0} \begin{cases} \frac{1}{\varepsilon}, & R' - \varepsilon < z < R' \\ 0, & z < R' - \varepsilon. \end{cases} \tag{3.47}$$

This regularization is in a way similar to treating the Higgs as a bulk field and then taking the limit $\beta \to \infty$, although without apparent divergences coming from taking β to be large. In any case one could also perform other regularization methods to remove the wavefunction ambiguities at the IR brane[2].

Now we can easily impose Dirichlet boundary conditions for the q_R, d_L profiles

[2]For example, we could have chosen instead to move the delta function location from R' to $(R' - \varepsilon)$, and enforce the usual boundary conditions on the fields at $z = R'$. Then, at the very end, we would take the limit $\varepsilon \to 0$ [25]. In that case we find

$$d_L(z), q_R(z) \quad \propto \quad v_4 Y_1^{5D} \; \theta(z - R' + \varepsilon) \qquad \text{for} \;\; R' - 2\varepsilon < z < R', \tag{3.48}$$

where we have used the step function $\theta(x) = 1$ for $x < 1$ and $\theta(x) = 0$ for $x > 0$. Inserting this

at IR brane

$$q_R(R') = d_L(R') = 0 \tag{3.49}$$

Integrating equations of motion (Eq. 3.43) from $(R' - \varepsilon < z < R')$ will lead to

$$\begin{aligned} q_R(R') - q_R(R' - \varepsilon) &= v_4 Y_1^{5D} R' d_R(R') & (3.50) \\ d_L(R') - d_L(R' - \varepsilon) &= -v_4 Y_1^{5D*} R' q_L(R') & (3.51) \end{aligned}$$

For the rectangular potential profiles q_R, d_L will drop to zero linearly in the region $R' - \varepsilon < z < R'$, so the profiles near the IR brane can be approximated by

$$\begin{aligned} q_R(z) &= v_4 Y_1^{5D} R' d_R(R') \left(\frac{z - R'}{\varepsilon}\right) \qquad \text{for} \quad R' - \varepsilon < z < R', & (3.52) \\ d_L(z) &= -v_4 Y_1^{5D*} R' q_L(R') \left(\frac{z - R'}{\varepsilon}\right) \qquad \text{for} \quad R' - \varepsilon < z < R'. & (3.53) \end{aligned}$$

From our previous discussion, the main contribution to the misalignment between SM fermion masses and Yukawa couplings come from the second term of Eq.(3.29), so plugging in the odd wavefunctions from Eq.(3.52), we get

$$\begin{aligned} \Delta_1^d &= 2(Y_2^{5D})^*(Y_1^{5D})^2 R'^3 v_4^3 d_R(R') q_L^*(R') \left(\frac{R}{R'}\right)^4 \int_{R'-\varepsilon}^{R'} dz \frac{1}{\varepsilon} \left(\frac{z - R'}{\varepsilon}\right)^2 \\ &= \frac{2}{3}(Y_2^{5D})^*(Y_1^{5D})^2 R'^3 v_4^3 d_R(R') q_L^*(R') \left(\frac{R}{R'}\right)^4 & (3.54) \end{aligned}$$

On the other hand, to leading order in Higgs vev, the SM fermion mass is given by

$$m_d \approx \left(\frac{R}{R'}\right)^4 v_4 Y_1^{5D} R' q_L^*(R') d_R(R') \tag{3.55}$$

---

into Eq. (3.29) we obtain the same misalignment as in Eq. (3.54), namely

$$\Delta_1^d \;\propto\; 2(v_4 R')^3 (Y_1^{5D})^2 Y_2^{5D*} \int_{R'-2\varepsilon}^{R'} dz\; \delta(z - R' + \varepsilon)\; [\theta(z - R' + \varepsilon)]^2 \;\propto\; \frac{2}{3}(v_4 R')^3 (Y_1^{5D})^2 Y_2^{5D*}.$$

Therefore, the misalignment can be expressed as

$$\Delta_1^d = \frac{2}{3} m_d Y_1^{5D} (Y_2^{5D})^* v_4^2 R'^2 = \frac{2}{3} |m_d|^2 m_d R'^2 \left(\frac{Y_2^{5D}}{Y_1^{5D}} \right)^* \frac{1}{f(c_q)^2 f(-c_d)^2} \tag{3.56}$$

As advertised before, this result agrees with the one obtained in the previous section for the bulk Higgs scenario, once we take $\beta \to \infty$ (Eq. 3.36). We again stress that this result shows that upon careful derivation, the misalignment obtained does not vanish in the particular case of a Brane localized Higgs. The main difference though, is the appearance of the independent couplings Y_2^{5D}, which in the bulk Higgs case are forced to be equal to Y_1^{5D} by 5D general covariance. These couplings Y_2^{5D} are not necessary for generating fermion masses, and so it is technically possible to set their values as small as necessary to suppress the obtained misalignment. Nevertheless this seems to go against the main philosophy of our approach which is to assume the value of all dimensionless 5D parameters of order one.

Again, the fact that Δ_1^d is non zero in the brane Higgs case is hard to understand in the mass insertion approximation since the contribution from each KK fermion (see Fig. 3.1) seems to be vanishing. In Appendix C.3 we show that to resolve this point we need to sum up all the KK modes of the mass insertion approximation, as already mentioned before.

The subleading contribution to the misalignment between SM fermion masses and Yukawa coupling can be calculated in a similar way as in the previous section, and the result is (for UV localized fermions)

$$\begin{aligned} \Delta_2^d &= m_d |Y_1^{5D}|^2 v_4^2 R'^2 \left[f(-c_d)^2 \frac{2c_q - 1}{2c_q + 1} + (c_{q,d} \to -c_{d,q}) \right] & (3.57) \\ &= m_d |m_d|^2 R'^2 \left[\frac{1}{f(c_q)^2} \left(\frac{2c_q - 1}{2c_q + 1} \right) + (c_{q,d} \to -c_{d,q}) \right] & (3.58) \end{aligned}$$

We can see that for the first two generations, we have $\Delta_2^d \ll \Delta_1^d$, and it agrees with Eq. (3.37) in the $\beta \to \infty$ limit. The result for both UV and IR localized fermions is given by

$$\Delta_2^d = m_d |m_d|^2 R'^2 \left[K(c_q) + K(-c_d)\right] \tag{3.59}$$

with

$$K(c) \equiv \frac{1}{1-2c}\left[-\frac{1}{\epsilon^{2c-1}-1} + \frac{\epsilon^{2c-1}-\epsilon^2}{(\epsilon^{2c-1}-1)(3-2c)} + \frac{\epsilon^{1-2c}-\epsilon^2}{(1+2c)(\epsilon^{2c-1}-1)}\right]. \tag{3.60}$$

One can see that Δ_1^d and Δ_2^d can be of the same order only for IR localized fermions.

3.4 Generalizing to three Generations

We can generalize the calculations presented in the sections 3.2 and B.11 to 3 generations. For simplicity we perform the analysis in the brane Higgs scenario here. To leading order in Yukawa, the SM fermion mass matrix is

$$\hat{m}^d_{\alpha\beta} = [\hat{F}_q \hat{Y}_1^{5D} \hat{F}_d]_{\alpha\beta} v_4 \tag{3.61}$$

where $\hat{}$ means a 3×3 matrix in flavor space and $\hat{F}_{q,d} = \mathrm{diag}[f(c_{q_i}, c_{d_i})]$. Using the same technique as before, we can easily show that the misalignment between fermion mass and Yukawa coupling matrix is $\hat{\Delta}^d = \hat{\Delta}_1^d + \hat{\Delta}_2^d$, with

$$\hat{\Delta}^d_{1,\alpha\beta} = \frac{2}{3}\left[\hat{F}_q \hat{Y}_1^{5D} (\hat{Y}_2^{5D})^\dagger \hat{Y}_1^{5D} \hat{F}_d\right]_{\alpha\beta} \left(v_4^3 R'^2\right) \tag{3.62}$$

$$= \frac{2}{3}\left[\hat{m}^d \frac{1}{\hat{F}_d} (\hat{Y}_2^{5D})^\dagger \frac{1}{\hat{F}_q} \hat{m}^d\right]_{\alpha\beta} \left(v_4^3 R'^2\right) \tag{3.63}$$

and

$$\hat{\Delta}^d_{2,\alpha\beta} = \left[\hat{m}^d \left(\hat{m}^{d\dagger}\hat{K}(c_q) + \hat{K}(-c_d)\hat{m}^{d\dagger}\right)\hat{m}^d\right]_{\alpha\beta} R'^2 \tag{3.64}$$

The subdominant contribution here (Eq. 3.64) agrees with the result found in [13]. The crucial observation is that $\hat{m}^d_{\alpha\beta}$ and $\hat{\Delta}^d_{\alpha\beta}$ are generally not aligned in flavor space. Thus when we diagonalize the quark mass matrix with a bi-unitary transformation $\hat{m}^d \to O^\dagger_{d_L}\hat{m}^d O_{d_R}$, the Yukawa couplings will not be diagonal. To be more specific, in models of flavor anarchy, we have (see Eq. (58) and (2.21))

$$(O_{d_L,d_R})_{\alpha\beta} \sim \frac{F_{q_\alpha,d_\alpha}}{F_{q_\beta,d_\beta}} \qquad \text{for} \quad \alpha < \beta \tag{3.65}$$

Then the off-diagonal Yukawa coupling will be (dominated by Eq. (3.62))

$$\begin{aligned} \hat{Y}^{\text{off}}_{\alpha\beta} &= -(O^\dagger_{d_L}\hat{\Delta}^d O_{d_R})_{\alpha\beta}\frac{1}{v_4} \\ &\sim \frac{2}{3}F_{q_\alpha}\bar{Y}^3 F_{d_\beta} v_4^2 R'^2 \end{aligned} \tag{3.66}$$

where $\bar{Y}$ is the typical value of the dimensionless 5D Yukawa coupling.

3.5 Estimates of Higgs FCNC in Flavor Anarchy

In this section, we estimate the off-diagonal couplings of Higgs to SM fermions (assuming again for simplicity a brane Higgs scenario). And then we do a numerical scan over anarchical Yukawa couplings to support our estimates. We first parametrize the Higgs Yukawa couplings as

$$\mathcal{L}_{HFV} = a^d_{ij}\sqrt{\frac{m^d_i m^d_j}{v_4^2}} H \bar{d}^i_L d^j_R + h.c. + (d \leftrightarrow u). \tag{3.67}$$

We can use Eq. (3.65) and (3.66) to estimate the sizes of $a_{ij}^{u,d}$. For example, we have

$$\begin{aligned} a_{12}^{d} &\sim \frac{2}{3} F_{q_1} \bar{Y}^3 F_{d_2} v^2 R'^2 \sqrt{\frac{v_4^2}{m_s m_d}} \\ &= \frac{2}{3} \frac{F_{q_1}}{F_{q_2}} \bar{Y}^2 v_4 R'^2 F_{q_2} \bar{Y} v_4 F_{d_2} \sqrt{\frac{v_4^2}{m_s m_d}} \\ &\sim \frac{2}{3} \lambda \bar{Y}^2 v_4^2 R'^2 \sqrt{\frac{m_s}{m_d}}, \end{aligned} \tag{3.68}$$

where $\lambda \approx 0.22$ is the Wolfenstein parameter, and we used $F_{q_1}/F_{q_2} \sim (O_{d_L})_{12} \sim (V_{CKM})_{12} \sim \lambda$. We can find the other $a_{ij}^{u,d}$'s in similar fashion. Here we present our results from estimates:

$$a_{ij}^{d} \sim \delta_{ij} - \frac{2}{3} \bar{Y}^2 v_4^2 R'^2 \begin{pmatrix} 1 & \lambda \sqrt{\frac{m_s}{m_d}} & \lambda^3 \sqrt{\frac{m_b}{m_d}} \\ \frac{1}{\lambda} \sqrt{\frac{m_d}{m_s}} & 1 & \lambda^2 \sqrt{\frac{m_b}{m_s}} \\ \frac{1}{\lambda^3} \sqrt{\frac{m_d}{m_b}} & \frac{1}{\lambda^2} \sqrt{\frac{m_s}{m_b}} & 1 \end{pmatrix} \tag{3.69}$$

$$a_{ij}^{u} \sim \delta_{ij} - \frac{2}{3} \bar{Y}^2 v_4^2 R'^2 \begin{pmatrix} 1 & \lambda \sqrt{\frac{m_c}{m_u}} & \lambda^3 \sqrt{\frac{m_t}{m_u}} \\ \frac{1}{\lambda} \sqrt{\frac{m_u}{m_c}} & 1 & \lambda^2 \sqrt{\frac{m_t}{m_c}} \\ \frac{1}{\lambda^3} \sqrt{\frac{m_u}{m_t}} & \frac{1}{\lambda^2} \sqrt{\frac{m_c}{m_t}} & 1 \end{pmatrix} \tag{3.70}$$

Note that the results we presented here are just estimates for the size of $a_{ij}^{u,d}$, not their signs or phases. However, for the third generation quarks, the corrections almost always suppress the Yukawa couplings if $Y_1 = Y_2$ (which is natural in bulk Higgs scenario) and are typically larger than the previous estimates. We argue this point in the next subsection.

3.5.1 Yukawa couplings of the third generation when $Y_1 = Y_2$

We can obtain a better estimate on the typical size of the diagonal entries of the Yukawa coupling matrices by going back to Eq. (3.63) and assume that $Y_1 = Y_2$. Its form simplifies further to

$$\hat{\Delta}^u_{1,\alpha\beta} = \frac{2}{3}R'^2 \left[\hat{m}^u \frac{1}{\hat{F}_u^2} (\hat{m}^u)^\dagger \frac{1}{\hat{F}_q^2} \hat{m}^u \right]_{\alpha\beta} \tag{3.71}$$

where we have written the misalignment in the up-sector. Now we perform the bi-unitary rotation needed to go to the physical fermion basis, and study the element (33) of the overall Yukawa coupling, i.e.

$$\begin{aligned} a_{tt} - 1 &= -\frac{2R'^2}{3m_t} \left[O^\dagger_{u_L} \hat{m}^u \frac{1}{\hat{F}_u^2} \hat{m}^{u\dagger} \frac{1}{\hat{F}_q^2} \hat{m}^u O_{u_R} \right]_{33} \\ &= -\frac{2R'^2}{3m_t} \left(m_u^{diag}\right)_{33} \left(O^\dagger_{u_R} \frac{1}{\hat{F}_u^2} O_{u_R} \right)_{3j} \left(m_u^{diag}\right)_{jj} \left(O^\dagger_{u_L} \frac{1}{\hat{F}_q^2} O_{u_L} \right)_{j3} \left(m_u^{diag}\right)_{33} \end{aligned} \tag{3.72}$$

First let's look at the contribution to a_{tt} when the "j" index is equal to 3 (i.e. in the middle mass matrix m_u^{diag} we have m_t). In this case, there will be 9 terms, each proportional to $-\frac{2R'^2\bar{Y}^2v_4^2}{3}$, and it is important to realize that every one of them will be real and negative, because $(O^\dagger_{u_R} \frac{1}{\hat{F}_u^2} O_{u_R})_{33} \geq 0$. When $j = 2$ (m_c) there will be only 4 terms $\sim \frac{2R'^2\bar{Y}^2v_4^2}{3}$ but every one of them will have generically a random complex phase (the 5 remaining terms are much smaller). For $j = 1$ (m_u) there is only one term $\sim \frac{2R'^2\bar{Y}^2v_4^2}{3}$ contributing, with the other 8 terms being again suppressed. So at the end of the day the dominant contribution to a_{tt} will consist of 14 terms, 9 of which are negative and the rest 5 have random complex phases. Generically each of these terms are of the same size $\sim \frac{2R'^2\bar{Y}^2v^2}{3}$ so from a statistical argument, $a_{tt} - 1$ should receive a negative contribution $\sim -9\left(\frac{2R'^2\bar{Y}^2v^2}{3}\right)$. This result is confirmed by

the numerical scan presented below.

One can perform the same analysis for the element (22) of the Yukawa matrix and realize that in this case the number of terms aligned (contributing constructively) is 4, and for the (11) element there are none. This means that the largest corrections are expected in the third generation Yukawa couplings, with a suppressed correction in second generation couplings and much more suppressed correction for first generation couplings. This structure in the corrections seems to be a result of the hierarchical structure of the flavor anarchy setup.

Finally, we must remind the reader that it was crucial to take $Y_1 = Y_2$ (which is required in the Bulk Higgs scenario) to obtain these predictions. In the case $Y_1 \neq Y_2$, there will be no alignment of terms, and we therefore generally expect smaller corrections to the third generation Yukawa couplings.

3.5.2 Validity of $\bar{Y} v_4 R'$ expansion

We managed to solve the fermion equations by expanding them in the parameter $(\bar{Y}^2 v_4^2 R'^2)$, and so our results can be trusted as long as

$$\bar{Y} \lesssim \frac{1}{v_4 R'} \quad \left(\sim 9 \text{ for } R'^{-1} = 1500\text{GeV}\right) \tag{3.73}$$

but we have seen in the previous subsection that the corrections to *htt* and *hbb* couplings do pick up an extra numerical factor of ~ 9 in the expansion parameter $(\bar{Y}^2 v_4^2 R'^2)$. This means that, at least for third generation fermions, our approximation is valid only for

$$\bar{Y} \lesssim \frac{1}{v_4 R' \sqrt{9}} \quad \left(\sim 3 \text{ for } R'^{-1} = 1500\text{GeV}\right) \tag{3.74}$$

Generically for the case with $\bar{Y} \gtrsim 3$ we will still have a large misalignment between the Higgs couplings and fermion masses but to be able to make valid predictions one would have to solve the equations of motion (Eq. 3.18 to 3.21) exactly or use a different perturbative parameter. In the numerical analysis presented below we performed a scan with $0.3 < |Y^{5D}_{1,2}| < 3$, where our expansion is valid. We then also allowed for slightly larger values of the Yukawas such that $1 < |Y^{5D}_{1,2}| < 4$. The average size of the couplings is still below 3, so for a KK scale of $R'^{-1} = 1500$ GeV or above, the results will still be precise enough, although approaching the edge of perturbative convergence.

3.5.3 Numerical Scan

We did a numerical scan over the input parameters $(Y^{5D}_1)_{ij}$, $(Y^{5D}_2)_{ij}$, c_{q_i}, c_{d_i}, c_{u_i} and we set $R'^{-1} = 1.5$ TeV. In our scan, we pick the points that give the correct SM quark masses and CKM matrix. Then we calculate the 4D effective Yukawa couplings of Higgs with SM quarks. We present here only the results for $|Y^{5D}_{1,2}| \in [0.3, 3]$. First, we scan the set of parameters with $Y^{5D}_1 = Y^{5D}_2$ which is motivated by bulk Higgs. Here are the results for this case:

$$a^d_{ij} = \begin{pmatrix} 0.99 - 1 & 0.006 - 0.019 & 0.004 - 0.012 \\ 0.006 - 0.019 & 0.96 - 0.99 & 0.007 - 0.02 \\ 0.042 - 0.10 & 0.075 - 0.18 & 0.85 - 0.93 \end{pmatrix} \tag{3.75}$$

$$a_{ij}^{u} = \begin{pmatrix} 0.99-1 & 0.06-0.16 & 0.09-0.21 \\ 0.003-0.008 & 0.94-0.98 & 0.03-0.09 \\ 0.009-0.02 & 0.05-0.14 & 0.71-0.82 \end{pmatrix} \tag{3.76}$$

The first and second numbers are the 25% and 75% quantiles of the distribution of $|a_{ij}|$ obtained from the scan (i.e. 50% of all the values we obtained in the scan for each $|a_{ij}|$ lie between these two quantiles). From the results we can see that the values of $a_{ij}^{u,d}$ from the scan are consistent with the estimates presented above (Eq 3.69 and 3.70), and the expected reduction of $h\bar{t}t$ coupling is confirmed. We can also easily see this reduction of third generation Yukawa couplings in Fig. 3.3.

For the case when Y_1^{5D} and Y_2^{5D} are completely uncorrelated (Brane Higgs) we get the following results:

$$a_{ij}^{d} = \begin{pmatrix} 0.99-1 & 0.01-0.026 & 0.005-0.012 \\ 0.012-0.03 & 0.98-1.01 & 0.008-0.02 \\ 0.05-0.12 & 0.07-0.2 & 0.96-1.03 \end{pmatrix} \tag{3.77}$$

$$a_{ij}^{u} = \begin{pmatrix} 0.98-1.01 & 0.07-0.17 & 0.08-0.19 \\ 0.004-0.009 & 0.97-1.02 & 0.025-0.067 \\ 0.007-0.016 & 0.04-0.11 & 0.9-0.99 \end{pmatrix} \tag{3.78}$$

We can see that the off-diagonal terms of $a_{ij}^{u,d}$ are of the same order as the previous case. However the diagonal entries do not have the suppression as in the $Y_1^{5D} = Y_2^{5D}$ case, see the discussion in Subsection 3.5.1.

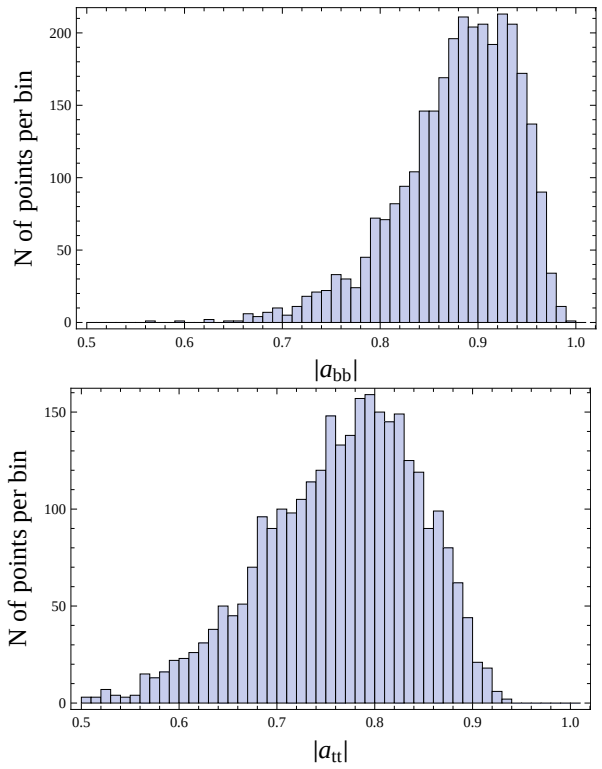

Figure 3.3: Distribution of the absolute value of the normalized Higgs couplings to $t\bar{t}$ and $b\bar{b}$, a_{tt} and a_{bb}, in our numerical scan, with a fixed KK scale of $R'^{-1} = 1500$ GeV (KK gluon mass $M_{KKG} = 2.45R'^{-1}$) and for 5D Yukawa couplings $|Y_{5D}^{ij}| \in [0.3, 3]$. The expected generic suppression for both couplings is demonstrated numerically quite clearly.

3.6 Lepton sector

Generically one can see that the same effects will lead to Higgs flavor violation in the lepton sector, the only difference is that in the lepton sector there are various ways to explain the large mixing angles and light masses for the neutrinos [7, 42, 43]. Now we want to look at Higgs flavor violation in the charged lepton sector, then depending on a given neutrino model, the left-handed charged lepton profiles can be either hierarchical and UV localized (i), or similar and UV localized (ii). The profiles of the right-handed charged leptons are always hierarchical and localized near the UV brane. We treat these two cases separately.

- Case (i) - left-handed and right-handed profiles are hierarchical. Then the profiles should satisfy the following relations:

$$f_L^i f_e^i \sim \frac{m_i^l}{\bar{Y} v_4}, \tag{3.79}$$

where $f_{L,e}$ are profiles of the left-handed and right-handed fields respectively, then the generational mixing is also hierarchical

$$(O_{L,e})^{i,j} \sim \frac{f_{L,e}^i}{f_{L,e}^j}, \qquad i < j. \tag{3.80}$$

We again parameterize our Lagrangian in the following form:

$$\mathcal{L}_{HFV} = a_{ij}^l \sqrt{\frac{m_i^l m_j^l}{v_4^2}} H \bar{L}^i e^j + h.c. \tag{3.81}$$

Where L, e are $SU(2)_L$ doublets and singlets respectively Then we can estimate a_{ij}^l

$$a_{ij}^l \sim \frac{2}{3} \bar{Y}^2 (v_4^2 R'^2) \sqrt{\frac{f_L^i f_e^j}{f_L^j f_e^i}} \tag{3.82}$$

One can see that our estimate depends on the profiles of the fermions, but the following relation will be valid

$$\sqrt{|a^l_{ij}|^2 + |a^l_{ji}|^2} \gtrsim \frac{4}{3}\bar{Y}^2(v_4^2 R'^2) = 0.16 \left(\frac{1500 \text{ GeV}}{1/R'}\right)^2 \left(\frac{\bar{Y}}{3}\right)^2 \tag{3.83}$$

This inequality is saturated when $\frac{f^i_L}{f^j_L} \sim \frac{f^i_e}{f^j_e} \sim \sqrt{\frac{m^l_i}{m^l_j}}$, i.e., when the hierarchy of charged lepton masses are explained equally by the profiles of left-handed and right-handed fields.

- Case (ii) - right-handed profiles are hierarchical and left-handed profiles are similar $f^1_L \sim f^2_L \sim f^3_L$. Then the profiles satisfy the following relations:

$$\begin{aligned} f^i_L f^i_e &\sim \frac{m^l_i}{\bar{Y} v_4} \\ \frac{f^i_L}{f^j_L} &\sim O(1), \qquad i < j \\ \frac{f^i_e}{f^j_e} &\sim \frac{m^l_i}{m^l_j}, \qquad i < j \end{aligned} \tag{3.84}$$

then we can estimate the parameter a^l_{ij} to be:

$$a^l_{ij} \sim \frac{2}{3}\bar{Y}^2(v_4^2 R'^2)\sqrt{\frac{f^j_e}{f^i_e}} \sim 0.08 \left(\frac{1500 \text{ GeV}}{1/R'}\right)^2 \left(\frac{\bar{Y}}{3}\right)^2 \sqrt{\frac{m^l_j}{m^l_i}} \tag{3.85}$$

These flavor violating Higgs Yukawa couplings to leptons can also lead to interesting collider signals, which will also be discussed in the next section.

3.7 Phenomenology

The FCNC generated by flavor violating Higgs Yukawa couplings will affect many low energy observables and also give possible signature at colliders. In this section, we first discuss bounds on Higgs flavor violation coming from $\Delta F = 2$

processes such as $\bar{K}-K$, $\bar{B}-B$, $\bar{D}-D$ mixing. And then we discuss possible signature at the LHC including suppression of htt coupling, rare top decay $t \to hc$ and flavor violating Higgs decay $h \to \tau\mu$.

3.7.1 Bounds from low energy physics

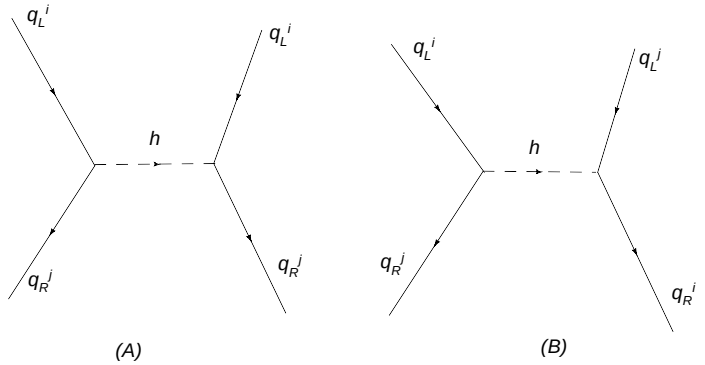

Figure 3.4: Contribution to $\Delta F = 2$ processes from Higgs exchange

The $\Delta F = 2$ process can be described by the general Hamiltonian [21, 29]

$$\mathcal{H}_{eff}^{\Delta F=2} = \sum_{a=1}^{5} C_a Q_a^{q_i q_j} + \sum_{a=1}^{3} \tilde{C}_a \tilde{Q}_a^{q_i q_j} \tag{3.86}$$

with

$$\begin{aligned} Q_1^{q_i q_j} &= \bar{q}_{jL}^{\alpha} \gamma_\mu q_{iL}^{\alpha} \bar{q}_{jL}^{\beta} \gamma^\mu q_{iL}^{\beta}, \\ Q_2^{q_i q_j} &= \bar{q}_{jR}^{\alpha} q_{iL}^{\alpha} \bar{q}_{jR}^{\beta} q_{iL}^{\beta}, \\ Q_3^{q_i q_j} &= \bar{q}_{jR}^{\alpha} q_{iL}^{\beta} \bar{q}_{jR}^{\beta} q_{iL}^{\alpha}, \\ Q_4^{q_i q_j} &= \bar{q}_{jR}^{\alpha} q_{iL}^{\alpha} \bar{q}_{jL}^{\beta} q_{iR}^{\beta}, \\ Q_5^{q_i q_j} &= \bar{q}_{jR}^{\alpha} q_{iL}^{\beta} \bar{q}_{jL}^{\beta} q_{iR}^{\alpha}, \end{aligned} \tag{3.87}$$

where α, β are color indices. The operators $\tilde{Q}_a$ are obtained from Q_a by exchange $L \leftrightarrow R$. For $\bar{K}-K$, $\bar{B}_d - B_d$, $\bar{B}_s - B_s$, $\bar{D}-D$ mixing, $q_i q_j = sd$, bd, bs and uc

respectively. Exchange of the Higgs can give rise to new contribution to C_2, $\tilde{C}_2$ and C_4. This can be seen in Fig. 3.4, where Fig. 3.4(A) gives C_2 and $\tilde{C}_2$, Fig. 3.4(B) gives C_4. These new contributions are

$$C_2^h = a_{ij}^2 \frac{m_i m_j}{v^2} \frac{1}{m_h^2} \tag{3.88}$$

$$\tilde{C}_2^h = a_{ji}^2 \frac{m_i m_j}{v^2} \frac{1}{m_h^2} \tag{3.89}$$

$$C_4^h = a_{ij} a_{ji} \frac{m_i m_j}{v^2} \frac{1}{m_h^2} \tag{3.90}$$

where m_h is the mass of physical Higgs. The model independent bound on the new physics contribution to these Wilson coefficients are given in [21]. We use the RGE from [41] and give the bounds renormalized at the scale $\mu_h = 200\ GeV$:

$$\mathrm{Im}C_K^2 \leq \left(\frac{1}{7 \times 10^7\ GeV}\right)^2, \quad \mathrm{Im}C_K^4 \leq \left(\frac{1}{1.3 \times 10^8\ GeV}\right)^2, \tag{3.91}$$

$$|C_D^2| \leq \left(\frac{1}{1.9 \times 10^6\ GeV}\right)^2, \quad |C_D^4| \leq \left(\frac{1}{2.9 \times 10^6\ GeV}\right)^2, \tag{3.92}$$

$$|C_{B_d}^2| \leq \left(\frac{1}{0.9 \times 10^6\ GeV}\right)^2, \quad |C_{B_d}^4| \leq \left(\frac{1}{1.4 \times 10^6\ GeV}\right)^2, \tag{3.93}$$

$$|C_{B_s}^2| \leq \left(\frac{1}{1 \times 10^5\ GeV}\right)^2, \quad |C_{B_s}^4| \leq \left(\frac{1}{1.7 \times 10^5\ GeV}\right)^2. \tag{3.94}$$

These bounds put constraints on both the Higgs flavor violating Yukawa couplings parametrized by a_{ij}, and on the Higgs mass m_h. If we assume that the phases of

$C^h_{2,4}$ are random, i.e., $\mathrm{Im}(C^h_{2,4}) \sim |C^h_{2,4}|$, we can then rewrite the previous bounds as

$$
\begin{aligned}
&0.25\left(\frac{350\ GeV}{m_h}\right)^2 \frac{\mathrm{Im}(a^d_{12})^2}{(0.032)^2} \leq 1, \quad 0.39\left(\frac{350\ GeV}{m_h}\right)^2 \frac{\mathrm{Im}(a^d_{21})^2}{(0.04)^2} \leq 1, \\
&1.11\left(\frac{350\ GeV}{m_h}\right)^2 \frac{\mathrm{Im}(a^d_{21}a^d_{12})}{(0.032\times 0.04)} \leq 1, \quad 0.018\left(\frac{350\ GeV}{m_h}\right)^2 \frac{|a^u_{12}|^2}{(0.15)^2} \leq 1, \\
&0.00005\left(\frac{350\ GeV}{m_h}\right)^2 \frac{|a^u_{21}|^2}{(0.008)^2} \leq 1, \quad 0.0021\left(\frac{350\ GeV}{m_h}\right)^2 \frac{|a^u_{12}a^u_{21}|}{(0.0012)} \leq 1 \\
&0.0002\left(\frac{350\ GeV}{m_h}\right)^2 \frac{|a^d_{13}|^2}{(0.01)^2} \leq 1, \quad 0.03\left(\frac{350\ GeV}{m_h}\right)^2 \frac{|a^d_{31}|^2}{(0.12)^2} \leq 1, \\
&0.006\left(\frac{350\ GeV}{m_h}\right)^2 \frac{|a^d_{13}a^d_{31}|}{(0.01\times 0.12)} \leq 1, \quad 0.00003\left(\frac{350\ GeV}{m_h}\right)^2 \frac{|a^d_{23}|^2}{(0.01)^2} \leq 1, \\
&0.003\left(\frac{350\ GeV}{m_h}\right)^2 \frac{|a^d_{32}|^2}{(0.15)^2} \leq 1, \quad 0.001\left(\frac{350\ GeV}{m_h}\right)^2 \frac{|a^d_{32}a^d_{23}|}{(0.1\times 0.01)} \leq 1
\end{aligned}
\tag{3.95}
$$

where we compare the a_{ij} elements with their estimated values, for a fixed average Yukawa coupling $\bar{Y} = 2$ and KK scale given by $1/R' = 1500$ GeV (see formulae for the estimates from Eqs. (3.69) and (3.70)). We also choose to compare the Higgs mass with a nominal value of $m_h = 350$ GeV. We can see that the bound on $\mathrm{Im}C^4_K$ coming from ϵ_K gives the strongest constraint on the Higgs mass. Specifically, we have

$$
m_h \gtrsim 350\ GeV \quad \text{for} \quad \mathrm{Im}(a^d_{21}a^d_{12}) = (0.04\times 0.032) \tag{3.96}
$$

for a fixed KK scale of $1/R' = 1.5$ TeV and average 5D Yukawa of $\bar{Y}_{5D} = 2$.

In Fig.3.5, we show the results of our numerical scan by plotting the bounds coming from ϵ_K in the (m_h-M_{KKG}) plane, where $M_{KKG} \approx 2.45R'^{-1}$ is the mass of the first KK gluon. In the left panel we show results for the case $|Y^{5D}_{ij}| \in [0.3, 3]$, and in the right panel we show results for the case $|Y^{5D}_{ij}| \in [1, 4]$. It can be seen quite

clearly that a larger 5D Yukawa coupling leads to a higher bound on the KK scale. Note that the bounds coming from KK gluon exchange are inversely proportional to the size of the 5D Yukawa couplings $\bar{Y}_{5D}$. This leads to an interesting observation

- The new contribution to ϵ_K coming from Higgs exchange has opposite dependence on the 5D Yukawa coupling as that of KK gluon exchange. Thus, increasing the overall size of Y_{5D} will alleviate pressure from KK gluon exchange but, as we have seen, this will also enhance the effect of Higgs mediated FCNC's.

With the chosen $\bar{Y}_{5D}$ (~ 2), we can see that for the region of parameter space with $M_{KKG} \sim 3$ TeV (accessible at the LHC), a Higgs mass $m_h < 400$ GeV is disfavored. On the other hand, if a light (< 150 GeV) Higgs is found in the LHC, we should expect sizable new physics contributions to $\Delta F = 2$ processes, just below current bounds.

3.7.2 Collider phenomenology

Besides low energy physics constraints, there could be very interesting signatures in colliders coming from the corrections to the Higgs Yukawa couplings. The modification of the top Yukawa coupling as well as contribution of the higher KK modes running in the loop can significantly modify hgg coupling which might lead to the striking signatures in the collider. In the case of a light Higgs boson (and assuming that somehow low energy FCNC bounds are overcome), the branchings of the Higgs can change substantially due to the generically reduced hbb couplings.

This would indirectly enhance the importance of $h \to \gamma\gamma$ signal, and maybe help overcome the overall reduction in the total production cross section due to reduced top Yukawa couplings. In Fig. 3.6, we plot the Higgs decay branching ratio for various final states versus the Higgs mass m_h [3]. We can see clearly that for a light Higgs, the reduction in the hbb coupling changes the branching ratio to other channels significantly. For a heavy Higgs, the branching for $h \to tt$ is reduced.

If kinematically accessible ($m_h < m_t$), the flavor violating htc couplings will allow the decay $t \to ch$ to occur. The branching ratio of this process is given by (see for example [13])

$$Br(t \to ch) = \frac{2(m_t^2 - m_h^2)^2 m_w^2}{(m_t^2 - m_w^2)^2(m_t^2 + 2m_w^2)g_2^2} \left\{ |a^u_{23}|^2 + |a^u_{32}|^2 + \frac{4m_c m_t}{m_t^2 - m_h^2} \mathrm{Re}[a^u_{23} a^u_{32}] \right\} \frac{m_c m_t}{v^2}. \tag{3.97}$$

If we take $m_h = 120$ GeV, then for $a^u_{23} \sim 0.08$ and $a^u_{32} \sim 0.14$, which are good estimates for $\bar{Y} = 2$ and a KK scale of $1/R' = 1500$ GeV (see Eq. (3.70)), we obtain a branching ratio of

$$Br(t \to ch) \sim 5 \times 10^{-5}. \tag{3.98}$$

The sensitivity of LHC for this rare top decay is $Br(t \to ch) \geq 6.5 \times 10^{-5}$ [45], precisely in the ball-park of our estimate. In Figure 3.7 we show the results of our two scans, each with a different average size of the 5D Yukawas. It is shown that observing the signal at the LHC is quite possible although it requires larger Yukawa couplings and a light Higgs. If observed, this signal would be very valuable in determining the structure of the 5D setup.

[3] We did not include $h \to \mu\tau$ mode on the plot because it is model dependent.

Another interesting collider signature for light Higgs might be the Higgs lepton flavor violating decay $h \to \mu\tau$. the LHC reach for this process was studied in [44] and it could be observable if $|a_{\mu\tau}, (a_{\tau\mu})| > 0.15$. One can see from equations (3.83) and (3.85) that for case (i), this decay is observable only for fairly large $\bar{Y}$ ($\gtrsim 3$) and low KK scale $1/R' \lesssim 1.5$ TeV, while for case (ii) there is an extra enhancement factor of $\sqrt{\frac{m_\tau}{m_\mu}} \sim 4$ for $a_{\mu\tau}$, so that in this case we expect larger parameter space to give us observable effects in the $h \to \mu\tau$ decay.

For a heavy Higgs ($m_h > m_t$), an interesting signal at the LHC might be the Higgs flavor violating decay $h \to tc$. A similar study on tc production from radion decay was considered in [20]. From Fig. 3.6 we can see that the branching for $h \to tc$ is in the range of 10^{-3} for a Higgs mass between $200 - 300$ GeV, and for the favorable parameter values of $\bar{Y}_{5D} \sim 2$ and $1/R' = 1500$ GeV. However, even with a branching fraction of 10^{-3} the signal would most likely be dominated by large backgrounds at the LHC. Larger flavor violating couplings are still possible for even larger values of the 5D Yukawas, although calculability and perturbativity become then a greater issue. More detailed analysis of the possibility and feasibility of this channel is left for future studies.

3.8 Summary

We presented analysis of the Higgs mediated flavor violation in the warped models. We have shown that the these effects are generic and cannot be decoupled by changing Higgs localization. We analyzed low energy bounds from neutral meson

oscillations, and we have shown that for the light Higgs, contribution to the ϵ_K mediated by the flavor violating couplings of the Higgs field becomes comparable to the contribution of the KK gluon analyzed in the previous chapter. We have also studied effects that might be interesting for the collider physics, such as modification of the Higgs branching fractions, and flavor violating Higgs and top decays.

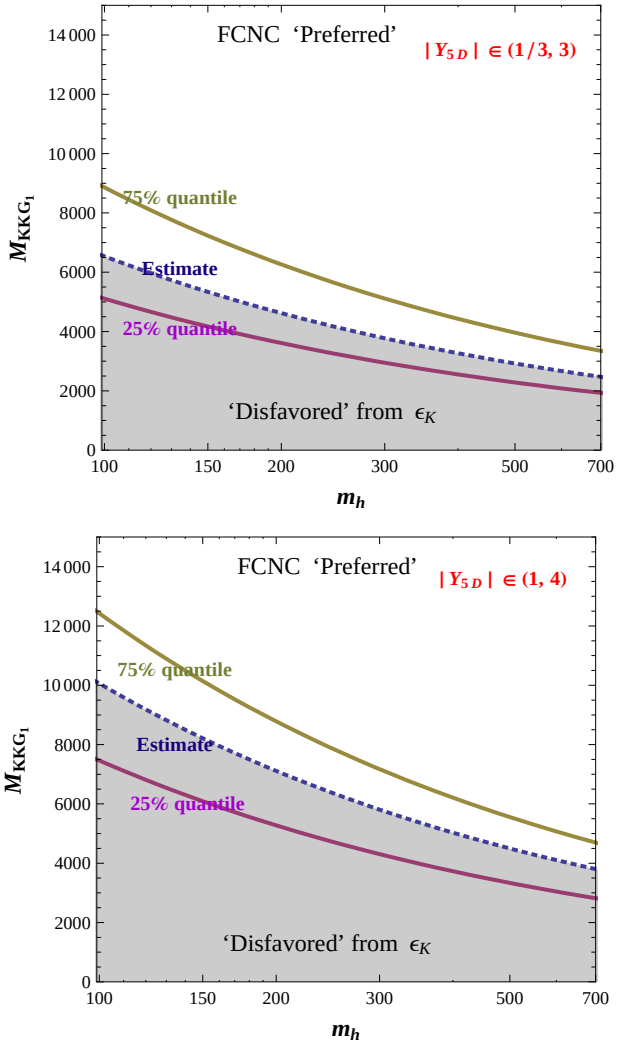

Figure 3.5: Generic bounds in the plane (m_h, M_{KKG_1}) coming from ϵ_K due to tree level Higgs exchange, where m_h is the Higgs boson mass and M_{KKG_1} is the mass of the first excited KK gluon. We perform a scan over 5D Yukawa matrices (such that $|Y_{5D}^{ij}| \in [0.3, 3]$ (left panel) and $|Y_{5D}^{ij}| \in [1, 4]$ (right panel)) and over fermion bulk c-parameters. In the scan, we choose $Y_1^{5D} = Y_2^{5D}$ and take the $\beta \to \infty$ limit (the result has only a mild dependence on β). The 25% quantile and 75% quantile curves trace the points in this plane where 25% and 75% of the randomly generated parameter points are safe from Higgs mediated FCNC's (and are otherwise in agreement with the rest of experimental constraints in the scenario). The "estimate" curve is based on the expected size of Higgs flavor violating couplings (see Eqs. (3.69) and (3.70)) for the chosen range of the 5D Yukawas.

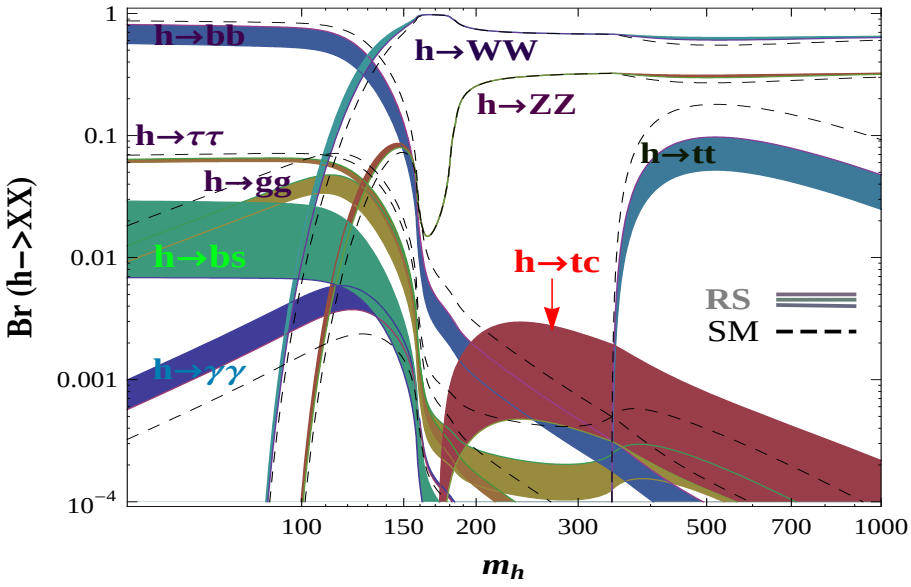

Figure 3.6: Higgs decay branching fractions as a function of its mass, for the case of 5D Yukawas such that $|Y_{5D}^{ij}| \in [1, 4]$ and for a KK scale $R'^{-1} = 1500$ GeV ($M_{KKG_1} = 2.45R'^{-1}$). The dashed curves represent the SM branching fractions, and the color bands correspond to 25% and 75% quantiles of our scan results. The $h \to tt$ curve shows a suppressed branching due to suppressed htt couplings. This same type of suppression happens in the hbb couplings, which in turn enhances important channels such as $h \to \gamma\gamma$. Of course Higgs production through gluon fusion is also suppressed due to suppressed htt couplings, but vector boson fusion is assumed to remain as in the SM, allowing one to probe at the LHC these relative changes in the couplings. We note also the appearance of two new important channels, $h \to bs$ and $h \to tc$, the second of which could be looked at at the LHC if the Higgs happens to be discovered (in the ZZ channel) in the appropriate mass regime.

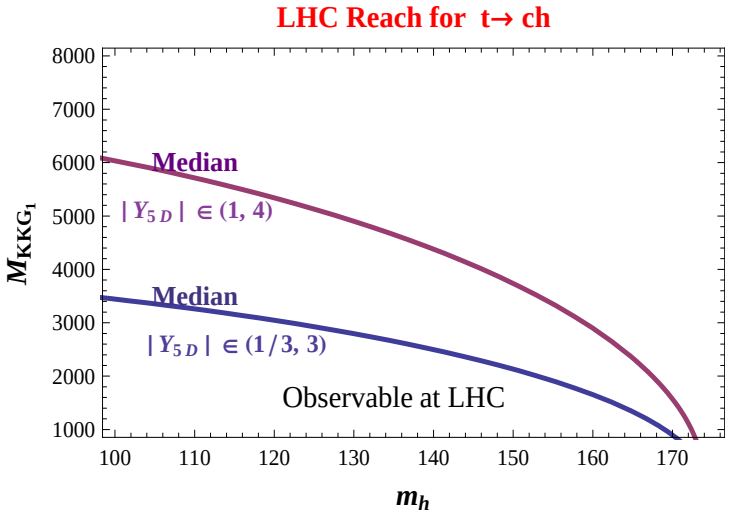

Figure 3.7: LHC observability of the exotic decay of the top quark $t \to ch$ in the plane (m_h, M_{KKG_1}). The two curves trace the region such that 50% of the generated points in our two scans (one with $|Y^{ij}_{5D}| \in [0.3, 3]$ and another with $|Y^{ij}_{5D}| \in [1, 4]$) will have a visible signal at the LHC.

Chapter 4

Radion mediated flavor violation

4.1 Radion and stabilization of the extra dimension

So far we have been ignoring all the new physics processes associated with the gravitational degrees of freedom. In this chapter we will analyze the properties and interactions of the radion, the four dimensional scalar degree of freedom of the five dimensional gravity multiplet.

In the original Randall-Sundrum (RS1) setup [1], the radion phenomenology was extensively studied and analyzed [46, 47, 48]. But it was not until relatively recently [49, 50, 51] that radion interactions with bulk SM fields were fully considered. In this chapter I will study the flavor structure of the radion interactions with SM fermions, and I will show that these interactions are generically flavor violating. Then I will proceed with the analysis of the phenomenological consequences of this flavor violation.

We can parametrize radion by the following scalar perturbation of the metric,

$$ds^2 = \left(\frac{R}{z}\right)^2 (e^{-2F}\eta_{\mu\nu}dx^\mu dx^\nu - (1+2F)^2 dz^2). \tag{4.1}$$

Demanding that the perturbed metric solves the Einstein equation and that the kinetic term of the radion field is properly normalized, we get

$$F = \frac{r(x)}{\Lambda_r}\frac{z^2}{R'^2}, \tag{4.2}$$

where $r(x)$ is the corresponding canonically normalized radion field with its associated interaction scale $\Lambda_r = \sqrt{6}\frac{R}{R'}M_{Pl}$.

In the original RS model (RS1) the interbrane distance was not fixed, thus the radion degree of freedom was massless (radion oscillations correspond to the change of the length of the extra dimension). One can address this problem of the stabilization of the interbrane distance [19] by simply adding an extra scalar field to the action

$$\begin{aligned} S_{bulk} &= \int d^4x \int dz\sqrt{g}\left(G^{AB}\partial_A\Phi\partial_B\Phi - m^2\phi^2\right) \\ S_{UV} &= \int \partial^4x\sqrt{g_{uv}}\lambda_{UV}(\Phi^2 - v^2) \\ S_{IR} &= \int \partial^4x\sqrt{g_{IR}}\lambda_{IR}(\Phi^2 - v^2). \end{aligned} \tag{4.3}$$

In the limit when $\lambda_{UV}, \lambda_{IR}$ are sufficiently large it becomes energetically favourable for the scalar field to be equal to $\Phi|_{UV,IR} = v_{UV,IR}$ at the boundaries, then interbrane distance will be stabilized and can be approximated as

$$kr \approx \frac{4}{\pi}\frac{k^2}{m^2}\ln\left(\frac{v_{UV}}{v_{IR}}\right). \tag{4.4}$$

So when v_{UV} and v_{IR} are of the same order, it is enough to have $\frac{k^2}{m^2} \sim 10$ to generate required hierarchy. It is important to note that the radion becomes massive after stabilization of the interbrane distance.

4.2 Couplings to fermions

In the discussion presented here we will not specify precise stabilization mechanism and treat radion mass as a free parameter, we also will neglect back reaction

of the radion on the metric and in this case it is generically expected for the radion to be the lightest new physics state [47, 4]. The couplings between bulk SM fermions and the radion are calculated in [50] in the case of one generation, with a brane localized Higgs. We are interested here in the flavor structure of these couplings when all families of fermions are considered, and for the more general case of a 5D bulk Higgs $\mathcal{H}$ [39]. To this end let us focus on the up-sector of the simple setup in which we consider the 5D fermions $\mathcal{Q}_i$, $\mathcal{U}_i$, with flavor indices $i, j = 1, 2, 3$. They contain the 4D SM $SU(2)_L$ doublet and singlet fermions respectively with a 5D action

$$\begin{aligned} S_{\text{fermion}} = & \int d^4x dz \sqrt{g} \Big[\frac{i}{2} \left(\bar{\mathcal{Q}}_i \Gamma^A \mathcal{D}_A \mathcal{Q}_i - \mathcal{D}_A \bar{\mathcal{Q}}_i \Gamma^A \mathcal{Q}_i \right) \\ & + \frac{c_{q_i}}{R} \bar{\mathcal{Q}}_i \mathcal{Q}_i + (\mathcal{Q} \to \mathcal{U}) + \left(Y_{ij} \sqrt{R}\ \bar{\mathcal{Q}}_i \mathcal{H} \mathcal{U}_j + h.c. \right) \Big] \end{aligned} \tag{4.5}$$

where $\frac{c_{q_i}}{R}$, $\frac{c_{u_i}}{R}$ are the 5D fermion masses, and we choose to work in the basis where they are diagonal in 5D flavor space (we will proceed in the same way as we did for the Higgs field by calculating exact wavefunctions in the presence of the Higgs vev). The bulk Higgs acquires a nontrivial vacuum expectation value $v(z)$ localized towards the IR brane solving the Planck-weak hierarchy problem. After writing the 5D fermions in two component notation, $\mathcal{Q}_i = \begin{pmatrix} \mathcal{Q}_L^i \\ \bar{\mathcal{Q}}_R^i \end{pmatrix}$ and $\mathcal{U}_i = \begin{pmatrix} \mathcal{U}_L^i \\ \bar{\mathcal{U}}_R^i \end{pmatrix}$, we perform a "mixed" KK decomposition as

$$\mathcal{Q}_L^i(x,z) = q_L^{ij}(z)\, Q_L^j(x) + ... \tag{4.6}$$

$$\bar{\mathcal{Q}}_R^i(x,z) = q_R^{ij}(z) \bar{U}_R^j(x) + ... \tag{4.7}$$

$$\mathcal{U}_L^i(x,z) = u_L^{ij}(z) Q_L^j(x) + ... \tag{4.8}$$

$$\bar{\mathcal{U}}_R^i(x,z) = u_R^{ij}(z)\, \bar{U}_R^j(x) + ... \tag{4.9}$$

where we have only written the 4D SM fermions $Q_L^j(x),\ U_R^j(x)$ and where $q_{L,R}^{ij}(z),\ u_{L,R}^{ij}(z)$ are the corresponding profiles along the extra dimension. The fields $Q_L^i(x)$ and $U_R^j(x)$ satisfy the Dirac equation

$$-i\bar{\sigma}^\mu \partial_\mu Q_L^i + m_{ij}\, \bar{U}_R^j = 0, \tag{4.10}$$

$$-i\sigma^\mu \partial_\mu \bar{U}_R^i + m_{ij}\, Q_L^j = 0, \tag{4.11}$$

with the 4D SM fermion mass matrix m_{ij} not necessarily diagonal in flavor space. The couplings between radion and SM fermions can be calculated by inserting the perturbed metric of Eq. (4.1) and the 5D fermion KK decompositions of Eqs. (4.6-4.9) into the action of Eq. (4.5). To proceed we used a perturbative approach treating the 4D fermion masses m_{ij} as small expansion parameters (i.e. we assumed $m_{ij}R' \ll 1$) keeping only first order terms. In this limit, the profiles $q_L^{ij}(z)$ and $u_R^{ij}(z)$ match the simple wave-functions for massless zero-modes. No other explicit profile solution is required since we just need to properly insert and use the KK equations for $q_R^{ij}(z)$ and $u_L^{ij}(z)$ into Eq. (4.5). A subtlety however is that the 5D bulk Higgs field perturbation contains itself some radion degree of freedom. This can be seen from solving the Higgs equations of motion in the perturbed background of Eq. (4.1), which requires the KK expansion of the 5D Higgs field to be of the form

$$\mathcal{H}(x,z) = v(z) - \frac{z^3 v'(z)}{R'^2}\left[1 - \left(\frac{R'}{z}\right)^2\right]\frac{r(x)}{\Lambda_r} + \cdots \tag{4.12}$$

where the ellipses contain the 4D light Higgs and the rest of the Higgs KK modes. This result gives an additional contribution to the radion coupling to fermions.

Combining all the contributions to the radion couplings will lead to the following formula

$$-\frac{r(x)}{\Lambda_r}\left(Q_L^i U_R^j + \bar{Q}_L^i \bar{U}_R^j\right) m_{ij}^u \left[\mathcal{I}(c_{q_i}) + \mathcal{I}(-c_{u_j})\right], \tag{4.13}$$

where we have defined

$$\mathcal{I}(c) = \left[\frac{(\frac{1}{2}-c)}{1-(R/R')^{1-2c}} + c\right] \approx \begin{cases} c & (\,c > 1/2\,) \\ \frac{1}{2} & (\,c < 1/2\,) \end{cases} \tag{4.14}$$

For one generation of fermions, this result agrees with the formulae obtained in [50] and it can also be understood from the following intuitive argument. When the 4D SM fermion mass is generated near the IR brane, its dependence on $\frac{1}{R'}$ is

$$m_{ij} \propto f(c_{q_i}) f(-c_{u_j}) \frac{R}{R'} \tag{4.15}$$

with $f(c)$ proportional to the zero mode wavefunction of the fermions evaluated at the IR brane

$$f(c) = \sqrt{\frac{1-2c}{1-(R/R')^{1-2c}}} \tag{4.16}$$

Since the radion is basically a fluctuation of the IR brane location, its couplings with the SM fermions can also be obtained by replacing $\frac{1}{R'} \to \frac{1}{R'}(1-\frac{r}{\Lambda_r})$ in the fermion mass matrix [50]. Then it is easy to check that we reproduce the result of Eq. (4.13). Non-univeralities in the term $\left[\mathcal{I}(c_{q_i}) + \mathcal{I}(-c_{u_j})\right]$ will lead to a misalignment between the radion couplings and the fermion mass matrix.[1] After diagonalization of the fermion mass matrix, flavor violating couplings will be generated and

[1]This will remain true in the presence of fermion brane kinetic mixings although the flavor structure of Eq. (4.13) will be modified.

can be parametrized as

$$\mathcal{L}_{FV} = \frac{r}{\Lambda_r}(\bar{U}_L^i U_R^j a_{ij}\sqrt{m_i m_j} + \text{h.c.}) \qquad (i \neq j) \tag{4.17}$$

where U^i are the quark mass eigenstates with masses m_i. The extension to the down quark sector and charged leptons is straightforward.

To study the consequences of this result, we will consider models with flavor anarchy i.e. where all the hierarchies in the fermion sector are explained by the warp factors and all 5D Lagrangian parameters are of the same order [6]. In this class of models the natural size of a_{ij} is

$$a_{ij} \sim (\Delta\mathcal{I}_{ij})\sqrt{\frac{f(c_{qi})f(-c_{uj})}{f(c_{qj})f(-c_{ui})}} \tag{4.18}$$

where $\Delta\mathcal{I}_{ij} \sim O(0.1)$ is the deviation of $\left[\mathcal{I}(c_{q_i}) + \mathcal{I}(-c_{u_j})\right]$ from its mean value.[2] We perform a scan over the 5D fermion masses and "anarchical" Yukawa couplings leading to the observed SM fermion masses and CKM mixing angles and obtain a distribution for the parameters a_{ij}. For example, the average values of the parameter a_{12}^d and a_{21}^d are of order ~ 0.07 and 70% of the time they are distributed between $0.03 < a_{12}^d,\, a_{21}^d < 0.12$. The average values of the parameter $a_{23}^u(a_{32}^u)$ are $\sim 0.08(0.05)$ and 70% of the times they are between $0.03 < a_{23}^u < 0.13$ $(0.01 < a_{32}^u < 0.09)$.

4.3 Radion phenomenology

The first thing to study is how constrained are the radion parameters due to low energy observables such as $\Delta F = 2$ processes. The strongest constraints

[2]This estimate is only valid for models that explain the Planck-weak hierarchy. But for little RS models [52], the deviation could be a few times larger.

come from the parameter ϵ_K of $K_0 - \bar{K}_0$ oscillations where a single radion exchange contributes to the standard dimension six operators $Q_2(Q_2') = (\bar{d}_{L(R)} s_{R(L)})(\bar{d}_{L(R)} s_{R(L)})$ and $Q_4 = (\bar{d}_R s_L)(\bar{d}_L s_R)$. The model independent bound on the size of new physics contributions to the imaginary part of the Wilson coefficient C_{4K} of the operator Q_4, renormalized at the scale 50 GeV, is $\mathrm{Im}C_4 \lesssim 1.2 \times 10^{-10}\mathrm{TeV}^{-2}$ [21].[3] From Eq. (4.17) it is easy to compute the contribution from a tree-level radion exchange as $\mathrm{Im}(C_4^{radion}) \approx m_d m_s \mathrm{Im}(a_{12}^d a_{21}^{d*})/(\Lambda_r^2 m_r^2)$ and therefore the experimental bound requires that

$$\frac{a_{ds}}{\Lambda_r m_r} < 0.44 \text{ TeV}^{-2}, \tag{4.19}$$

where we have defined $a_{ds} \equiv \sqrt{|a_{12}^d a_{21}^{d*}|}$ and assumed an order one phase. In Fig. 4.1, we show the bounds for different values of a_{ds} in the (m_r, Λ_r) plane. The scale Λ_r is directly related to the lightest KK gluon mass by $M_1^{\mathrm{KKG}} \simeq \Lambda_r/(M_{Pl}R)$, and so one can easily convert bounds on the KK mass into bounds on Λ_r.[4] It is also interesting to note that the bounds from flavor physics give strong constraints for a very light radion, precisely the hardest possibility to probe at the LHC due to its dominant hadronic decay channels. A light radion with flavor violating couplings can also become a top quark decay product, in processes such as $t \to rc$ or $t \to ru$, where u

[3] We used the RG equations in [41]. Constraints on the coefficient C_2 of Q_2 are weaker by a factor of five and the bounds from B_d mixing are weaker by an order of magnitude, so we ignored them in the present analysis.

[4] Note that the value of $M_{Pl}R$ is generally assumed to be at least larger than a few but as argued in [53] it might even be lower than one and still remain in the domain of validity of the theory.

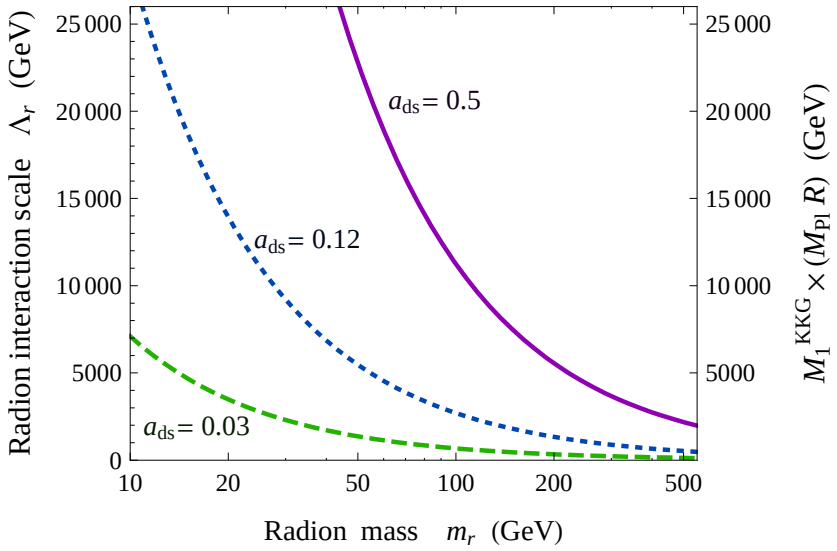

Figure 4.1: Bounds in the $(m_r - \Lambda_r)$ plane coming from ϵ_K for different values of the flavor violating parameter $a_{ds} = \sqrt{|a^d_{12} a^{d*}_{21}|}$. In flavor anarchy models [6], typical values for a_{ds} range between 0.03 and 0.12. In the Little RS scenario [52] this parameter can reach values a few times larger. One can relate the scale Λ_r to the mass of the lightest KK gluon as $M_1^{\rm KKG} \simeq \Lambda_r/(M_{Pl}R)$, as shown on the right-hand side of the figure.

and c are the up and charm quarks. We have checked that, due to the suppressed couplings coming from Λ_r, this signal [**?**] will not be visible at the LHC unless the flavor violating parameters a_{i3} or a_{3i} take unnaturally large values of order one.

For a heavier radion ($\gtrsim$ 200 GeV), the most promising discovery channel would be $r \to ZZ \to 4l$ due to its clean signal. Translating the LHC Higgs search analysis [54] into radion LHC reach, one finds that both ATLAS and CMS should separately be able to claim discovery for $\Lambda_r \lesssim 5$ TeV with 30 fb^{-1} of data[55]. To study the flavor structure of such a heavy radion, we consider the channel $r \to \bar{t}c, t\bar{c}$. The signal we focus on is $p\,p \to tc \to b\,l\,\nu\,c$, where l stands for electrons

and muons. In this case, the main backgrounds are: (i) $p,p \to t\,j \to b\,l\,\nu\,j$; (ii) $p,p \to W\,j\,j \to l\,\nu\,j\,j$, where one of the light jet is mistagged as a bottom quark; (iii) $p\,p \to W\,\bar{b}\,b \to b\,\bar{b}\,l\,\nu$, where one of the b-jet is mistagged; (iv) $p\,p \to \bar{t}\,t \to b\,l^+\,\nu\,\bar{b}\,l^-\,\bar{\nu}$ where one b-jet is mistagged and one of the charged lepton is lost in the beam pipe ($|y_l| > 2.5$) or it is merged with one of the jets ($\Delta R_{jl} < 0.6$). We use CalcHEP [56] and PYTHIA 2.6 [57] to obtain both signal and background cross sections and estimate the potential LHC reach for this signal. For this we fix the radion interaction scale to $\Lambda_r = 2$ TeV, and use three different values for its mass, $m_r = 250, 300$ and 350 GeV. We impose lepton and jet acceptance cuts on the transverse momenta $p_T^{j,l} > 20$ GeV, on the rapidities, $|y_{j,l}| < 2.5$, and on the angular separation $\Delta R_{lj} > 0.6$ and $\Delta R_{jj} > 0.6$. We assume that the neutrino momentum can be reconstructed. We demand additionally that the total invariant mass of the event reconstructs to the radion's mass $M_{bl\nu j} \in (m_r - 5\ \text{GeV}, m_r + 5\ \text{GeV})$, and that the $bl\nu$ invariant mass reconstructs to the top mass $M_{bl\nu} \in (170\ \text{GeV}, 180\ \text{GeV})$. We also tighten the rapidity cut on the light jet, $|y_j| < 1.5$. We assume that the radion would have been discovered through the $r \to ZZ$ channel and thus its mass m_r is known. Because the radion decay width is extremely small ($\Gamma_r < 0.15$ GeV in this mass range), the window to use for the total invariant mass is controlled by the experimental jet energy resolution (we used a window of ± 5 GeV). The results are shown in Table. 4.1. As noted in [51], a small amount of Higgs-radion mixing [46], parametrized by the Lagrangian parameter ξ, can dramatically reduce the principal radion decay channels. This could then enhance secondary decay channels, such as $r \to \gamma\gamma$, and in this case $r \to \bar{t}c(t\bar{c})$. In Fig. 4.2 we plot contours for the LHC reach

(we use the evidence criterion of signal significance $S/\sqrt{B} = 3$) in the (a_{tc} vs. ξ) plane, for $m_r = 250$ GeV and different values of Λ_r. We can see that at least for some ranges of ξ, the LHC should be able to probe typical values of a_{tc} in flavor anarchy models. Of course a more realistic study of this signal should be carried out, including a full detector simulation as well as the hadronic decay mode of the intermediate W boson.

m_r	250 GeV	300 GeV	350 GeV
Signal	$a_{tc}^2 \times 21$ fb	$a_{tc}^2 \times 15$ fb	$a_{tc}^2 \times 9$ fb
Background	280 fb	199 fb	136 fb

Table 4.1: Signal and background for different radion masses with $\Lambda_r = 2$ TeV (and no Higgs-radion mixing). We multiplied by a K-factor of 2.4 for the signal, to account for QCD corrections in the radion production from gluon fusion.

4.4 Summary

We studied radion couplings to fermions in the warped models where SM is in the 5D bulk, and we have shown that these couplings are generically flavor violating. Then we analyzed constraints from low energy observables, which become very strong for the sub hundred GeV radion. Then we discussed possibilities of observing radion flavor violating decays at LHC, and presented signals and backgrounds for different masses of the radion.

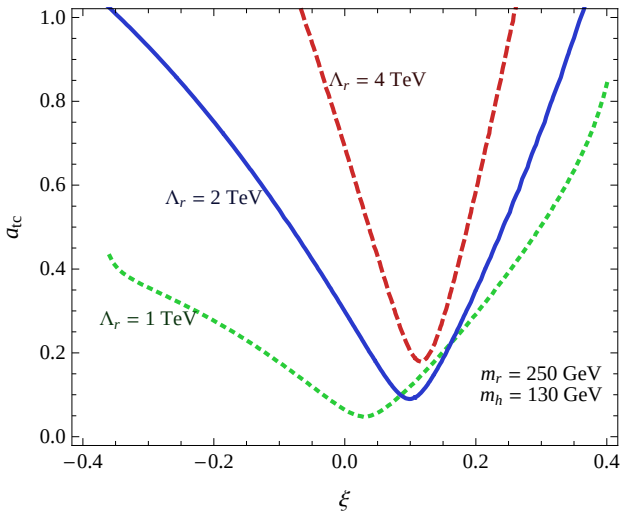

Figure 4.2: Contours in the $(\xi - a_{tc})$ plane of the estimated signal significance $S/\sqrt{B} = 3$ for the process $(pp \to r \to tc)$ at the LHC for 300 fb^{-1} of data. ξ is the Higgs-radion mixing parameter and a_{tc} is the flavor violating parameter which gives rise to the radion coupling to top-charm.

Chapter 5

Conclusions and outlook

I will conclude by summarizing the results presented in this thesis. Warped extra dimensions present a very nice extension of the Standard Model which can address the gauge hierarchy problem as well as explain hierarchies of the fermion masses. In this thesis, we presented an analysis of the flavor violation in the warped models. In the second chapter we analyzed the bounds arising from ϵ_k parameter of $K_0 - \bar{K}_0$ oscillations and exotic decays of b quark $b \to s\gamma$. We found that the constraints from these two processes are complementary, in a sense that they have opposite dependence on the Yukawa couplings of the original five dimensional Lagrangian. We also found that the bound arising from ϵ_k can be relaxed if the Higgs becomes a bulk field. The discussion presented in the thesis was carried out within a two site model, which provides us with an economical description of the five dimensional warped model. Later we matched the two site model to the warped models so the bounds presented can be used for both models. This results in a overall bound of $O(5)$ TeV on the mass of the lightest new physics spin one resonance.

In the third chapter, we presented an analysis of the flavor violation in the Higgs sector. We have shown that generically in the models with warped extra dimensions, simple relation between Higgs Yukawa couplings and masses of the SM fermions is modified. This effect arises from the mixing of SM fermions with their

KK partners due to the Higgs vev and leads to the flavor violating couplings between SM fermions and Higgs boson. In the previous analysis, these effects for the light SM fermions were mistakenly assumed to be negligible, but we have shown that the contribution to ϵ_k mediated by Higgs can be very important and comparable to the contribution of the KK gluon. We checked that these effects are independent of the localization of the Higgs field in the bulk, and cannot be decoupled. Moreover, we have shown that these effects might change top Yukawa coupling by up to 20%, which can be an interesting signal for the collider phenomenology. We also discussed possible exotic decays of the top quark $t \to ch$ and Higgs $h \to tc, h \to \tau\mu$ and we have found that for considerable part of the parameter space these effects might be seen at LHC.

In the last chapter, we discussed radion physics. We derived flavor structure of the couplings of the radion to the fermions in the models where SM fermions are in the bulk. We have shown that these couplings are generically misaligned with SM fermions masses. This leads to flavor changing neutral currents mediated by the radion, and if the radion is light enough, low energy observables such as ϵ_k will put strong constraints on the model parameters. For a heavier radion, we studied possibilities of the flavor changing neutral decays such as $r \to tc$. Although challenging, we still have found an interesting region of the radion parameter space where this effect can be observed, gaining very valuable information on the flavor substructure of the whole model.

At the end I would like to say that the models with warped extra dimension provide a very well motivated extension of the SM, which can address most of the

puzzles of nature. In this thesis, we have shown that RS models, with the lightest new physics states at the few TeV scale, are on the edge of being ruled out by various low energy constraints, and at the same time these models predict a very rich collider phenomenology, so in the nearest future we will be able to tell whether this is the right way to go.

Chapter A

Kaluza Klein decomposition

In this chapter I will discuss Kaluza Klein decomposition in Randall-Sundrum models, I will start with the simplest example of the scalar field, then I will discuss fermions and gauge bosons.

A.1 Scalar field in the bulk

Let us consider a scalar field in extra dimension, the action in this case will be given by

$$S_{scalar} = \int dz \left(\frac{R}{z}\right)^5 \left(\frac{1}{2}\left(\frac{z}{R}\right)^2 (\partial_\mu \phi)^2 - \frac{1}{2}\left(\frac{z}{R}\right)^2 (\partial_z \phi)^2 - \frac{1}{2} M^2 \phi^2\right) \tag{A.1}$$

Now we can apply variational principle to derive equations of motion for the field ϕ, but we have to remember that our fifth dimension is finite and the total divergence term will not vanish any more, leading to the additional terms on the boundaries

$$-\left(\frac{R}{z}\right)^3 \delta\phi \partial_z \phi|_R^{R'}. \tag{A.2}$$

In order to have a consistent theory we need to vanish these terms. We can achieve this by imposing boundary conditions on the field at the UV and IR branes. There are two sets of the boundary conditions we can impose, on each of the branes

$$\begin{aligned} \partial_z \Phi(z)|_{UV,IR} = 0 \;\; \text{Neumann, even} \\ \Phi(z)|_{UV,IR} = 0 \;\; \text{Dirichlet, odd} \end{aligned} \tag{A.3}$$

In the future we will denote the even, odd boundary conditions by $(+,(-))$ respectively. For any field we have to specify both boundary conditions at UV and IR branes so in the notation $\Phi(+,+)$ first sign refers to the UV and the second one to the IR boundary conditions. The Euler-Lagrange equations will look like:

$$-\partial_z^2\Phi + \frac{3}{z}\partial_z\Phi + \Box\Phi + M^2R_0^2\frac{\Phi}{z^2} = 0. \tag{A.4}$$

Now we can decompose our field in terms of the KK modes.

$$\Phi(z) = \sum_n f^n(z)\phi^n(x) \tag{A.5}$$

where each of the $f^n(z)$ satisfies,

$$-\partial_z^2 f^n(z) + \frac{3}{z}\partial_z f^n(z) - m_n^2 f^n(z) + M^2R_0^2\frac{f^n(z)}{z^2} = 0, \tag{A.6}$$

and $f^n(z)$ are normalized in the following way

$$\int_R^{R'} dz \left(\frac{R}{z}\right)^3 \left(f^n(z)\right)^2 = 1. \tag{A.7}$$

The general solution of this equation will be given by

$$\begin{aligned} \Phi &= N_n z^2 \left(J_\alpha(m_n z) + b_n Y_\alpha(m_n z)\right), \\ \alpha &= \sqrt{4 + M^2R^2}, \end{aligned} \tag{A.8}$$

where N_n is a normalization constant, coefficients b_n are fixed from the boundary condition, and KK masses can be found by solving the following equations:

$$\begin{aligned} \phi(+,+) : b_n &= -\frac{J_{\alpha-1}(m_nR') + \frac{2-\alpha}{m_nR'}J_\alpha(m_nR')}{Y_{\alpha-1}(m_nR') + \frac{2-\alpha}{m_nR'}Y_\alpha(m_nR')} = -\frac{J_{\alpha-1}(m_nR) + \frac{2-\alpha}{m_nR}J_\alpha(m_nR)}{Y_{\alpha-1}(m_nR) + \frac{2-\alpha}{m_nR'}Y_\alpha(m_nR)} \\ \phi(-,-) : b_n &= -\frac{J_\alpha(m_nR')}{Y_\alpha(m_nR')} = -\frac{J_\alpha(m_nR)}{Y_\alpha(m_nR)} \\ \phi(-,+) : b_n &= -\frac{J_\alpha(m_nR)}{Y_\alpha(m_nR)} = -\frac{J_{\alpha-1}(m_nR') + \frac{2-\alpha}{m_nR'}J_\alpha(m_nR')}{Y_{\alpha-1}(m_nR') + \frac{2-\alpha}{m_nR'}Y_\alpha(m_nR')} \\ \phi(+,-) : b_n &= -\frac{J_{\alpha-1}(m_nR) + \frac{2-\alpha}{m_nR}J_\alpha(m_nR)}{Y_{\alpha-1}(m_nR) + \frac{2-\alpha}{m_nR'}Y_\alpha(m_nR)} = -\frac{J_\alpha(m_nR')}{Y_\alpha(m_nR')}. \end{aligned} \tag{A.9}$$

In the limit when $m_n R' >> 1$ KK masses become equally separated (in this limit Bessel function can be expressed in terms of trigonometrical functions) and for example for $(+,+)$ case

$$m_n \simeq \frac{\pi}{R'}\left(n + \frac{\alpha}{2} - \frac{3}{4}\right) \tag{A.10}$$

A.2 Fermions in the bulk

In this section we will show some details of the calculations for the discussion of the fermions in section 1.3.0.1. Let us consider now a single fermion in the bulk, then the action will be:

$$S = \int dz \left(\frac{R}{z}\right)^5 \left[\frac{i}{2}\bar{\psi} e_A^M \Gamma^A D_M \psi - \frac{i}{2}\left(D_M\psi\right)^\dagger e_A^M \Gamma^A \psi - c\bar{\psi}\psi\right] \tag{A.11}$$

where Γ^A are 5D γ matrices of Dirac equation, e_A^M and D_M are funfbeins and covariant derivatives, and for the RS metric they are equal to:

$$\begin{aligned} \Gamma^A = (\gamma^\mu, -i\gamma^5) \quad e_M^A = \frac{R}{z}\delta^{AM} \\ D_\mu = \partial_m u - \frac{i}{2}\gamma_5\gamma_\mu\frac{R}{z}. \end{aligned} \tag{A.12}$$

So finally the action becomes equal to

$$\int dz \left(\frac{R}{z}\right)^4 \left[\frac{i}{2}\bar{\psi}\Gamma^M\partial_M\psi - \frac{i}{2}(\partial_M\psi)^\dagger\gamma_0\Gamma^M\psi - \frac{c\bar{\psi}\psi}{z}\right]. \tag{A.13}$$

Then Euler-Lagrange equations will look like

$$\begin{aligned} &\frac{\partial\mathcal{L}}{\partial\bar{\psi}} = \frac{1}{z^4}(\frac{i}{2}\Gamma^M\partial_M\psi - \frac{c\psi}{z}) \\ &\partial_M\frac{\partial\mathcal{L}}{\partial(\partial_M\bar{\psi})} = \partial_M(-\frac{i}{2z^4}\Gamma^M\psi) = -\frac{i}{2z^4}\Gamma^M\partial_M\psi + \frac{2\gamma_5}{z^5}\psi \\ &i\partial\!\!\!/\psi + \gamma^5\partial_z\psi - \frac{2}{z}\gamma^5\psi - \frac{c}{z}\psi = 0 \end{aligned} \tag{A.14}$$

and in the 4D momentum space

$$\left(\not{p} + \gamma_5 \partial_z - \frac{2}{z}\gamma_5 - \frac{c}{z}\right)\psi = 0. \tag{A.15}$$

Now we can rewrite this equation using 4D chiral chiral fields ψ_L, ψ_R

$$\begin{aligned} \not{p}\psi_L + \left(\partial_z - \frac{2+c}{z}\right)\psi_R = 0 \\ \not{p}\psi_R + \left(-\partial_z - \frac{-2+c}{z}\right)\psi_R = 0 \end{aligned} \tag{A.16}$$

Performing KK decomposition for the fields $\psi_{L,R}$

$$\psi_{L,R}(x,z) = \sum_n \psi^{(n)}_{L,R}(x) f^n_{L,R}(c,z) \tag{A.17}$$

will lead us to the coupled differential equations for the left handed and right handed profiles

$$\begin{aligned} m_n f_R + \left(-\partial_z + \frac{2}{z} - \frac{c}{z}\right) f_L = 0 \\ m_n f_L + \left(\partial_z - \frac{2}{z} - \frac{c}{z}\right) f_R = 0. \end{aligned} \tag{A.18}$$

One can see that left handed and right handed profiles satisfy the following equations

$$\begin{aligned} -m_n^2 f_R - \partial_z^2 f_R + \frac{4}{z}\partial_z f_R + \frac{c^2 - c - 6}{z^2} f_R = 0, \\ -m_n^2 f_L - \partial_z^2 f_L + \frac{4}{z}\partial_z f_L + \frac{c^2 + c - 6}{z^2} f_R = 0, \end{aligned} \tag{A.19}$$

where the general solutions are given by

$$\begin{aligned} f_R(z) = N_n z^{5/2}\left[J_{-1/2+c}(m_n z) + b_n Y_{-1/2+c}(m_n z)\right], \\ f_L(z) = N_n z^{5/2}\left[J_{1/2+c}(m_n z) + b_n Y_{1/2+c}(m_n z)\right]. \end{aligned} \tag{A.20}$$

Coefficients b_n and KK masses m_n are fixed from boundary conditions similar to those presented for the scalar field and normalization is fixed by the condition

$$\int_R^{R'} \left(\frac{R}{z}\right)^4 \left(f_{L,R}^n\right)^2 dz = 1. \tag{A.21}$$

For the $(+,+)$ boundary condition we will have a massless mode in the KK decomposition with the following profile

$$f_0(c,z) = f(c) \left(\frac{z}{R}\right)^{2-c} \frac{1}{\sqrt{R_0}} \left(\frac{R}{R'}\right)^{1/2-c} \tag{A.22}$$

where

$$f(c) = \sqrt{\frac{1-2c}{1-(R'/R)^{2c-1}}}. \tag{A.23}$$

A.2.1 KK decomposition of gauge boson

Now we will consider the gauge bosons in the bulk, the 5D action will be given by

$$\int_R^{R'} dz \left(\frac{R}{z}\right)^5 F_{MN} F^{MN}, \tag{A.24}$$

where F_{MN} is five dimensional field strength. Again in order to have a consistent theory we have to impose boundary conditions on the field A_M. One can see that A_μ and fifth component A_5 of the vector field satisfy opposite boundary conditions. For $A_\mu(+,+)$ boundary conditions we will have a massless vector boson in the KK decomposition, and for the $A_\mu(-,-)$ case (which corresponds to the $A_5(+,+)$ boundary conditions) we will have a massless scalar in the spectrum (A_5 is scalar from 4D point of view). It is obvious now that for the SM gauge bosons we have to

impose even $A_\mu(+,+)$ boundary conditions on both UV and IR branes. Performing KK decomposition

$$\begin{aligned} A_\mu(z,x) &= \sum_n A_\mu^n(x) f_A^n(z) \\ \partial_z^2 f_A^n - \frac{\partial_z}{z} f_A^n + m_n^2 &= 0 \end{aligned} \tag{A.25}$$

leads to the following solution

$$\begin{aligned} f_A^n(z) &= N_n z \left(J_1(m_n z) + b_n Y_1(m_n z) \right) \\ b_n &= -\frac{J_0(m_n R')}{Y_0(m_n R')} = -\frac{J_0(m_n R)}{Y_0(m_n R)} \end{aligned} \tag{A.26}$$

The mass of the lightest KK mode will be equal to $m_{KK}^1 = 2.54 R'^{-1}$ It is interesting that in the y coordinates the profile looks very simple and can be roughly approximated by

$$f_A^1(y) \sim \begin{cases} 0 < y < \pi r - \frac{1}{k} & -\frac{1}{\pi r \sqrt{k}} \\ \pi r - \frac{1}{k} < y < \pi r & \sqrt{k} \end{cases} \tag{A.27}$$

It is important to point out that the zero mode for $A_\mu(+,+)$ has a flat $f_A^0 = const$ profile, which is required by 4D gauge invariance.

Chapter B

Matching 4D and 5D theories

B.1 Matching gauge couplings

In order to make predictions in the warped models we need to know the couplings of the five dimensional lagrangian, so we need to know how to relate them to the couplings of the SM. Let us look on the action of the gauge field, generically we can rewrite it as

$$\int d^4x \left[-\frac{1}{4g_{UV}^2} TrF_{\mu\nu}^2 - \frac{1}{4g_{IR}^2} TrF_{\mu\nu}^2 - \int dz \left(\frac{R}{z}\right) \frac{1}{4g_{5D}^2} TrF_{\mu\nu}^2 \right] \tag{B.1}$$

where $-\frac{1}{4g_{UV,IR}^2}$ refer to the terms localized on the UV and IR branes respectively. Then using the fact that the zero mode of the gauge boson is flat we should match couplings in the following way

$$\frac{1}{g^2} = \frac{1}{g_{UV}^2} + \frac{1}{g_{IR}^2} + \frac{R \ln(R'/R)}{g_{5D}^2}, \tag{B.2}$$

but because we are matching our couplings at the TeV scale we have to add running of the UV localized term which modifies equation to

$$\frac{1}{g^2} \approx \frac{1}{g_{UV}^2} + \frac{1}{g_{IR}^2} + \ln(R'/R) \left(\frac{R}{g_{5D}^2} + \frac{b}{8\pi^2} \right) \tag{B.3}$$

[58, 59], where b comes from one loop running effects.

Let us apply now this discussion to the matching of the QCD coupling, this becomes especially important for the calculation of the ϵ_k. The value of the 5D coupling $g_5\sqrt{k}$ can be fixed by matching it to the $4D$ QCD coupling,

- $g_5\sqrt{k} \sim 3$ for matching at the *loop* level, i.e., including the b^{QCD} term with zero bare/tree-level brane kinetic terms and with a Planck-weak hierarchy. Clearly, this is the *smallest* allowed value of g_* for this hierarchy.

- $g_5\sqrt{k} \sim 6$ for matching at the *tree*-level, i.e., neglecting the b^{QCD} term, with no brane kinetic terms[1].

In general, the value of $g_5\sqrt{k}$ can be even larger than above if we allow non-zero (positive) brane kinetic terms (on the Planck or TeV brane). In particular, with non-zero *Planck* brane localized kinetic terms, the couplings of (lightest) gauge KK are still set by $g_5\sqrt{k}$ since these modes are localized near TeV brane. Thus, the KK coupling (measured in units of SM gauge coupling) also increases as these brane kinetic terms are increased. On the other hand, allowing (sizeable) TeV brane localized kinetic terms has a more interesting effect as follows. The value of $g_5\sqrt{k}$ (again measured in units of the SM gauge coupling) increases as in the case of the Planck brane localized kinetic terms, but the KK gauge coupling is clearly determined by the kinetic term localized on the TeV brane where the KK modes are localized (instead of being set by $g_5\sqrt{k}$). As the size of the brane kinetic terms increases, it turns out that the gauge KK coupling (measured in units of the SM gauge coupling as usual) becomes weaker [60]. At the same time, the mass of the lightest KK mode becomes smaller in such a way that ratio

$$\frac{\text{KK coupling constant}}{\text{Lightest KK mass in units of } ke^{-k\pi R}} \tag{B.4}$$

[1]Equivalently, choosing the tree-level brane kinetic term to cancel the loop contribution": see discussion in [11].

stays roughly the same (for moderately large brane terms), up to $O(1)$ factors. The flavor-violating amplitude (in units of $ke^{-k\pi R}$) depends on precisely the above ratio. So it is clear that large TeV brane terms can allow lighter KK states to satisfy the flavor constraints, but it will *not* allow a reduction in the scale $ke^{-k\pi R}$ which might be the one more relevant (than the lightest KK mass scale) for the fine tuning in EWSB. Although a detailed analysis of TeV brane kinetic terms is beyond the scope of this paper, it is important to keep in mind that such terms can affect the bounds on the scale $ke^{-k\pi R}$ by $O(1)$ factors.

B.1.0.1 Perturbativity bound on size of $5D$ gauge coupling

On the other hand, an *upper* bound on g_5^{QCD} coupling can also be obtained from the condition of perturbativity of the $5D$ QCD theory in the following way. We can estimate the loop expansion parameter for this theory by comparing the one-loop correction to the tree-level value of a coupling (or comparing a two-loop correction to a one-loop effect). This loop expansion parameter grows with energy (or number of active KK modes) due to the non-renormalizability of $5D$ couplings. So, the number of KK modes below the $5D$ cut-off, denoted by N_{KK}, can then be estimated by setting this loop expansion parameter to be ~ 1 (see, for example [61]). As an example, we can *estimate* the one-loop correction to the tree-level value of the three KK gluon coupling arising from this interaction itself. Including color and helicity factors of ~ 3 each for this loop diagram (see, for example, reference [62]),

we find:

$$\frac{\left(g_5^{QCD}\sqrt{k}\right)^2 3\times 3}{16\pi^2} N_{KK} \;\sim\; 1 \tag{B.5}$$

where $\sim \left(g_5^{QCD}\sqrt{k}\right)$ is coupling of 3 KK gluons and the single power of N_{KK} (i.e., single KK sum) follows from KK number conservation at the purely KK gluon vertices. Equivalently, the dimension of g_5^{QCD} being $-1/2$ implies that the $5D$ loop expansion parameter is $\sim (g_5^{QCD})^2 E/\left(16\pi^2\right)$ with $E/k \sim$ being the number of active KK modes.

We can also instead consider the one-loop self-corrections to the coupling of KK gluon to two KK fermions, where the helicity factor of 3 is absent (in this sense, the estimate in Eq.(B.5) is conservative). The estimate in Eq. (B.5) leads to the following values of the number of KK modes below cutoff:

- $N_{KK} \sim 2$ for $g_5^{QCD}\sqrt{k} \sim 3$ which is again the smallest $g_5^{QCD}\sqrt{k}$ allowed for Planck-weak hierarchy (i.e., with loop-level matching of the $5D$ coupling to the $4D$ coupling and with no bare/tree-level brane kinetic terms).

- Whereas for $g_5^{QCD}\sqrt{k} \sim 6$ (i.e., with tree-level matching of the $5D$ coupling to the $4D$ coupling with no brane kinetic terms), there seems to be hardly any energy regime where the $5D$ theory is weakly coupled, i.e., $N_{KK} < 2$.

This conclusion about perturbativity for the $g_5^{QCD}\sqrt{k} \sim 6$ case is valid even if we do *not* include the helicity factor of ~ 3 as would be the case for the estimate of loop expansion parameter using the KK gluon coupling to two KK fermions (instead of coupling of three KK gluon coupling). So with this perturbativity motivation

(and using the correspondence in Eq. B.3), we have focused on using $g_{s*} \sim 3$ in our analysis of the two-site model, but of course, one should understand that these conclusions are just estimates.

B.1.1 ϵ_k in the bulk Higgs

In this section we will prove that bulk Higgs will relax the ϵ_k bound. First thing to note is that from analysis of the fermion KK modes the following relation is approximately true

$$\frac{f_0(c, R')}{f_n(c, R')} \approx \frac{f(c)}{\sqrt{2}} \tag{B.6}$$

Also we will assume the Higgs is a 5D scalar defined in the model [39] in this case the Higgs *vev* profile, is given by brane:

$$v(\beta, z) = v_4 z_v \sqrt{\frac{2(1+\beta)}{z_h^3(1-(z_h/z_v)^{2+2\beta})}} \left(\frac{z}{z_v}\right)^{2+\beta}. \tag{B.7}$$

The couplings between fermion zero modes and Higgs (Y_0), fermion KK modes and Higgs (Y_{KK}), fermion zero modes and gauge KK modes (g_{KK}) are given by overlap integrals of the their profiles multiplied by the $5D$ couplings:

$$\begin{aligned}
Y_0\left(c_L, c_R, \beta\right) &= Y_5^{bulk} \int dz \left(\frac{R}{z}\right)^5 v(\beta, z) f_{0L}(c_L, z) f_{0R}(c_R, z)/v_4 \\
Y_{KK}\left(c_L, c_R, \beta\right) &= Y_5^{bulk} \int dz \left(\frac{R}{z}\right)^5 v(\beta, z) f_{nL}(c_L, z) f_{mR}(c_R, z)/v_4 \\
g_{KK}\left(c_L\right) &= g_5 \int dz \left(\frac{R}{z}\right)^4 f_{Glue}^n(z) f_{0L}(c_L, z) f_{0L}(c_L, z)
\end{aligned} \tag{B.8}$$

where Y_5^{bulk} is defined by $\mathcal{S} \ni \int d^4x dz \sqrt{G}\, Y_5^{bulk} H(x,z) \overline{\Psi(x,z)} \Psi'(x,z)$ (with Ψ and Ψ' being $SU(2)_L$ doublet/singlet and G is the determinant of the metric) and has

mass dimension $-1/2$ just like g_5. Again, Y_{KK} defined above is for KK modes with same chirality as the zero-mode. A similar expression can be obtained for the overlap integrals giving the coupling between KK gluon and two KK fermions which was used to obtain Eq. (B.3).

It is useful to know approximate formulae for these overlap integrals which comes from the the relations of Eq. A.27. For example

$$g_{KK} \approx \left(g_5\sqrt{k}\right)\left(-\frac{1}{k\pi r_c} + f(c_L)f(c_R)\right) \tag{B.9}$$

where pre-factor of "1" that multiplies $f(c_L)f(c_R)$ is almost c-independent for $0.4 \lesssim c \lesssim 0.7$ that is of interest for down-type quarks.

Similarly, we define the parameter $a(\beta, c_L, c_R)$ by

$$Y_0\left(c_L, c_R, \beta\right) = a(\beta, c_L, c_R) Y_{KK}\left(c_L, c_R, \beta\right) f(c_L)f(c_R) \tag{B.10}$$

We find (numerically) that, for fixed Higgs vev profile, the $c_{L,R}$ dependence of a is *very* mild for the range $0.4 \lesssim c \lesssim 0.7$ that is of interest for the down-type quarks and hence we set $c_L = c_R = 0.55$ henceforth when we quote values of a. We give a table for a vs. the parameter β of bulk Higgs (see Table B.1). We see that $a \sim O(1)$ as expected. In detail, the Higgs and KK fermion profiles are localized near the TeV brane so that Y_{KK} is dominated by overlap of profiles in this region. So, we get $Y_{KK} \sim Y_5\sqrt{k}$ (with a mild dependence on c and β), where the $5D$ Yukawa is made dimensionless simply by a factor of $\sim \sqrt{k}$ coming from the normalized profiles at the TeV brane: see Eqs. (B.7). Even though the fermion zero-modes (except for top quark) are localized near the Planck brane, their overlap with the Higgs is still dominated by the region near the TeV brane for the choices of c's relevant for

β	a	M_{KK} ($g_5^{QCD}\sqrt{k}=3$, $Y_{KK}=6$)	M_{KK} ($g_5^{QCD}\sqrt{k}=6$, $Y_{KK}=6$)
0	1.5	3.7 TeV	7.4 TeV
1(two-site)	1	5.5 TeV	11 TeV
2	0.75	7.3 TeV	14.6 TeV
∞ (brane)	0.5	11 TeV	22 TeV

Table B.1: The values of the parameter a (relating zero to KK mode Yukawa couplings: see Eq. (B.10)) in 1st column for different values of the parameter β (2nd column) which determines the profile of the bulk Higgs (Eq. (B.7)). The two-site model and brane Higgs case are also shown as corresponding to specific values of β (see discussion in text). The bound on M_{KK} (from ϵ_K *only*, based on the estimate in Eq. (B.15)) for the purely composite sector (or KK) gauge coupling $g_5^{QCD}\sqrt{k}=3$ (3rd column) and $g_5^{QCD}\sqrt{k}=6$ (last column) are also shown. We fix the composite/KK Yukawa coupling $Y_{KK}=6$ for all entries in the table and $c_L=c_R=0.55$ in order to obtain the value of a.

quark masses[2]. Therefore, using the ratio of fermion zero and KK mode profiles (f's) given in Eq. (B.6), we expect $Y_0 \sim Y_{KK} f(c_L) f(c_R) \sim \left(Y_5\sqrt{k}\right) f(c_L) f(c_R)$, i.e., $a \sim O(1)$. Note that $f(c)$'s can be hierarchical even with small variations in c's, resulting in a solution to the flavor hierarchy problem in the sense that $4D$ Yukawa

[2]For larger values of c's (i.e., fermion zero-modes localized closer to the Planck brane) as relevant for Dirac neutrino masses, the overlaps with Higgs can be dominated by the region near the Planck brane instead [7].

matrix (Y_0) can be hierarchical without any (large) hierarchies in the $5D$ theory, i.e., with anarchic $5D$ Yukawa matrix (or Y_{KK}) and $O(1)$ c's.

The following observation about the parameter a is crucial for the analysis of ϵ_K in next section. Since the fermion zero modes profiles peak near the Planck brane while the fermion KK mode profiles peak near the TeV brane, it is clear that the overlaps of profiles of fermion zero modes with Higgs increase while those of fermion KK modes with Higgs decrease as the Higgs wavefunction moves farther *away* from the TeV brane. Therefore, as seen from this table,

- as we *decrease* the parameter β determining the Higgs profile in Eq. (B.7) – thereby localizing the Higgs away from the TeV brane, the parameter a in Eq. (B.10) *increases*.

We thus expect the opposite limit, $\beta \to \infty$, to reproduce brane Higgs scenario. In fact, for brane-localized Higgs, couplings of fermions to Higgs are simply given by wavefunctions of fermions at TeV brane, i.e., there is *no* overlap integral to be performed:

$$\begin{aligned} Y_0^{brane} &= \left(Y_5^{brane} k\right) f_L f_R \\ Y_{KK}^{brane} &= \left(2 Y_5^{brane} k\right) \end{aligned} \tag{B.11}$$

with $\mathcal{S} \ni \int d^4x \sqrt{G} Y_5^{brane} H(x) \overline{\Psi_L(x, z_v)} \Psi'_R(x, z_v)$. Note that dimension of Y_5 changes from $-1/2$ to -1 as we switch from bulk Higgs to brane-localized Higgs. The factor of two in Y_{KK}^{brane} in second line of Eq. (B.11) comes from the fact that the normalized KK wavefunction at TeV brane is $\approx \sqrt{2k}$ (see Eq. (A.20)). From Eqs. (B.10) and (B.11), the model with brane-localized Higgs (effectively) has $a = 1/2$. And,

the numerical calculation of the overlap integrals for bulk Higgs shows that indeed $a \to 1/2$ for $\beta \to \infty$ (see Table B.1), in agreement with the above expectation.

Now we can see the similarity between the two-site model and the bulk Higgs scenario. First, we compare the gauge couplings between the two cases: Eq. (B.9) and $\mathcal{L}^{SM-SM}$ term of Eq. (2.16), using Eq. (B.3). From these equations, we can make the following identifications:

$$\begin{aligned} s_{L,R} &\leftrightarrow f_{L,R} \\ \frac{1}{k\pi r_c} &\leftrightarrow \tan^2\theta \end{aligned} \tag{B.12}$$

As mentioned above, f_{L_i,R_i} can be hierarchical with small variations in $5D$ fermion mass parameters (c). Therefore, our choice of hierarchical elementary/composite mixing angles ($s_{q,u,d}$) in the two-site model is justified.

We turn to Yukawa couplings and compare Eq. (B.10) with $\mathcal{L}_Y^{\text{SM-SM}}$ term of Eq. (2.15). First, just like for the gauge couplings, we should identify the Higgs coupling to heavy fermions in the two-site model with the Higgs coupling to KK fermions in the $5D$ model[3], i.e.,

$$Y_* \leftrightarrow Y_{KK} \tag{B.13}$$

(In particular, both are assumed to be anarchic.) Then we can see that the two-site and $5D$ Yukawa coupling equations match if $a = 1$. Therefore, we conclude that

- the two-site model "mimics" the bulk Higgs scenario with $\beta \approx 1$ (which has $a \approx 1$). This result is also shown in Table B.1.

[3]Note that, for a fixed β, Y_{KK} is only mildly sensitive to $c_{L,\,R}$'s.

B.1.2 Bound from ϵ_K

Following the arguments of the analysis of ϵ_K for the two-site model, it is clear that, in the bulk Higgs scenario, we get from KK gluon exchange

$$C_{4\,\text{estimate}}^{5D}\left(M_{KK}\right) = \frac{\left(g_5\sqrt{k}\right)^2}{Y_{KK}^2 a\left(\beta\right)^2}\frac{2m_s m_d}{v^2}\frac{1}{M_{KK}^2}, \tag{B.14}$$

where "estimate" has the same meaning as in our analysis of the two-site model. Thus the constraint from ϵ_K is

$$M_{KK} \gtrsim 11\frac{g_5\sqrt{k}}{Y_{KK}a(\beta)}\text{TeV} \tag{B.15}$$

The bounds on M_{KK} for different values of β (i.e., choices of Higgs profiles), including the brane Higgs case and the two-site model is shown in Table B.1 for $g_5^{QCD} = 3, 6$ and $Y_{KK} = 6$.

Now we can compare our results to previous analysis: references [11, 12] used a brane-localized Higgs, i.e., $a \sim 1/2$, with $Y_5^{brane}k \sim 3$, i.e., $Y_{KK} \sim 6$ (from Eq. B.11). They obtained the bound on KK scale of $\sim$ 20(10) TeV for the case of $g_5^{QCD}\sqrt{k} \sim 6(3)$ which agrees with our results in Table B.1. However, from Table B.1, we see that

- for *same* $g_5\sqrt{k}$ and KK Yukawa (Y_{KK}), the bound on M_{KK} from ϵ_K is lowered for a *bulk* Higgs (instead of brane-localized Higgs).

Of course, this reduction in the KK scale for a bulk Higgs relative to the case of brane localized Higgs is due to a smaller coupling of SM fermions to the KK gluon for the bulk Higgs case, i.e., the zero-mode fermions being localized a bit farther

from the TeV brane (where gauge KK modes are localized), than for the brane-localized Higgs case. The crucial point is that, even with this shift of zero-mode fermion profiles relative to the brane-localized Higgs case, the bulk Higgs set-up can maintain the *same* (i.e., SM) value of the zero-mode Yukawa (for the *same* KK Yukawa) as in brane-localized Higgs case. Here, we use the result (explained above) that the ratio of zero-mode to KK Yukawa couplings (denoted by a above) is larger for the bulk Higgs case than for brane-localized Higgs (for fixed fermion profiles).

We remind the reader that we are *not* considering models where Higgs is the 5^{th} component of $5D$ gauge field here. In the Higgs-as-A_5 model, the SM Higgs also has a profile which is peaked near the TeV brane *in a specific gauge* [63]. However, for this model, it was shown in reference [11] that the lower limit on the KK mass scale is ~ 10 TeV for the choices $g_5^{QCD}\sqrt{k} \sim 3$ and $g_5^{EW}\sqrt{k}$ (which is the "effective" $5D$ Yukawa) ~ 6. For larger $g_5^{QCD}\sqrt{k}$ and/or smaller $g_5^{EW}\sqrt{k}$, the bound on KK scale is higher.

B.1.3 Perturbativity limit on size of KK Yukawa

Finally, we wish to illustrate why ϵ_K *by itself* might allow *a few*, say, ~ 3 TeV KK scale, even with *anarchy* in $5D$ flavor parameters, i.e., mixing angles of size as in Eq. (2.21). The point is that the bound on KK scale from ϵ_K depends on size of KK Yukawa as seen in Eq. (B.15). Instead of using $b \to s\gamma$ in order to constrain Y_{KK} (as we did for the two-site model), we can use perturbativity of the $5D$ theory.

Proceeding in the same way as for the gluon coupling, we can estimate N_{KK} from the loop expansion parameter associated with the Yukawa coupling being ~ 1.

For example, we can compare the one-loop correction to the tree-level value of the coupling of Higgs to two KK fermions from this coupling itself (there are no color or helicity factors here). For *brane*-localized Higgs, we get

$$\frac{Y_{KK}^{brane\,2}}{16\pi^2} N_{KK}^2 \;\sim\; 1 \tag{B.16}$$

where N_{KK}^2 (i.e., *double* KK sum) in this loop diagram follows from absence of KK number conservation at the Higgs vertices in the brane-localized Higgs case. One can also derive such growth of the loop expansion parameter with N_{KK} from dimensional analysis, namely, $[Y_5^{brane}] = -1$ such that the $5D$ loop expansion parameter is $\sim Y_5^{brane\,2} E^2/(16\pi^2)$. So, for the brane-localized Higgs case, we get $Y_{KK}^{brane} \sim 4\pi/N_{KK}$ and the choice of $Y_{KK} \sim 6$ (i.e., $Y_5^{brane} k \sim 3$) in references [11, 12] for brane Higgs corresponds to $N_{KK} \sim 2$.

On the other hand, the loop expansion parameter for the *bulk* Higgs case is

$$\frac{Y_{KK}^{bulk\,2}}{16\pi^2} N_{KK} \;\sim\; 1 \tag{B.17}$$

where the *single* power of N_{KK} follows from the single KK sum due to KK number conservation at Higgs vertices for the bulk Higgs case. Equivalently, we can use dimensional analysis, i.e., $[Y_5^{bulk}] = -1/2$ so that the $5D$ loop expansion parameter $\sim Y_5^{bulk\,2} E/(16\pi^2)$ just like for $5D$ gauge theory. Hence, we have for bulk Higgs case, $Y_{KK}^{bulk} \sim 4\pi/\sqrt{N_{KK}}$, i.e.,

- for same N_{KK}, we find that Y_{KK} can be larger for bulk Higgs by $\sim \sqrt{N_{KK}}$ than for the brane-localized Higgs case. Thus the KK mass bound can be lowered even further (*beyond* the point related to the factor a discussed above) as seen from Eq (B.15).

And, in particular,

- we get $Y_{KK}^{bulk} \sim 6\sqrt{2}$ for $N_{KK} \sim 2$ (same as the choice made in references [11, 12]) so that choosing in addition the Higgs profile with $\beta \sim 0$ (so that $a \sim 1.5$) and $g_* \sim 3$, we see from Eq. (B.15) that $M_{KK} \sim 2.6$ TeV might be allowed by ϵ_K constraint.

However, such a low KK scale and large Y_{KK} in the $5D$ model will most likely be very strongly constrained by $\mathrm{BR}\,(b \to s\gamma)$ just as in the case of the two-site model. Note that the bulk Higgs couplings other than $Y_{0,\,KK}$ – for example the mixed (i.e., zero-KK fermion) ones – might not *exactly* mimic the corresponding ones in the two-site model so that our results for $b \to s\gamma$ in the two-site model cannot be directly used for the $5D$ model[4]. A detailed calculation of $b \to s\gamma$ for the $5D$ model is beyond the scope of this work.

B.2 Model Independent Loop Calculation

We work in *non*-unitary gauge for the electroweak gauge sector of the SM, where we must include the would-be Goldstone bosons in the loop. The model-*independent* interaction between a *charged* Higgs, SM down-type quarks (d) and an up-type heavy quark (U) can be parametrized as follows:

$$\mathcal{L} \supset \bar{U}[\alpha_{1i}(1+\gamma_5) + \alpha_{2i}(1-\gamma_5)]d_i\ H^- + h.c. \tag{B.18}$$

[4]Of course, the amplitude for $b \to \gamma$ in the $5D$ model is expected to be of similar size to (i.e., differing only by $\sim O(1)$ factors from) that in the two-site model.

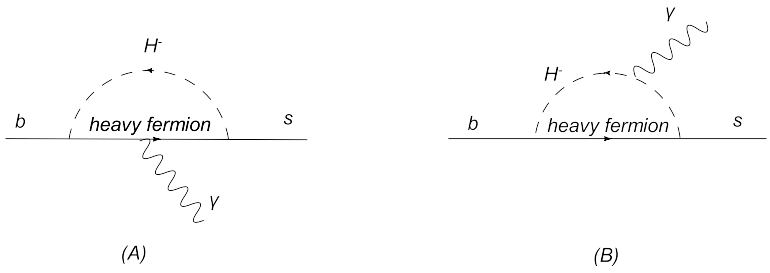

Figure B.1: Feynman diagrams for b → s γ via charged Higgs

where *all quarks are in mass eigenstate basis (including effects of EWSB)*. We focus on the dominant contributions to the dipole moment operator for $b \to s\gamma$ generated by these interactions – the relevant diagrams contain the charged Higgs and heavy fermion in the loop with the SM fermions as external legs (see Fig. B.1 (A) and (B)). We will then apply the results obtained in this section for the *specific* case of the two-site model and calculate the effective dipole operator for *one* generation in Appendix B.3 and $b \to s\gamma$ in appendix B.3.1.

For the first diagram (see Fig. B.1 (A)), with photon line attached to the heavy fermion, we get the effective operator[5]

$$\mathcal{H}_1^{eff} = \frac{ieQ_U}{8\pi^2}\frac{(2\epsilon\cdot p)}{M_w^2}\left\{A_1\bar{s}(1+\gamma_5)b + B_1\bar{s}(1-\gamma_5)b\right\} \tag{B.19}$$

with

$$A_1 = (\alpha_{2b}\alpha_{2s}^* m_b + \alpha_{1b}\alpha_{1s}^* m_s)f_1(t) + (\alpha_{2s}^*\alpha_{1b})M_* f_2(t) \tag{B.20}$$

$$B_1 = (\alpha_{1b}\alpha_{1s}^* m_b + \alpha_{2b}\alpha_{2s}^* m_s)f_1(t) + (\alpha_{1s}^*\alpha_{2b})M_* f_2(t)$$

[5]We used Feynman gauge in this calculation. Since we are considering only the dominant diagrams here, the result will be different by $O(\frac{M_w^2}{M_*^2})$ if we use another non-unitary gauge. Such differences can be neglected for our purpose here. Of course including the other diagrams (with W/Z) will produce a gauge-invariant result.

and

$$f_1(t) = -\frac{t[t(t-6)+3]+6t\ln(t)+2}{12(t-1)^4}; \qquad f_2(t) = -\frac{(t-4)t+2\ln(t)+3}{2(t-1)^3} \tag{B.21}$$

where M_* is the mass of the heavy fermion, Q_U is the charge of the heavy fermion, $t = M_*^2/M_w^2$. This result can also be used for the diagram with *neutral* Higgs (including physical Higgs and the neutral would-be-Goldstone boson) in the loop.

The result for the second diagram(See Fig. B.1 B), with photon attached to the charged Higgs, is

$$\mathcal{H}_2^{eff} = \frac{-ie}{8\pi^2}\frac{(2\epsilon\cdot p)}{M_w^2}\{A_2\bar{s}(1+\gamma_5)b + B_2\bar{s}(1-\gamma_5)b\} \tag{B.22}$$

with

$$A_2 = (\alpha_{2b}\alpha_{2s}^* m_b + \alpha_{1b}\alpha_{1s}^* m_s)g_1(t) + (\alpha_{1b}\alpha_{2s}^*)M_* g_2(t) \tag{B.23}$$

$$B_2 = (\alpha_{1b}\alpha_{1s}^* m_b + \alpha_{2b}\alpha_{2s}^* m_s)g_1(t) + (\alpha_{1s}^*\alpha_{2b})M_* g_2(t)$$

and

$$g_1(t) = \frac{2t^3-6t^2\ln(t)-6t+1+3t^2}{12(t-1)^4}; \qquad g_2(t) = \frac{t^2-2t\ln(t)-1}{2(t-1)^3} \tag{B.24}$$

These results (Eq. B.19 and B.22) can be applied to calculate $\Gamma(b\to s\gamma)$ if we find the couplings α_{1i}, α_{2i} (see Eq. B.18).

B.3 Mass matrix diagonalization and dipole moment operator for one generation

Having performed a calculation of the dipole operator for $b \to s$ generated by general couplings of bottom and strange quarks to Higgs and heavy fermions, we

now consider this contribution specifically in the two-site model. As explained in section 2.4.1, we have to consider the mixing between the SM and heavy fermions of all three generations induced after EWSB. Diagonalization of this mixing will give the couplings to Higgs in mass eigenstate basis for the quarks which we can then plug into the model-independent results of appendix B.2 in order to calculate $b \to s\gamma$. In this section, we will first consider *analytically* the simpler *one* generation case, i.e., a calculation of $(g-2)_\mu$, which will be generalized (numerically) to the case of three generations for calculating $b \to s\gamma$ in the next sub-section. This result for the dipole operator for one generation was also used in section 2.4.1 to obtain an *estimate* for $b \to s\gamma$ (after multiplying by an estimate for the generational mixing factors).

The one generation mass matrix for down type quarks (including effects of EWSB) is (see Eq. (2.15))

$$(\bar{b}_L \quad \bar{\tilde{B}}_L \quad \bar{B}_L) M_* \begin{pmatrix} x s_q s_b & 0 & x s_q \\ 0 & x & 1 \\ x s_b & 1 & x \end{pmatrix} \begin{pmatrix} \tilde{b}_R \\ B_R \\ \tilde{B}_R \end{pmatrix} + h.c. \tag{B.25}$$

where $x = vY_*/\left(M_*\sqrt{2}\right)$, $\tilde{B}$ and B are composite $SU(2)_L$ singlet and doublet fermions respectively. It can be diagonalized by bi-unitary transformation to first order in x.

$$O_{D_L} = \begin{pmatrix} 1 & x s_q/\sqrt{2} & -x s_q/\sqrt{2} \\ -x s_q & 1/\sqrt{2} & -1/\sqrt{2} \\ 0 & 1/\sqrt{2} & 1/\sqrt{2} \end{pmatrix}; \qquad O_{D_R} = \begin{pmatrix} 1 & x s_b/\sqrt{2} & x s_b/\sqrt{2} \\ -x s_b & 1/\sqrt{2} & 1/\sqrt{2} \\ 0 & 1/\sqrt{2} & -1/\sqrt{2} \end{pmatrix} \tag{B.26}$$

$$O_{D_L}^{\dagger}\begin{pmatrix} xs_qs_b & 0 & xs_q \\ 0 & x & 1 \\ xs_b & 1 & x \end{pmatrix} O_{D_R} = \mathrm{diag}(\ xs_qs_b\ , 1+x\ , 1-x\ ) \tag{B.27}$$

Similarly we can get the up-type diagonalization matrix (O_{U_L}) and (O_{U_R}). We define the mass eigenstates as

$$\begin{pmatrix} b_L^{SM} \\ B_{1L} \\ B_{2L} \end{pmatrix} = O_{D_L}^{\dagger}\begin{pmatrix} b_L \\ \tilde{B}_L \\ B_L \end{pmatrix} \qquad \begin{pmatrix} b_R^{SM} \\ B_{1R} \\ B_{2R} \end{pmatrix} = O_{D_R}^{\dagger}\begin{pmatrix} \tilde{b}_R \\ B_R \\ \tilde{B}_R \end{pmatrix}, \tag{B.28}$$

where b^{SM} is the SM bottom quark with mass $vY_*s_qs_b$. B_1 is the heavy state with mass $(1+x)M_*$ and B_2 is the heavy state with mass $(1-x)M_*$. Similar mass eigenstates can be defined for up-type quarks (t^{SM}, T_1, T_2).

The coupling between down type and up type quarks through charged Higgs is

$$Y_*(\bar{b_L^{SM}} \quad \bar{B}_{1L} \quad \bar{B}_{2L})\ O_{D_L}^{\dagger}\begin{pmatrix} s_qs_t & 0 & s_q \\ 0 & -1 & 0 \\ s_t & 0 & 1 \end{pmatrix} O_{U_R}\begin{pmatrix} t_R^{SM} \\ T_{1R} \\ T_{2R} \end{pmatrix} H^- \tag{B.29}$$

We can find the couplings between b_L^{SM} and heavy up-type quarks

$$Y_*H^-\bar{b}_L^{SM}\left[\frac{(1+x)}{\sqrt{2}}s_qT_{1R} + \frac{(x-1)}{\sqrt{2}}s_qT_{2R}\right] \tag{B.30}$$

Similarly, we have the coupling coming from another chirality

$$Y_*(\bar{b_R^{SM}} \quad \bar{B}_{1R} \quad \bar{B}_{2R})\ O_{D_R}^{\dagger}\begin{pmatrix} -s_qs_b & 0 & -s_b \\ 0 & 1 & 0 \\ -s_q & 0 & -1 \end{pmatrix} O_{U_L}\begin{pmatrix} t_L^{SM} \\ T_{1L} \\ T_{2L} \end{pmatrix} H^- \tag{B.31}$$

which gives us the coupling

$$Y_* H^- \bar{b}_R^{\rm SM} \left[-\frac{(1+x)}{\sqrt{2}} s_b T_{1L} + \frac{(x-1)}{\sqrt{2}} s_b T_{2L} \right] \tag{B.32}$$

Altogether, we have the charged Higgs coupling between SM bottom quark and heavy up-type quark

$$\begin{aligned} Y_* H^- \bar{b}^{\rm SM} \left[(\frac{1+\gamma_5}{2})(1+x)\frac{s_q}{\sqrt{2}} - (\frac{1-\gamma_5}{2})(1+x)\frac{s_b}{\sqrt{2}} \right] T_1 + \\ Y_* H^- \bar{b}^{SM} \left[(\frac{1+\gamma_5}{2})\frac{x-1}{\sqrt{2}} s_q + (\frac{1-\gamma_5}{2})\frac{x-1}{\sqrt{2}} s_b \right] T_2 \end{aligned} \tag{B.33}$$

Based on our parametrization of the couplings (see Eq. B.18), we extract (we ignore the subscript "b" in $\alpha_{1,2}$ here)

$$\begin{aligned} \alpha_1^{(1)} &= -\frac{(1+x)s_b}{2\sqrt{2}} Y_* \\ \alpha_1^{(2)} &= \frac{(x-1)s_b}{2\sqrt{2}} Y_* \\ \alpha_2^{(1)} &= \frac{(1+x)s_q}{2\sqrt{2}} Y_* \\ \alpha_2^{(2)} &= \frac{(x-1)s_q}{2\sqrt{2}} Y_* \end{aligned} \tag{B.34}$$

The contribution from heavy up-type quark to the dipole moment operator would be (see Eq. B.19 and B.22)

$$\mathcal{H}^{\rm dipole}_{\text{charged Higgs}} = \frac{ie}{8\pi^2}\frac{(2\epsilon\cdot p)}{M_w^2} K \left[\bar{b}^{SM}(1-\gamma_5) b^{\rm SM} + \bar{b}^{\rm SM}(1+\gamma_5) b^{SM} \right] \tag{B.35}$$

with

$$\begin{aligned} K \quad &= \sum_{i=1}^{2} \left(|\alpha_1^{(i)}|^2 + |\alpha_2^{(i)}|^2 \right) m_b \left[\frac{2}{3} f_1(t_i) - g_1(t_i) \right] \\ &+ \sum_{i=1}^{2} (\alpha_1^{(i)*} \alpha_2^{(i)}) M_i \left[\frac{2}{3} f_2(t_i) - g_2(t_i) \right]. \end{aligned} \tag{B.36}$$

Substituting Eq. (B.34) in (B.36) one can see that the first term is sub-leading due to additional powers of s_b,s_q. For the second term we use the approximation

$$\frac{2}{3}f_2(t_i) - g_2(t_i) \approx -\frac{5}{6}\frac{M_w^2}{(M_*)^2(1 \pm x)^2} \tag{B.37}$$

It gives us

$$K \approx \frac{5x}{24}s_q s_b \frac{M_w^2}{(M_*)^2}(Y_*)^2 \tag{B.38}$$

And the final result is

$$\mathcal{H}^{\text{dipole}}_{\text{charged Higgs}} = \frac{5}{12}(Y_*)^2 m_b \frac{ie}{16\pi^2}\frac{(2\epsilon \cdot p)}{(M_*)^2}[\bar{b}^{\text{SM}}(1-\gamma_5)b^{SM} + \bar{b}^{SM}(1+\gamma_5)b^{\text{SM}}] \tag{B.39}$$

Note that we have chosen *not* to combine the two terms in $\Big[...\Big]$ in the above equation. The reason is that when we apply the above result to $b \to s\gamma$, then the two terms with *different* chirality structure will be multiplied by different mixing angles and hence it is useful to keep track of the two terms separately even for the case of one generation.

The contribution from neutral Higgs can be calculated in a similar fashion. The coupling between down-type quarks and neutral Higgs is

$$Y_* H^0 \begin{pmatrix} \bar{b}_L^{\text{SM}} & \bar{B}_{1L} & \bar{B}_{2L} \end{pmatrix} O_{D_L}^\dagger \begin{pmatrix} s_q s_b & 0 & s_q \\ 0 & 1 & 0 \\ s_b & 0 & 1 \end{pmatrix} O_{D_R} \begin{pmatrix} b_R^{\text{SM}} \\ B_{1R} \\ B_{2R} \end{pmatrix} + h.c. \tag{B.40}$$

From this we can find the coupling between SM b quark and heavy down-type fermions:

$$Y_* H^0 \left\{ \bar{b}_L^{\text{SM}} \left[\frac{1-x}{\sqrt{2}} s_q B_{1R} - \frac{1+x}{\sqrt{2}} s_q B_{2R} \right] + \bar{b}_R^{SM} \left[\frac{1-x}{\sqrt{2}} s_b B_{1L} + \frac{1+x}{\sqrt{2}} s_b B_{2L} \right] \right\} + h.c \tag{B.41}$$

which gives us (see Eq. B.18)

$$\alpha_1^{(i)} = Y_* \frac{s_b}{2\sqrt{2}}(1-x,\ 1+x) \tag{B.42}$$
$$\alpha_2^{(i)} = Y_* \frac{s_q}{2\sqrt{2}}(1-x,\ -1-x)$$

Follow the same procedure as before, including only the first diagram (Fig. B.1A). We get

$$\mathcal{H}^{\text{dipole}}_{\text{neutral Higgs}} = -\frac{1}{4}(Y_*)^2 m_b \frac{ie}{16\pi^2}\frac{(2\epsilon\cdot p)}{(M_*)^2}[\bar{b}^{SM}(1-\gamma_5)b^{SM} + \bar{b}^{SM}(1+\gamma_5)b^{SM}] \tag{B.43}$$

B.3.1 Three generation calculation

Generalizing to three generations, the mass matrix Eq. (B.25) becomes 9×9. However, since analytical diagonalization of this 9×9 matrix is difficult, we do it numerically and extract the parameters α_1, α_2 (see Eq. (B.18) which parametrize general interaction between fermions and Higgs field, keeping in mind that $\alpha_{1,2}$ will now have six components $\alpha_{1,2}^{(1,2,\ldots 6)}$ because we have six heavy mass eigenstates). Then using these α's in the formulae from the loop calculation in Eqs. (B.19) and (B.22), we will get *exact* values for the C_7 and C_7' coefficients in the amplitude for $b\to s\gamma$ (instead of the estimates presented in section 2.4.1). Similarly, applying the above diagonalization to Eq. (2.16) allows us to calculate the flavor-violating couplings of heavy gluon to the SM fermions *after* EWSB (including effects of SM-heavy fermion mixing) which generate contributions to ϵ_K. The results of the numerical scan in section 2.6 are based on these calculations.

B.4 Details of Scan

All the masses and mixings in the fermion sector (including SM and heavy) can be parametrized by the composite site Yukawa couplings ($Y^*_{u,d}$) and the elementary/composite mixings ($s_{q,d,u}$). Of course, we must choose Y_* and $s_{q,u,d}$ to give the observed quark masses and CKM angles. We would like the composite site Yukawa couplings to be "anarchical", i.e., of the same order, and $s_{q,d,u}$ to be hierarchical[6] in order to explain SM fermion masses and mixing, and their approximate values are given by (60). We choose to scan over the following independent variables

- Elementary-composite mixing angles $s_{q,u,d}$
- SM rotation matrices $O_{U_R}, O_{U_L}, O_{D_R}$ (O_{D_L} is fixed by $O_{D_L} = O_{U_L} \cdot V_{CKM}$)

(This choice is equivalent to treating $Y_*^{u,d}$ and $s_{q,u,d}$ as the independent variables which are scanned.) We randomly vary each set of the independent variables around their "natural" size by a factor of three, where the natural sizes for the $s_{q,u,d}$ are defined to be Eq. (60) and that for $O_{U_R}, O_{U_L}, O_{D_R}$ in Eq. (2.21) by replacing "$\sim$" by "$=$" in both these equations. Then we calculate corresponding $Y_{*u,d}$[7]

$$Y_u = \frac{\sqrt{2}}{v}(O_{U_L}) \cdot M_u^{diag} \cdot (O_{U_R})^\dagger; \qquad Y_d = \frac{\sqrt{2}}{v}(O_{D_L}) \cdot M_d^{diag} \cdot (O_{D_R})^\dagger$$

$$Y_*^{u,d} \approx s_Q^{-1} Y_{u,d} s_{u,d}^{-1} \tag{B.44}$$

[6] As mentioned earlier, these assumptions can be justified by the correspondence with the $5D$ model to be discussed later.

[7] We are ignoring the mixing between the SM and heavy fermions induced by EWSB in the last relation here which results in an error of $Y_*^2 v^2/M_*^2 \sim$ a few % (for the our choice of parameters) in the determination of Y_*.

Then we check whether our $Y_{*u,d}$ are "anarchical", i.e., whether they satisfy the following condition

$$\begin{aligned}\frac{\mathrm{Max}(|Y_{*u}|)}{3} &< \mathrm{G.M.}(|Y_{*u}|) < 3 * \mathrm{Min}(|Y_{*u}|) \\ \frac{\mathrm{Max}(|Y_{*d}|)}{3} &< \mathrm{G.M.}(|Y_{*d}|) < 3 * \mathrm{Min}(|Y_{*d}|)\end{aligned} \tag{B.45}$$

where G.M. stands for the geometrical mean. If these Yukawas satisfy "anarchy" condition, we proceed to calculate new physics contribution to $\Gamma(b \to s\gamma)$, $\mathrm{Im}\, C_4^K$ (as described in section B.3.1) and $\delta g_{Z\bar{b}_L b_L}$ as in Eq. (2.45). On the other hand, if these Yukawas do not satisfy the anarchy condition, then we discard them. We have checked that the couplings ($Y_{*u,d}$) generated in this way are random, i.e., that there is no correlation between different elements of the matrices. The results of the scan are presented in Fig. B.2 to B.7.

B.5 Sub-leading effects

B.5.1 ϵ_K

Similarly to the heavy gluon exchange, heavy EW gauge boson exchange generates $(V-A)\times(V+A)$ operators, but it gives $C_5\,(M_*)$ only and of smaller size than $C_4\,(M_*)$ from heavy gluon due to smaller values of gauge couplings and gauge quantum numbers in the heavy EW boson exchange than in heavy gluon exchange. Moreover, the model-*independent* constraint from UTfit [21] on C_5 (renormalized at a few TeV scale) is weaker than for C_4. So, we find that constraint on M_* from heavy EW gauge boson exchange in the two-site model is weaker than that from heavy gluon exchange:

see also discussion in [12].

We have also checked that the constraint from $(V-A)\times(V-A)$ and $(V+A)\times(V+A)$-type operators from heavy gauge boson exchange in the two-site model can be weaker than from $(V-A)\times(V+A)$ operator from heavy gluon exchange. In detail, such exchange generates the Wilson coefficient $C_1\,(M_*)$. Firstly, the model-independent bound on C_1 (renormalized at a few TeV scale) is weaker than for C_4 due to the absence of matrix element *and* RGE enhancement for C_1 relative to C_4. Secondly, in the two-site model, the size of C_1 can be effectively *controlled* by a single parameter, namely, the amount of elementary-composite mixing of b_L – the point being that the other down-type elementary-composite mixings are then fixed: the ones for d_L, s_L via CKM mixing angles and then, for given composite Yukawa, the right-handed ones by SM Yukawa (as discussed earlier).[8] Usually, one chooses s_{q3} to satisfy the constraint from $Zb\bar{b}$ (as discussed earlier) and simultaneously to obtain the correct top Yukawa, i.e., $Y_* s_{q3} \sim O(1)$, assuming SM t_R is fully composite. For the choice of $M_* \sim$ a few TeV and $Y_* \sim$ a few, we then find $s_{q3} \sim 1/$ (a few). With this size of s_{q3} and once we choose M_* to satisfy the ϵ_K-constraint from $(V-A)\times(V+A)$ operators, we find that both $(V-A)\times(V-A)$ and $(V+A)\times(V+A)$-type operators do not give as strong a constraint as from heavy gluon contribution to the $(V-A)\times(V+A)$ operator: see also [12] for a related discussion.

[8] Contrast this case to that for $C_{4,\,5}$ above whose size was *fixed* in terms of SM fermion Yukawa couplings/masses (due to a combination of left and right-handed elementary-composite mixings involved in C_4).

B.5.2 Other B-physics observables

It is easy to compute $B_{d,\,s}$ mixing amplitudes in the two-site model. The main new physics contribution comes from the flavor violating couplings of heavy gluon, just like for $\Delta S = 2$ process discussed earlier. We have checked that bounds on $B_{d,\,s}$ mixing amplitude is satisfied once ϵ_K is safe: see also [11, 12] for related discussions.

In detail, the $(V-A)\times(V+A)$ type operator generated in the two-site model is less constrained in the $B_{d,\,s}$ systems than in the K system for the following reasons. Firstly, the model-independent constraint on $C_{4,\,5}^{new}\left(M_*\right)/C_1^{SM}\left(M_W\right)$ is weaker in the $B_{d,\,s}$ system than in the K system since there is no matrix element enhancement for $C_{4,5}$ in the $B_{d,\,s}$ mixing operators (unlike for K mixing). Secondly, in the two-site model, the size of $C_{4,\,5}^{new}\left(M_*\right)/C_1^{SM}\left(M_W\right)$ for $B_{d,\,s}$ mixing turns out (due to the particular values of down-type quark masses) to be smaller than in K mixing. For the $(V \pm A) \times (V \pm A)$ type operator, the analysis is similar to that for K mixing.

Besides $\Delta F = 2$ processes, there are also new physics contribution to $\Delta F = 1$ processes in the two-site model. For example, the non-universal shift (in gauge eigenstate basis) in the Z couplings for b_L (vs. d_L, s_L) will lead to flavor-violating couplings to Z once we transform to mass eigenstate basis, resulting in the (flavor-violating) processes $b \to s f \bar{f}$, where f = quark, lepton. We have checked that the new physics contribution to $b \to s l^+ l^-$ process is below the experimental bound once we satisfy $\delta g_{Z b_L^- b_L}/g_{Z b_L^- b_L} \lesssim 0.25\%$ as required by the flavor-preserving $Z b \bar{b}$ data: see also [13] for a related discussion.

We also checked the new physics contribution to the time-dependent CP asym-

metry in $b \to s\gamma$, i.e., S_{CP} which requires an interference between the C_7 and C_7' amplitudes: $S_{CP} \sim C_7' C_7/(|C_7|^2 + |C_7'|^2)$. In the SM, $S_{CP} \sim m_s/m_b$ due to the suppression of C_7' by m_s/m_b relative to C_7 [64]. In the two-site model, new physics contribution will generically give $C_7' \sim C_7^{SM}$ so that we expect S_{CP} to be sizable in the two-site model. However, we found that there is no significant constraint coming from S_{CP} because of the large experimental uncertainty at present [31].

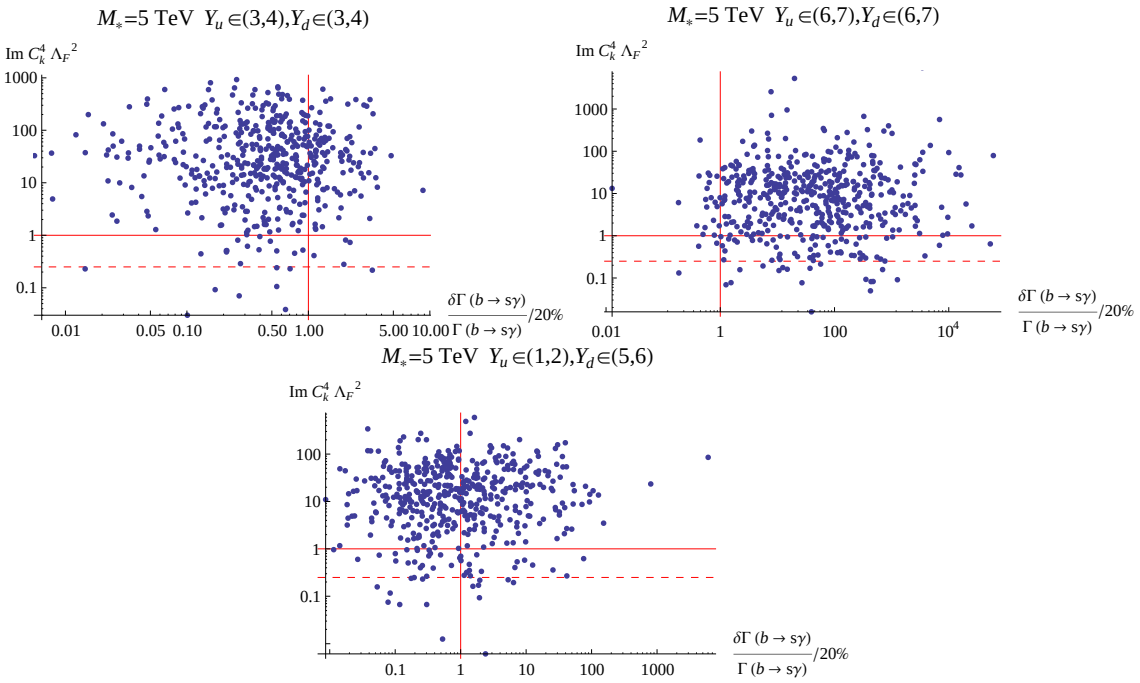

Figure B.2: Scatter plot for shift in BR($b \to s\gamma$) and Im (C_{4K}) for $M_* = 5$ TeV, the composite site gauge coupling $g_{s*} = 3$ and different values of $Y_*^{u,d}$ (defined here as the geometric *mean* of the composite site Yukawa couplings $|Y_{*ij}^{u,d}|$). The allowed region is below and to the left of the (red) solid lines. For $g_{s*} = 6$, the allowed region is below the dashed line and to the left of the solid (red) line. (see discussion in section 2.6).

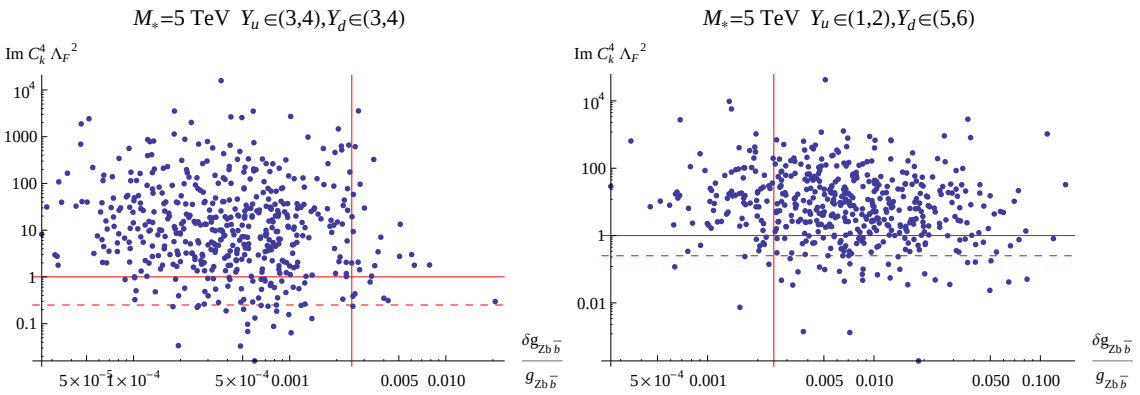

Figure B.3: Scatter plot for $\delta g_{Z\bar{b}_L b_L}$ and Im (C_{4K}) for $M_* = 5$ TeV, the composite site gauge coupling $g_{s*} = 3$ and for different values of $Y_*^{u,d}$ (defined here as the geometric *mean* of the composite site Yukawa couplings $|Y_{*ij}^{u,d}|$). The allowed region is below and to the left of the (red) solid lines. For $g_{s*} = 6$, the allowed region is below the dashed line and to the left of the solid (red) line. (see discussion in section 2.6).

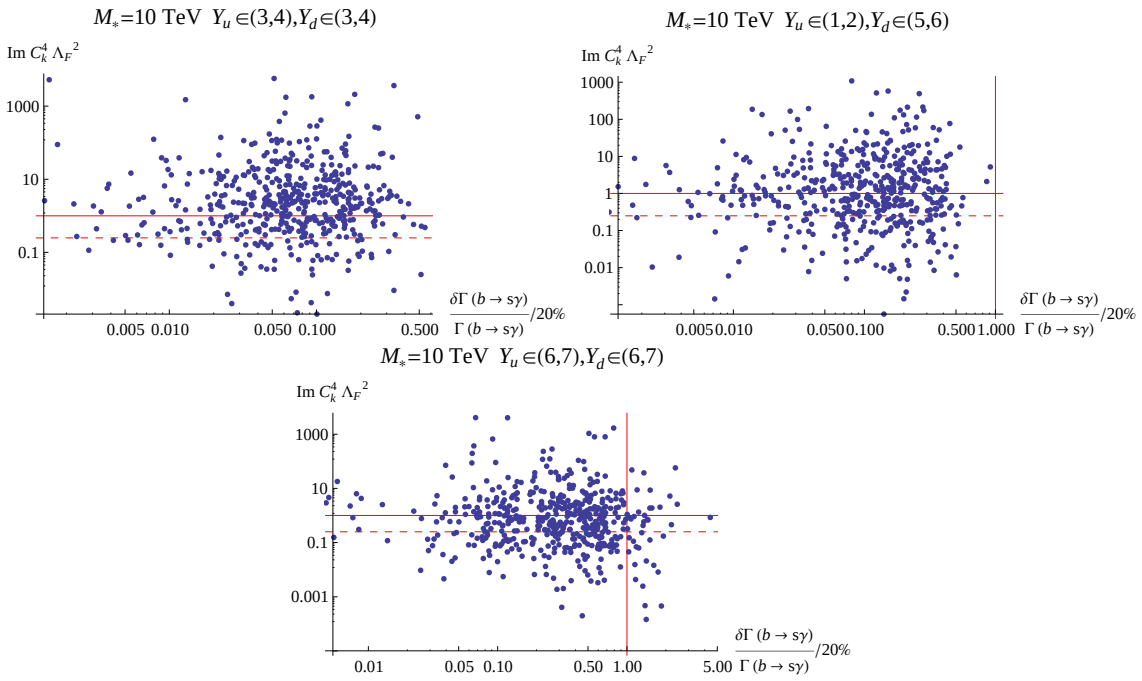

Figure B.4: Same as Fig. B.2, but with $M_* = 10$ TeV.

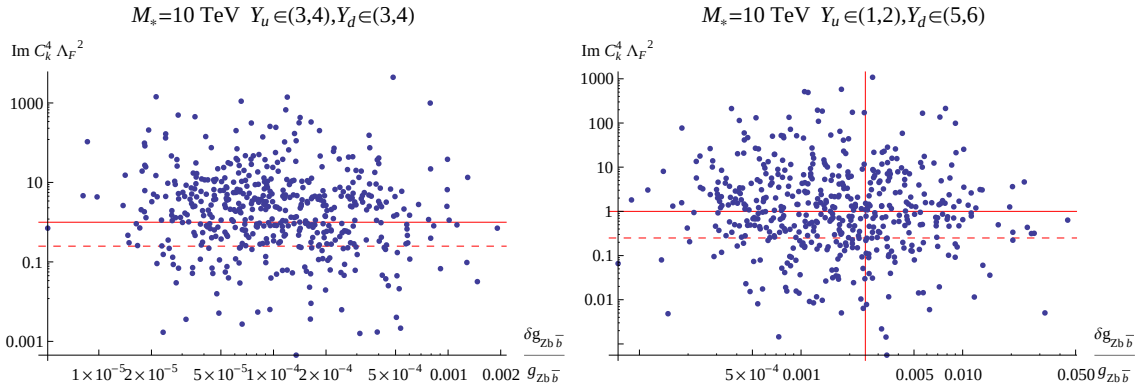

Figure B.5: Same as Fig. B.3, but with $M_* = 10$ TeV.

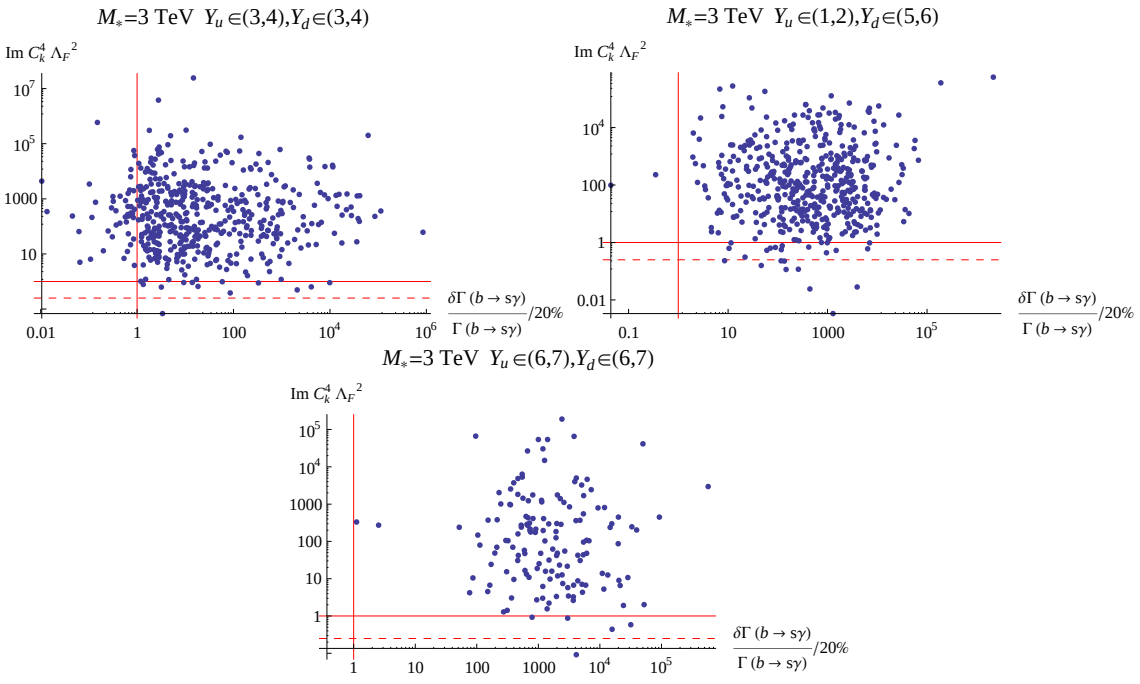

Figure B.6: Same as Fig. B.2, but with $M_* = 3$ TeV.

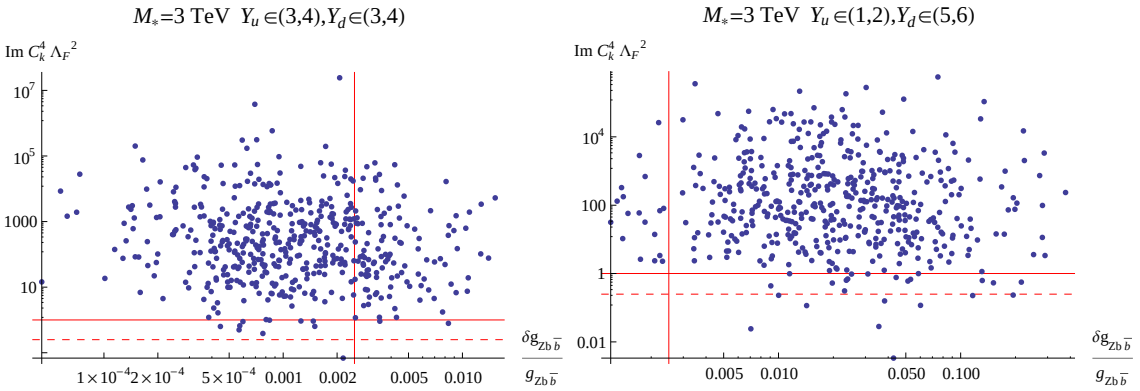

Figure B.7: Same as Fig. B.3, but with $M_* = 3$ TeV.

Chapter C

Higgs and Radion

C.1 General misalignment formulae

Here we present the result for the misalignment for general fermions (both UV and IR localized). The largest contribution (second term of Eq. 3.29) is

$$\begin{aligned}\Delta_1^d \quad &= 2m_d^3 R'^2 \frac{2+c_d-c_q+\beta}{(1+2c_d)(1-2c_q)}\left[\frac{\epsilon^{1+2c_d}}{3-c_d-c_q+\beta}-\frac{1}{4+c_d-c_q+\beta}-\frac{\epsilon^{2-2c_q+2c_d}}{3-c_d-c_q+\beta}\right.\\ &\frac{\epsilon^{-2c_q+1}}{3+c_d+c_q+\beta}-\frac{\epsilon^{-2c_q+2c_d+2}}{4+2\beta}(\epsilon^{-1-2c_d}-1)\\ &-\frac{\epsilon^{-2c_q+2c_d+2}}{4+2\beta}(\epsilon^{-1+2c_q}-1)+\frac{\epsilon^{2c_d+1}}{5-2c_q+2\beta}(\epsilon^{-1-2c_d}-1)\\ &\left.+\frac{\epsilon^{-2c_q+1}}{5+2c_d+2\beta}(\epsilon^{-1+2c_q}-1)+\frac{\epsilon^{2+2c_d-2c_q}}{6+c_d-c_q+3\beta}(\epsilon^{-1-2c_d}-1)(\epsilon^{-1+2c_q}-1)\right]. \quad \text{(C.1)}\end{aligned}$$

For the case of the UV localized fermions ($c_q > 0.5, c_d < -0.5$) the 3rd, 4th and 9th terms are dominating and we recover Eq. (3.36). For the subleading contribution of the misalignment Δ_2^d (first term of Eq. 3.29) we get:

$$\begin{aligned}\Delta_2^d = \frac{m_d^3 R'^2}{1-2c_q}\left[-\frac{1-\epsilon^2}{\epsilon^{2c_q-1}-1}+\frac{\epsilon^{2c_q-1}-\epsilon^2}{(\epsilon^{2c_q-1}-1)(3-2c_q)}+\frac{\epsilon^{1-2c_q}-\epsilon^2}{(1+2c_q)(\epsilon^{2c_q-1}-1)}\right.\\ \left.-\frac{1}{4+c_d-c_q+\beta}+\frac{2\epsilon^{1-2c_q}}{3+c_q+c_d+\beta}+\frac{(\epsilon^{2c_q-1}-1)\epsilon^{1-2c_q}}{5+2c_d+2\beta}+(c_{d,q}\leftrightarrow -c_{q,d})\right] \quad \text{(C.2)}\end{aligned}$$

For the UV localized fermions ($c_q > 0.5, c_d < -0.5$) the 3rd, 5th and 6th terms are important and we recover Eq. (3.37).

C.2 Misalignement due to $v(z) \neq h(z)$

In this section we discuss the possible flavor violation coming from the the misalignment between the physical Higgs profile and the Higgs vev profile. The profile of the KK Higgs modes are given by [39]

$$h_m(z) = Bz^2(Y_{1+\beta}(mR)J_\beta(mz) + J_{1+\beta}(mR)Y_\beta(mz)). \tag{C.3}$$

where the mass of the KK mode is determined by the boundary conditions. Then for the lightest mode (physical Higgs) we can expand the Bessel functions using $(m \ll 1/z)$

$$h(z) = A(m_H)z^{2+\beta}\left(1 - \frac{m_H^2 z^2}{4(\beta+1)}\right) \tag{C.4}$$

where the constant $A(m_H)$ is fixed by requiring the Higgs profile normalization. One can see that in the limit $(m_H = 0)$, the profiles of the physical Higgs and the profile of its vev become proportional to each other. Then, the normalization constants of the Higgs field and the Higgs vev, $A(m_H)$ and $V(\beta)$ (Eq. 3.10), will be related by

$$A(m_H)|_{m_H=0} \equiv A(0) = \frac{V(\beta)}{v_4} \tag{C.5}$$

and so the profile of the Higgs will be given by

$$\begin{aligned} h(z) &= A(0)z^{2+\beta}\left[1 + \frac{m_H^2 R'^2}{2(4+\beta)} - \frac{m_H^2 z^2}{4(1+\beta)} + O\left((m_H^2 R'^2)^2\right)\right] \\ &= \frac{v(z)}{v_4}\left[1 + \frac{m_H^2 R'^2}{2(4+\beta)} - \frac{m_H^2 z^2}{4(1+\beta)} + O\left((m_H^2 R'^2)^2\right)\right]. \end{aligned} \tag{C.6}$$

This will lead to a new contribution to the shift Δ^d

$$\Delta_3^d = -m_d(m_H^2 R'^2)\left[\frac{1}{2(4+\beta)} - \frac{2+\beta+c_d-c_q}{4(1+\beta)(4+\beta+c_d-c_q)}\right], \tag{C.7}$$

but one can see that in the limit $\beta \to \infty$ this contribution decouples. Moreover, even for finite β, the numerical size of this type of flavor misalignment is small.

C.3 Convergent infinite sum in the mass insertion approximation

In this appendix, we address again the "contradiction" between the mass insertion approximation and the 5D calculation when the Higgs is on the IR brane. We will prove that one can obtain the result of Eq. 3.56 from direct calculations of the Feynman diagrams in the insertion approximation.

Naively, the importance of the Y_2 term looks counter intuitive because the profiles q_R, d_L do vanish at IR brane. Indeed if one follows the insertion approximation (see Fig. 3.1) then the coupling between q_R^{KK}, d_L^{KK} and the Higgs vanish, so there will be no contribution to fermion masses and Yukawa couplings out of that diagram. However there is a subtlety in this approach, since we are expanding in KK modes by using the profiles for the case $\langle H \rangle = 0$. This means that after electroweak symmetry breaking, we should include the mixing between the whole tower of KK modes induced by a nonzero Higgs vev. Naively the heavier KK modes should decouple so that their contribution should not qualitatively affect the final result. But this appears not to be the case.

For simplicity we will start our discussion from the case of a flat extra dimension. Now, the fermion profiles are given by sine and cosine functions instead of Bessel functions, and the derivation becomes much more transparent. At the same time when the Higgs is localized on one of the branes, we still have the same issue

for any Yukawa coupling between odd modes and the Higgs i.e., the term $Y_2 q_R d_L$ naively should not lead to any misalignment between fermion masses and Yukawa couplings.

The profiles of the even KK modes are given by

$$\begin{aligned} q_L^n(d_R^n) &= \frac{1}{\sqrt{\pi R}}\cos\left(\frac{nz}{R}\right), \qquad n = \pm 1, \pm 2, ... \\ q_L^0(d_R^0) &= \frac{1}{\sqrt{2\pi R}} \end{aligned} \tag{C.8}$$

and the odd KK mode profiles are

$$\begin{aligned} q_R^n &= \frac{1}{\sqrt{\pi R}}\sin\left(\frac{nz}{R}\right) \qquad n = \pm 1, \pm 2, ... \\ d_L^n &= -\frac{1}{\sqrt{\pi R}}\sin\left(\frac{nz}{R}\right) \qquad n = \pm 1, \pm 2, ... \end{aligned} \tag{C.9}$$

The coupling $Y_2 H Q_R D_L \delta(y - \pi R)$ should vanish because Q_R and D_L are vanishing at $y = \pi R$, but in the diagram (Fig. 3.1) we have to include all the KK modes, so we will have an infinite sum of zeroes, and in order to treat all the infinities accurately we will again use the rectangular regulator Eq.(3.47) for the delta function.

Let us define the following quantities:

$$\begin{aligned} &Y^e_{mn} - \text{coupling between “m” and “n” even KK modes} \\ &Y^o_{mn} - \text{coupling between “m” and “n” odd KK modes} \end{aligned} \tag{C.10}$$

then

$$\begin{aligned} Y^e_{mn} = &\quad \frac{(-1)^{m+n}}{2\pi\varepsilon}\left[\frac{\sin\left(\frac{(n-m)\varepsilon}{R}\right)}{n-m} + \frac{\sin\left(\frac{(n+m)\varepsilon}{R}\right)}{n+m}\right] = \frac{(-1)^{n+m}}{2\pi R}\left[1 + O\left((n,m)^2\left(\frac{\varepsilon}{R}\right)^2\right)\right], \\ Y^o_{mn} = &\quad -\frac{(-1)^{m+n}}{2\pi\varepsilon}\left[\frac{\sin\left(\frac{(n-m)\varepsilon}{R}\right)}{n-m} - \frac{\sin\left(\frac{(n+m)\varepsilon}{R}\right)}{n+m}\right] = -\frac{(-1)^{n+m}}{3\pi R}\left(\frac{\varepsilon}{R}\right)^2 mn \\ &\left[1 + O\left((n,m)^4\left(\frac{\varepsilon}{R}\right)^4\right)\right] \end{aligned} \tag{C.11}$$

In a similar way one can calculate the coupling between the 0 and the n-th even KK modes:

$$Y^e_{0n} = Y_1 \frac{(-1)^n}{\pi\sqrt{2}\varepsilon} \frac{\sin\left(\frac{n\varepsilon}{R}\right)}{n} = Y_1 \frac{(-1)^n}{\pi\sqrt{2}R}\left[1 + O\left(\frac{n\varepsilon}{R}\right)\right] \tag{C.12}$$

As we said before to find the $O(v^3 R'^2)$ misalignment between fermion masses and Yukawa couplings, it is sufficient to consider the contribution of the diagram with three Higgs insertions (see Fig. 3.1) and sum over all KK modes. However, for KK modes with $|n|, |m| \gtrsim R/\varepsilon$, the sinusoidal oscillation of the odd wavefunction inside the Higgs profile will tend to make the $Y^o_{m,n}$ coupling vanish. Thus we need to sum up $|n|, |m|$ only up to $\sim R/\varepsilon$, and the estimate of that sum will be:

$$\begin{aligned} \Delta^d_1 &\sim v^2 \sum_{|n|,|m|=1}^{R/\varepsilon} Y^e_{0n} \frac{R}{n} Y^o_{nm} \frac{R}{m} Y^e_{0m} \\ &\sim \frac{Y_1^2 Y_2 v^2}{R} \sum_{n,m=1}^{R/\varepsilon} \left(\frac{\varepsilon}{R}\right)^2 \end{aligned} \tag{C.13}$$

One can see that all of the terms up to $n \lesssim R/\varepsilon$ are of the same order, and so the sum should be finite and proportional to $\frac{Y_1^2 Y_2 v^2}{R}$. Exact resummation gives us

$$\Delta^d_1 = \frac{Y_1^2 Y_2 v^3}{6\pi R} \tag{C.14}$$

It is important to mention that to account for the flavor mixing effects one has to sum at least the first R/ε terms. And the lightest mode is an admixture of the zero mode and the first R/ε KK modes. This should not be surprising because the zero Higgs vev expansion should include all KK modes up to the value of the cutoff and the cutoff is related to the inverse of the Higgs wavefunction width. In our case the

width of the Higgs profile is ε so we have to sum all the modes with masses up to $1/\varepsilon$.

In the case of the warped geometry things become a little bit more complicated, because the sine and cosine are replaced by the Bessel functions:

$$\begin{aligned} f^e(z,m_n) &= (Rz)^{5/2}\frac{1}{N\sqrt{R\ln(R'/R)}}\left[J_\alpha(m_n z)+b_\alpha(m_n)Y_\alpha(m_n z)\right] \\ f^e(z,m_n) &= (Rz)^{5/2}\frac{1}{N\sqrt{R\ln(R'/R)}}\left[J_{\alpha-1}(m_n z)+b_\alpha(m_n)Y_{\alpha-1}(m_n z)\right] \end{aligned} \quad \text{(C.15)}$$

where

$$\begin{aligned} \alpha &= c+\frac{1}{2} \\ b_\alpha(m_n) &= \frac{J_{\alpha-1}(m_n R)}{Y_{\alpha-1}(m_n R)}=\frac{J_{\alpha-1}(m_n R')}{Y_{\alpha-1}(m_n R')} \end{aligned} \quad \text{(C.16)}$$

but for the cases when the mass of the KK mode is $\frac{1}{R'} \ll m \ll \frac{1}{R}$ the expressions for the profiles simplify significantly

$$\begin{aligned} m_n R' &\sim \pi(n+c/2+1/2) \\ J_\alpha(m_n z) &\sim \sqrt{\frac{2}{\pi m_n z}}\cos(m_n z-\pi/2(c+1)) \\ J_{\alpha-1}(m_n z) &\sim \sqrt{\frac{2}{\pi m_n z}}\cos(m_n z-\pi/2c) \end{aligned} \quad \text{(C.17)}$$

so the ratio

$$\frac{f^o(z,m_n)}{f^e(z,m_n)}|_{z=R'-\varepsilon} \sim \frac{\sin(m_n\varepsilon)}{\cos(m_n\varepsilon)} \sim \sin(m_n\varepsilon) \quad \text{(C.18)}$$

and so it becomes obvious that

$$Y^o_{nl} \sim \sin(m_n\varepsilon)\sin(m_l\varepsilon). \quad \text{(C.19)}$$

One can see that Y^o_{nl} has the same dependence on the KK numbers as in the flat case, and on the masses of the KK modes $m_n \sim \pi n/R'$ for large n, so the calculation for the warp geometry will proceed exactly as in the flat geometry case.

There is yet another way to understand this result[1]. Instead of operator $Y_2 H \overline{u}_L q_R$ we can consider the following effective operator localized at the IR brane:

$$\frac{Y_2(\partial_z \overline{u}_L)(\partial_z q_R) H \ \delta(z-R')}{\Lambda^2} \tag{C.20}$$

Then the contribution to the diagram (Fig. 3.1) will be

$$\begin{aligned} \Delta_1^d &\sim \sum_{n,l \lesssim \frac{\Lambda}{M_{kk}}} \frac{Y_1 v}{m_n} \frac{Y_2 m_n m_l}{\Lambda^2} \frac{Y_1 v}{m_l} \\ &\sim \frac{Y_1^2 Y_2 v^2}{\Lambda^2} \sum_{n,l \lesssim \frac{\Lambda}{M_{kk}}} \\ &\sim \frac{Y_1^2 Y_2 v^2}{M_{kk}^2} \end{aligned} \tag{C.21}$$

and we can see that the effect of every KK mode becomes equally important and we again have to sum up all the modes up to the value of the cutoff Λ, obtaining a cutoff independent finite result. On the other hand it is easily seen that this operator corresponds to giving Higgs some finite width $\sim \frac{1}{\Lambda}$. Indeed if will use the boundary conditions for the profiles $u_L|_{R'} = q_R|_{R'} = 0$ we will get

$$-\left.\frac{\partial_z \overline{u}_L}{\Lambda}\right|_{R'} = \left(\overline{u}_L - \frac{\partial_z \overline{u}_L}{\Lambda}\right)_{R'} = \overline{u}_L \left(R' - \frac{1}{\Lambda}\right) + O\left(\frac{1}{\Lambda^2}\right) \tag{C.22}$$

so the operator (C.20) is equivalent to

$$\frac{(\partial_z \overline{u}_L)(\partial_z q_R) H \delta(z-R')}{\Lambda^2} \Leftrightarrow (\overline{u}_L q_R) H \delta\left(z - R' - \frac{1}{\Lambda}\right) \tag{C.23}$$

[1]We thank Raman Sundrum for suggesting it.

This result is not surprising because the width of the Higgs profile should be related to the value of the inverse cutoff.

C.4 Interactions of the radion

In this appendix I will present the couplings of the radion to the SM fields[50]. Because the radion is part of the of the five dimensional gravity multiplet it should couple to matter via energy momentum tensor. Using the precise form of radion excitation (4.1) we can derive that it will couple to energy momentum tensor in the following way,

$$S_{radion} = -\frac{1}{2}\int d^5x\sqrt{g}T^{MN}\delta g_{MN} = \int d^5x\sqrt{g}\left(F(TrT^{MN} - 3T^{55}g_{55})\right). \quad \text{(C.24)}$$

C.4.1 Couplings to the massive vector bosons

Now we can derive interactions of the radion with all SM fields. Let us start with interactions of the radion with massive vector bosons. Using Eq. (C.24) and (4.2) we can see that these interaction will be

$$-\frac{2r}{\Lambda_r}M_w^2 - \frac{r}{\Lambda}\frac{1}{\ln\frac{R'}{R}}W_{\mu\nu}W_{\mu\nu} + \frac{r}{\Lambda}W_{\mu\nu}W_{\mu\nu}M_w^2R'^2\left[\frac{1}{8\ln\frac{R'}{R}} - \frac{1}{4}\right] \quad \text{(C.25)}$$

where $W_{\mu\nu}$ is a field strength for the massive vector boson.

C.4.2 Interactions of the radion with massless vector bosons

The simplest way to derive this coupling is to observe that radion degrees of freedom correspond to the change of the length of extra dimension, so we can derive its coupling by making substitution,

$$R' \to R' \left(1 + \frac{r}{\Lambda}\right). \tag{C.26}$$

Starting from gauge coupling matching relation (B.3) we will get

$$\frac{1}{g^2(q)} \approx \frac{1}{g_{UV}^2} + \frac{1}{g_{IR}^2} + \left(\frac{R}{g_{5D}^2}\right) \ln(R'/R) + \frac{b_{UV}}{8\pi^2} \ln \frac{1}{Rq} + \frac{b_{IR}}{8\pi^2} \ln \frac{1}{R'q} \tag{C.27}$$

where now $b_{UV,IR}$ are beta functions of the fields localized at UV and IR branes respectively, and making substitution (C.26) we will get

$$-\frac{r}{4\Lambda} \left(\frac{R}{g_{5D}^2} - \frac{b_{IR}}{8\pi^2}\right) F^{\mu\nu} F_{\mu\nu}. \tag{C.28}$$

But from low energy theorems we know that heavy fields become decoupled and do not contribute to the gauge coupling running, so we have to subtract their contribution

$$\frac{b_H^i}{8\pi^2} \ln \frac{m_i}{q} \sim \frac{b_H(q)}{8\pi^2} \ln \frac{1}{qR'} \tag{C.29}$$

where b^H stands for the contribution of the heavy fields, and we have assumed that the heavy states have mass of order R'^{-1}. Then the radion couplings become equal to

$$-\frac{r}{4\Lambda} \left(\frac{R}{g_{5D}^2} - \frac{b_{IR} - b_H}{8\pi^2}\right) F^{\mu\nu} F_{\mu\nu} \tag{C.30}$$

where the $-b_H$ automatically counts the contribution of the triangle diagrams. The gauge coupling matching condition modifies to,

$$\frac{R}{g_{5D}^2} = \frac{1}{\ln\frac{R'}{R}}\left[\frac{1}{g^2(q)} - \frac{1}{g_{UV}^2} - \frac{1}{g_{IR}^2} - \frac{b_{IR}}{8\pi^2}\ln\frac{1}{qR'} - \frac{b_{UV}}{8\pi^2}\ln\frac{1}{qR} + \frac{b_H}{8\pi^2}\ln\frac{1}{R'q}\right]. \quad \text{(C.31)}$$

Then the interaction of the radion will be given by

$$-\frac{r}{4\Lambda\ln\frac{R'}{R}}\left[\frac{R}{g^2(q)} - \left(\frac{1}{g_{UV}^2} + \frac{1}{g_{IR}^2}\right)\frac{b-b_H}{8\pi^2}\ln\left(\frac{R'}{R}\right)\right]F^{\mu\nu}F_{\mu\nu} \quad \text{(C.32)}$$

where $b = b_{UV} + b_{IR}$ is total beta function corresponds to the trace anomaly and b_H corresponds to the contribution of the heavy quarks from triangle diagrams.

Bibliography

[1] L. Randall and R. Sundrum, Phys. Rev. Lett. **83**, 3370 (1999); [arXiv:hep-ph/9905221]; L. Randall and R. Sundrum, Phys. Rev. Lett. **83**, 4690 (1999). [arXiv:hep-th/9906064].

[2] J. M. Maldacena, Adv. Theor. Math. Phys. **2**, 231 (1998) [Int. J. Theor. Phys. **38**, 1113 (1999)] [arXiv:hep-th/9711200]; S. S. Gubser, I. R. Klebanov and A. M. Polyakov, Phys. Lett. B **428**, 105 (1998) [arXiv:hep-th/9802109]; E. Witten, Adv. Theor. Math. Phys. **2**, 253 (1998) [arXiv:hep-th/9802150].

[3] N. Arkani-Hamed, M. Porrati and L. Randall, JHEP **0108**, 017 (2001) [arXiv:hep-th/0012148];

[4] R. Rattazzi and A. Zaffaroni, JHEP **0104**, 021 (2001) [arXiv:hep-th/0012248].

[5] S. J. Huber and Q. Shafi, Phys. Lett. B **498**, 256 (2001) [arXiv:hep-ph/0010195].

[6] K. Agashe, G. Perez and A. Soni, Phys. Rev. D **71**, 016002 (2005) [arXiv:hep-ph/0408134].

[7] K. Agashe, T. Okui and R. Sundrum, arXiv:0810.1277 [hep-ph].

[8] K. Agashe, R. Contino and R. Sundrum, Phys. Rev. Lett. **95**, 171804 (2005) [arXiv:hep-ph/0502222].

[9] K. Agashe and G. Servant, Phys. Rev. Lett. **93**, 231805 (2004) [arXiv:hep-ph/0403143] and JCAP **0502**, 002 (2005) [arXiv:hep-ph/0411254].

[10] R. Contino, T. Kramer, M. Son and R. Sundrum, JHEP **0705**, 074 (2007) [arXiv:hep-ph/0612180].

[11] C. Csaki, A. Falkowski and A. Weiler, JHEP **0809**, 008 (2008); [arXiv:0804.1954 [hep-ph]].

[12] M. Blanke, A. J. Buras, B. Duling, S. Gori and A. Weiler, JHEP **0903**, 001 (2009) [arXiv:0809.1073 [hep-ph]].

[13] S. Casagrande, F. Goertz, U. Haisch, M. Neubert and T. Pfoh, JHEP **0810**, 094 (2008) [arXiv:0807.4937 [hep-ph]].

[14] K. Agashe, A. Azatov and L. Zhu, arXiv:0810.1016 [hep-ph].

[15] O. Gedalia, G. Isidori and G. Perez, arXiv:0905.3264 [hep-ph].

[16] A. J. Buras, B. Duling and S. Gori, arXiv:0905.2318 [hep-ph].

[17] K. Agashe and R. Contino, Phys. Rev. D **80**, 075016 (2009) [arXiv:0906.1542 [hep-ph]].

[18] A. Azatov, M. Toharia and L. Zhu, Phys. Rev. D **80**, 035016 (2009) [arXiv:0906.1990 [hep-ph]].

[19] W. D. Goldberger and M. B. Wise, Phys. Rev. Lett. **83**, 4922 (1999) [arXiv:hep-ph/9907447].

[20] A. Azatov, M. Toharia and L. Zhu, Phys. Rev. D **80**, 031701 (2009) [arXiv:0812.2489 [hep-ph]].

[21] M. Bona *et al.* [UTfit Collaboration], JHEP **0803**, 049 (2008) [arXiv:0707.0636 [hep-ph]].

[22] T. Gherghetta and A. Pomarol, Nucl. Phys. B **586**, 141 (2000); [arXiv:hep-ph/0003129]; Y. Grossman and M. Neubert, Phys. Lett. B **474**, 361 (2000); [arXiv:hep-ph/9912408].

[23] D. B. Kaplan, Nucl. Phys. B **365**, 259 (1991).

[24] H. Davoudiasl, J. L. Hewett and T. G. Rizzo, Phys. Lett. B **473**, 43 (2000) [arXiv:hep-ph/9911262]; A. Pomarol, Phys. Lett. B **486**, 153 (2000) [arXiv:hep-ph/9911294]; S. Chang, J. Hisano, H. Nakano, N. Okada and M. Yamaguchi, Phys. Rev. D **62**, 084025 (2000) [arXiv:hep-ph/9912498].

[25] C. Csaki, C. Grojean, J. Hubisz, Y. Shirman and J. Terning, Phys. Rev. D **70**, 015012 (2004) [arXiv:hep-ph/0310355].

[26] M. E. Peskin and T. Takeuchi, Phys. Rev. D **46**, 381 (1992).

M. E. Peskin and T. Takeuchi, Phys. Rev. Lett. **65**, 964 (1990).

[27] C. Csaki, J. Erlich and J. Terning, Phys. Rev. D **66**, 064021 (2002) [arXiv:hep-ph/0203034].

[28] K. Agashe, A. Delgado, M. J. May and R. Sundrum, JHEP **0308**, 050 (2003) [arXiv:hep-ph/0308036].

[29] A. J. Buras, [arXiv:hep-ph/9806471].

[30] M. Misiak *et al.*, Phys. Rev. Lett. **98**, 022002 (2007) [arXiv:hep-ph/0609232].

[31] Heavy Flavor Averaging Group, http://www.slac.stanford.edu/xorg/hfag/rare/winter08/radll/btosg.pdf

[32] T. Huber, J. Phys. Conf. Ser. **110**, 052024 (2008) [arXiv:0712.3158 [hep-ph]].

[33] K. Agashe, G. Perez and A. Soni, Phys. Rev. Lett. **93**, 201804 (2004) [arXiv:hep-ph/0406101].

[34] K. Agashe, R. Contino, L. Da Rold and A. Pomarol, Phys. Lett. B **641**, 62 (2006) [arXiv:hep-ph/0605341].

[35] W. Buchmuller and D. Wyler, Nucl. Phys. B **268**, 621 (1986).

[36] F. del Aguila, M. Perez-Victoria and J. Santiago, Phys. Lett. B **492**, 98 (2000) [arXiv:hep-ph/0007160]; JHEP **0009**, 011 (2000) [arXiv:hep-ph/0007316].

[37] K. S. Babu and S. Nandi, Phys. Rev. D **62**, 033002 (2000) [arXiv:hep-ph/9907213].

[38] G. F. Giudice and O. Lebedev, Phys. Lett. B **665**, 79 (2008) [arXiv:0804.1753 [hep-ph]].

[39] G. Cacciapaglia, C. Csaki, G. Marandella and J. Terning, JHEP **0702**, 036 (2007), [arXiv:hep-ph/0611358].

[40] H. Davoudiasl, B. Lillie and T. G. Rizzo, JHEP **0608**, 042 (2006), [arXiv:hep-ph/0508279].

[41] J. A. Bagger, K. T. Matchev and R. J. Zhang, Phys. Lett. B **412**, 77 (1997).

[42] G. Perez and L. Randall, arXiv:0805.4652 [hep-ph];

[43] K. Agashe, arXiv:0902.2400 [hep-ph].

[44] T. Han and D. Marfatia, Phys. Rev. Lett. **86**, 1442 (2001) [arXiv:hep-ph/0008141].

[45] J. A. Aguilar-Saavedra and G. C. Branco, Phys. Lett. B **495**, 347 (2000), [arXiv:hep-ph/0004190].

[46] G. F. Giudice, R. Rattazzi and J. D. Wells, Nucl. Phys. B **595**, 250 (2001) [arXiv:hep-ph/0002178].

[47] C. Csáki, M. L. Graesser and G. D. Kribs, Phys. Rev. D **63**, 065002 (2001) [arXiv:hep-th/0008151].

[48] S. Bae, P. Ko, H. S. Lee and J. Lee, arXiv:hep-ph/0103187.

[49] T. G. Rizzo, JHEP **0206**, 056 (2002)

[50] C. Csaki, J. Hubisz and S. J. Lee, Phys. Rev. D **76**, 125015 (2007) [arXiv:0705.3844 [hep-ph]].

[51] M. Toharia, arXiv:0809.5245 [hep-ph].

[52] H. Davoudiasl, G. Perez and A. Soni, Phys. Lett. B **665**, 67 (2008)

[53] K. Agashe, H. Davoudiasl, G. Perez and A. Soni, Phys. Rev. D **76**, 036006 (2007)

[54] G. L. Bayatian *et al.* [CMS Collaboration], J. Phys. G **34**, 995 (2007), [ATLAS Collaboration], CERN-OPEN-2008-020, Geneva, 2008, to appear.

[55] M.Toharia , private communication.

[56] A. Pukhov, [arXiv:hep-ph/0412191].

[57] T. Sjostrand, S. Mrenna and P. Skands, JHEP **0605**, 026 (2006)

[58] A. Pomarol, Phys. Rev. Lett. **85**, 4004 (2000) [arXiv:hep-ph/0005293]; L. Randall and M. D. Schwartz, Phys. Rev. Lett. **88**, 081801 (2002) [arXiv:hep-th/0108115] and JHEP **0111**, 003 (2001) [arXiv:hep-th/0108114]; K. Agashe, A. Delgado and R. Sundrum, Nucl. Phys. B **643**, 172 (2002) [arXiv:hep-ph/0206099] and Annals Phys. **304**, 145 (2003) [arXiv:hep-ph/0212028]; R. Contino, P. Creminelli and E. Trincherini, JHEP **0210**, 029 (2002) [arXiv:hep-th/0208002].

[59] W. D. Goldberger and I. Z. Rothstein, Phys. Rev. Lett. **89**, 131601 (2002) [arXiv:hep-th/0204160]. W. D. Goldberger and I. Z. Rothstein, Phys. Rev. Lett.

89, 131601 (2002) [arXiv:hep-th/0204160]; Phys. Rev. D **68**, 125011 (2003) [arXiv:hep-th/0208060] and

[60] H. Davoudiasl, J. L. Hewett and T. G. Rizzo, Phys. Rev. D **68**, 045002 (2003) [arXiv:hep-ph/0212279];

[61] T. Appelquist, H. C. Cheng and B. A. Dobrescu, Phys. Rev. D **64**, 035002 (2001) [arXiv:hep-ph/0012100].

[62] K. w. Choi and I. W. Kim, Phys. Rev. D **67**, 045005 (2003) [arXiv:hep-th/0208071].

[63] R. Contino, Y. Nomura and A. Pomarol, Nucl. Phys. B **671**, 148 (2003) [arXiv:hep-ph/0306259].

[64] D. Atwood, M. Gronau and A. Soni, Phys. Rev. Lett. **79**, 185 (1997) [arXiv:hep-ph/9704272].